LIGHT-RESPONSIVE SPIROPYRAN BASED POLYMER: SYNTHESIS AND PHOTOCHROMIC BEHAVIOUR

by
Claudia Ventura
MSc Organic and Biomolecular chemistry

Dublin City University

This thesis is submitted to Dublin City University for the degree of Doctor of Philosophy (PhD) in the School of Chemical Sciences

Supervised by Dr. Andreas Heise

December 2013

I hereby certify that this material, which I now submit for assessment on the programme of study leading to the award of Doctor of Philosophy is entirely my own work, that I have exercised reasonable care to ensure that the work is original, and does not to the best of my knowledge breach any law of copyright, and has not been taken from the work of others save and to the extent that such work has been cited and acknowledged within the text of my work.

Signed: _____

Claudia Ventura

ID No.: 59105178

Date: _____

To my father

A papy

ACKNOWLEDGEMENTS

First of all I want to thank Dr. Andreas Heise for giving me the chance to work in his group, for always encouraging and supporting me during my PhD and for being an example to follow both as a supervisor and as a person.

Thanks to Jin, Fabrice, Mark, Zeliha, Anton, Ida, Tushar, Marcello, Jaco and all the people that within the School of Chemistry helped me, each one in their own way, during my years in DCU.

Thanks to Dr. Robert Byrne and Dr. Silvia Giordani for contributing with their knowledge and their experience to the realization of my work.

I want to thank my parents for their endless affection and their constant support all my life, for having been my solid points, for having taught me love and for having passed on to me the real values of life and an immense love for studying and researching.

Thanks to my siblings Cristiano and Elena for sharing with me joys, disappointments, adventures and discoveries, hurts and highs, every bright and dark moment of my life, always holding my hand for better or for worse. They have been the best gift my parents ever made.

I want to thank boyfriend Paul for being such an exceptional partner. His constant love and care and his consistent support in every possible way fill my life. Thank you for all the time you spent helping me and for never stop believing in me.

I want to thank my best friend Bianca for being omnipresent in my life, even when she is thousands kilometers away. Her support, encouragements and positive energy have played a key role in my life, especially in the last six atrocious months.

Thanks to Giada, Francesca, Giulia, Ana, Giulia, Serena, Alessio and all my friends for their affection and their never-ending support, each one in their own way makes my life overflowing with joy, love and positive energy. Friends are the family we choose.

LIST OF ABBREVIATIONS

4BriBu	Pentaerythritol tetrakis(2-bromoisobutyrate)
ACN	Acetonitrile
AHMA	6-azidohexyl methacrylate
ATRP	Atom Transfer Radical Polymerization
bis-BSP-PEG	Double end-functionalized with 1'-(propargyl)-3',3'-dimethyl-6-nitrospiro[2H-1-benzopyran-2,2'-indoline] poly ethylene glycol
bis-BSP-PPO	Double end-functionalized with 1'-(propargyl)-3',3'-dimethyl-6-nitrospiro[2H-1-benzopyran-2,2'-indoline] poly propylene oxide
bis-N_3-PEG	Double azide end-functionalized poly ethylene glycol
bis-N_3-PPO	Double azide end-functionalized poly propylene oxide
Bis-SP	1,4-bis((6-tert-butyl-1',3',3'-trimethylspiro[chromene-2,2'-indoline]-8-yl)methyl)piperazine
BMC	Benzomerocyanine
BMC-1-PMMA	Benzomerocyanine form of 1'-(2-bromoisobutyryloxyethyl)-3',3'-dimethyl-6-nitrospiro[2H-1-benzopyran-2,2'-indoline] functionalized poly(methyl methacrylate)
BMC-2-PMMA	Benzomerocyanine form of 1',3',3'-trimethyl-6-(2-bromoisobutyryloxy)spiro[2H-1-benzopyran-2,2'-indoline] functionalized poly(methyl methacrylate)
BMC-alkyne	Benzomerocyanine form of 1'-(propargyl)-3',3'-dimethyl-6-nitrospiro[2H-1-benzopyran-2,2'-indoline]
BMC-Br-1	Merocyanine form of 1'-(2-bromoisobutyryloxyethyl)-3',3'-dimethyl-6-nitrospiro[2H-1-benzopyran-2,2'-indoline]
BMCH	protonated BMC
BMCH-alkyne	Protonated benzomerocyanine form of 1'-(propargyl)-3',3'-dimethyl-6-nitrospiro[2H-1-benzopyran-2,2'-indoline]
BMC-PMMA	Benzomerocyanine form of 1’-(2-hydroxyethyl)-3’,3’-dimethyl-6-nitrospiro[2H-1-benzopyran-2,2’-indoline] functionalized poly(methyl methacrylate)

bpy	2,2'-bipyridine
BSP	Benzospiropyran
BSP-1-PMMA	1'-(2-bromoisobutyryloxyethyl)-3',3'-dimethyl-6-nitrospiro[2H-1-benzopyran-2,2'-indoline] functionalized poly(methyl methacrylate)
BSP-2-PMMA	1',3',3'-trimethyl-6-(2-bromoisobutyryloxy)spiro[2H-1-benzopyran-2,2'-indoline] functionalized poly(methyl methacrylate)
BSPA	1'-(2-acryloxyethyl)-3',3'-dimethyl-6-nitrospiro[2H-1-benzopyran-2,2'-indoline]
BSP-alkyne	1'-(propargyl)-3',3'-dimethyl-6-nitrospiro[2H-1-benzopyran-2,2'-indoline]
BSP-Br-1	1'-(2-bromoisobutyryloxyethyl)-3',3'-dimethyl-6-nitrospiro[2H-1-benzopyran-2,2'-indoline]
BSP-Br-2	1',3',3'-trimethyl-6-(2-bromoisobutyryloxy)spiro[2H-1-benzopyran-2,2'-indoline]
BSPMA	1'-(2-methacryloxyethyl)-3',3'-dimethyl-6-nitrospiro[2H-1-benzopyran-2,2'-indoline]
BSP-OH-1	1’-(2-hydroxyethyl)-3’,3’-dimethyl-6-nitrospiro[2H-1-benzopyran-2,2’-indoline]
BSP-OH-2	1',3',3'-trimethyl-6-hydroxyspiro[2H-1-benzopyran-2,2'-indoline]
BSP-PEG	End-functionalized with 1'-(propargyl)-3',3'-dimethyl-6-nitrospiro[2H-1-benzopyran-2,2'-indoline] poly ethylene glycol
BSP-PMMA	1’-(2-hydroxyethyl)-3’,3’-dimethyl-6-nitrospiro[2H-1-benzopyran-2,2’-indmnoline] functionalized poly(methyl methacrylate)
$CDCl_3$	Deuterated chloroform
CH_3OH	methanol
CRP	Controlled Radical Polymerization
CuAAC	Copper-catalyzed Azide-Alkyne 1,3-dipolar Cycloaddition

DCM	Dichloromethane
DIPEA	N,N-diisopropyl ethyl amine
DMAEMA	2-(dimethylamino)ethyl methacrylate
DMANF	2-*N*,*N*-dimethylamino-7-nitrofluorene
DMF	Dimethylformamide
DNA	Deoxyribonucleic acid
EBiB	Ethyl 2-bromoisobutyrate
ESI	Electrospray ionization
Et2O	Diethyl ether
Et2O	Diethyl ether
Et_3N	Triethylamine
EtOH	Ethanol
FT-IR	Fourier Transform Infrared Spectroscopy
GPC	Gel Permeation Chromatography
GSH	Glutathione
H-bonds	Hydrogen bonds
HEMATMS	2-(trimethylsilyloxy) ethyl methacrylate
HMTETA	1,1,4,7,10,10-hexamethyltriethylenetetraamine
IPA	Isopropyl alcohol
LED	Light-emittind diode
MALDI-ToF	Matrix-Assisted Laser Desorption/Ionitiation Time of Flight-mass spectroscopy
MC	Merocyanine
MCH	Protonated merocyanine form of 1'-(2-hydroxyethyl)-3',3'-dimethyl-6-nitrospiro[2H-1-benzopyran-2,2'-indoline]
MC-OH	Merocyanine form of 1'-(2-hydroxyethyl)-3',3'-dimethyl-6-nitrospiro[2H-1-benzopyran-2,2'-indoline]
MMA	Methyl methacrylate
M_n	Number-average molecular weights
M_w	Weight-average molecular weights
N_3-PEG	azide end-functionalized poly ethylene glycol
n-BA	n-butyl acrylate

NMR	Nuclear Magnetic Resonance
NO_2	nitro group
PAHMA	poly(6-azidohexyl methacrylate)
PAiBEMA	Poly(2-azidoisobutyryloxyethyl methacrylate)
PBiBEMA	Poly(2-bromoisobutyryloxyethyl methacrylate)
PBSPHMA	poly(BSP hexyl methacrylate)
PDI	polydispersity index
PEG	Polyethylene glycol
PEO	Poly(ethylene oxide)
PHMTETA	Poly(trimethylsilyloxyethyl methacrylate)
PMDETA	N,N,N',N'',N''-pentamethyldiethylenetriamine
PMMA	Poly(methyl methacrylate)
PPO	Poly propylene oxide
RAFT	Reversible Addition Fragmentation chain Transfer
SdP	Solvent dipolarity
SEC	Size Exclusion Chromatograms
SP	Spiropyran
SP-OH	1'-(2-Hydroxyethyl)-3',3'-dimethyl-6-nitrospiro[2H-1-benzopyran-2,2'-indoline]
TBAF	Tetrabutylammonium fluoride
TFA	Trifluoroacetic acid
THF	Tetrahydrofuran
TPMA	Tris[(2-pyridyl)methyl]amine
ttbP9	3,20-di-*tert*-butyl-2,2,21,21-tetramethy 5,7,9,11,13,15,17,19-docosanonaene
UV	Ultraviolet
Vis	Visible

TABLE OF CONTENTS

ABSTRACT

Photo-responsive polymers have been investigated intensively as important elements for the development of smart materials and devices. Our interest is in polymers functionalized with spiropyran (SP), a well-known photocromic molecule that has the ability to reversibly switch from an uncharged, colorless, benzospiropyran form, to a zwitterionic, planar, highly colored merocyanine (MC) form upon exposure to ultraviolet (UV) or visible light. Controlled radical polymerization (CRP) is a particularly attractive method to produce spiropyran-derivitized polymers as the synthesis of polymers with photochromic units present in defined positions, either along the polymer chain or as the polymer end-group, is readily achievable. This thesis initially documents firstly the synthesis of polymers that possess a single SP terminal unit, produced by atom transfer radical polymerization (ATRP), and their light responsiveness. The second part of this work reports the synthesis and the characterization of a SP derivative with a propyne functional group and the study of its photochromism. The alkyne functionality of the BSP compound was exploited to demonstrate a BSP-based polymeric system that utilizes commercially available polymers, through copper(I) catalyzed azide/alkyne reaction (CuAAC). The third part of this work consists of synthesizing well-defined polymeric systems with complex architectures, such as star or graft copolymer, that bear a high density of SP units in the side chain. The strategy employed consists of combining ATRP and the CuAAC.

Chapter 1

Introduction

1.1 Photocromism of spiropyran

Photochromism is the reversible conversion of a single chemical species between two isomeric forms induced by absorption of electromagnetic radiation, resulting in a change in absorption spectra.[1,2]

The family of spiropyrans is one of the most extensively studied class of photochromic organic molecules since the discovery of their photochromic properties in 1952 by Fisher and Hirshberg[3,4] spiropyrans have been widely investigated for several applications such as self-developing photography, displays, filters, lenses,[4] sensors and biomolecules activity regulation.[5] Structurally spiropyrans present a substituted *2H*–pyran linked to a second heterocyclic system by a common tetrahedral sp^3 carbon atom. The two heterocyclic parts of the molecule are held orthogonal by the spiro carbon atom (**Scheme 1.1**).[6]

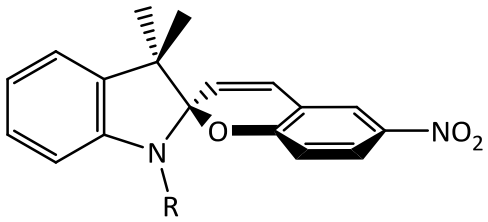

Scheme 1.1 Representation of the structure of spiropyrans, showing that the two halves of the molecule are positioned perpendicular to each other**.**

Upon UV-light irradiation the colorless, uncharged, non-planar, closed form of spiropyran (SP) switches to a colored, zwitterionic, planar, open isomer, called merocyanine (MC). The latter reverts back thermodynamically under dark condition or when irradiated with visible light (in particular white or green light) (**Scheme 1.2**).[7]

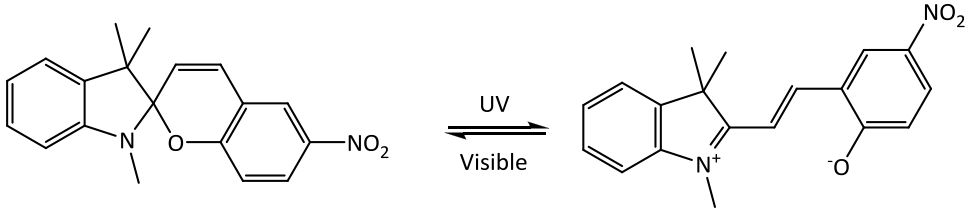

SP MC

Scheme 1.2 The photoinduced (UV and Vis) transformation of spiropyran.

The structural transformation from SP to MC is due to the pyran ring cleavage followed by a molecular rotation.[2,8-11] Upon UV light exposure the spiro C-O bond is cleaved heterolytically and the hybridization of the involved carbon atom changes from sp^3 to sp^2, enabling the planar structure. Consequently the π systems of the two parts of the molecules, previously isolated, become extensively conjugated. The so-generated extended conjugated system, the MC form, is strongly colored because it has the ability to absorb photons of visible radiation. The final result is the shift of the UV absorption in the visible region.[1]

As already mentioned the SP and MC isomers produce two different absorption spectra and it is evident and intuitive, as they are strongly structural diverse, that they also differ in various physical and chemical properties, including dipole moment and geometrical structure.[2,7,12] The growing interest in spiropyrans derives indeed from the significant difference between the two generated isomers, their molecular stability and the reversibility of the isomerization.[7,10]

One of the unique features of the MC form is the presence of a phenolate group which can bind divalent metal ions,[8,13,14] H^+,[15,16] amino acids[17,18] and DNA.[19] Therefore the MC form possesses particular coordination properties that are not shown by the SP isomer.[20] The mentioned bindings are photo-reversible: upon illumination with white or green light, MC releases the guest and reverts to the SP form. Basically the spiropyran compounds represent a bistable molecular system[10] responsive to external inputs such as light, proton and metal ions. Exploiting and manipulating this characteristic numerous molecular switches, logic gates, sensors and receptors have been developed.[18] The following two examples are discussed in more detail.

In 2001 Raymo and Giordani[21] demonstrated the efficacy of a common spiropyran as a molecular switch and showed the simplicity of generating a complex logic circuit based on it. They induced selectively, with light and chemical stimuli, three different states of the spiropyran: SP-OH, MC-OH and MCH, the protonated form of the MC-OH (**Figure 1.1**). They achieved control of the system by switching completely from one state to the others, generating a unique optical response. Basically the light and chemical stimulations were transduced in optical outputs,

through several logic operations, as shown in **Figure 1.1**. This spiropyran-based system operates as a nine-element logic circuit.

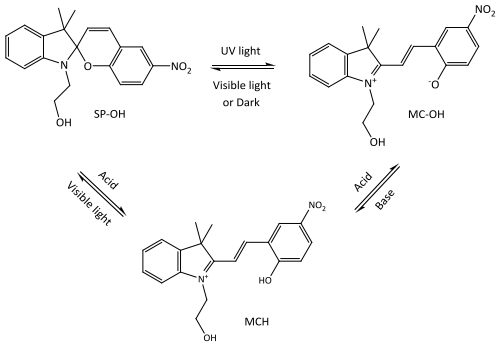

Input Data			Output Data	
Ultraviolet Light	Visible Light	H^+	Absorption at 401 nm	Absorption at 563 nm
*I*1	*I*2	*I*3	*O*1	*O*2
0	0	0	0	0
0	0	1	1	0
0	1	0	0	0
1	0	0	0	1
0	1	1	0	0
1	0	1	1	0
1	1	0	0	1
1	1	1	1	0

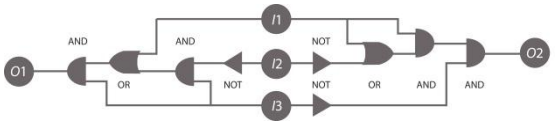

Figure 1.1 (Left) The switching cycle associated with the three states SP-OH, MC-OH and MCH. (Right) Truth table for the three-state molecular switch where a *0* indicates that the corresponding signal is *Off* and a *1* that it is *On* and the logic circuit equivalent to the three-state molecular switch transduces the inputs *I*1-*I*3 into the outputs *O*1 and *O*2 through AND,NOT, and OR operations.[21]

As already mentioned, SP have been widely investigated as molecular sensors and recently Albiz' group has developed a bis-spiropyran ligand (Bis-SP, **Scheme 1.3**) for dipolar compounds.[18] In Albiz work the high selectivity and the photocontrolled reversibility of Bis-SP towards reduced glutathione (GSH, **Scheme 1.3**), one of the principal cellular thiol compound with several important functions in the body, is very well demonstrated.[18]

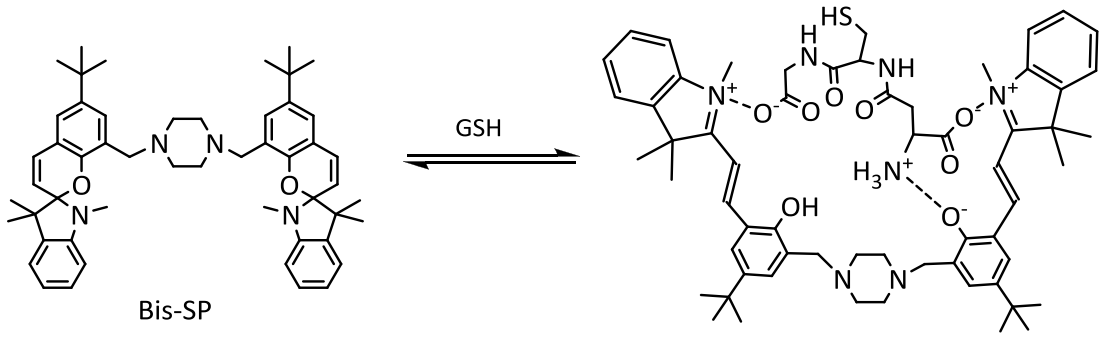

Scheme 1.3 Possible scheme of the photochemical ring-opening of Bis-SP in the presence of GSH.[18]

Since the Bis-SP responds to the GSH binding with an absorption in the visible region and a fluorescence emission, the GSH complexation is also detectable by measuring the change in fluorescence, in other words the Bis-SP is a fluorescent probe. Furthermore, this system has the capability of penetrating the cell membrane and is exploitable for glutathione imaging in living cell.

1.1.1 Structural conformation of SP

As previously mentioned, the spiro carbon atom of SP links two isolated orthogonal π systems. Therefore, the absorption spectrum of SP in its closed form is merely the sum of the spectra of the two halves of the molecule, with absorbance bands only in the UV region and no bands in the visible region.[6] Upon exposure to UV light the C-O of the closed SP cleavages leading to an open, planar MC structure which allows the conjugation between the two π systems of the molecule, resulting in a strong absorbance band in the visible region of the spectrum, 500-600 nm.[1,6]

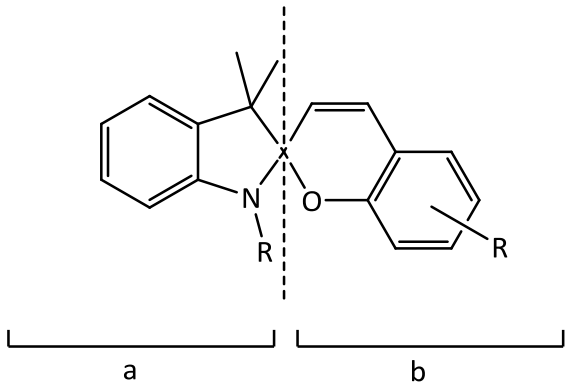

Figure 1.2 Schematic representation of SP. The structure of the molecule consists of an indoline part (a) attached through an insulating spiro carbon atom to a *2H*–pyran (b).

An important stereoelectronic effect that influences the SP behaviour is the interaction between the n_N electrons and the σ*orbital of the C_{spiro}-O bond. Indeed, the structure of the SP spiro center is favourable to negative hyperconjugation, which consists in a partial donation of the lone electron pair of the nitrogen atom to the vacant antibonding σ^*_{C-O} orbital, leading to a shortening of the C_{spiro}-N bond and to an elongation of the C_{spiro}-O bond (**Figure 1.3**, A). Consequently, while the C_{spiro}-N bond results strengthen, the C_{spiro}-O bond is weakened and prone to cleavage in the SP-MC isomerization process. This effect is only partially compensated by the

interaction being between the n_O electrons and the $\sigma^*_{C\text{-}N}$ orbital (**Figure 1.3**, B), this interaction considerably weaker than $n_N \rightarrow \sigma^*_{C\text{-}O}$, since the more electronegative oxygen centre is a poorer electron donor than nitrogen and therefore the energy gap between the interacting orbitals is larger. It has been demonstrated that electron-withdrawing substituents on the benzene ring of the pyran fragment strengthen the $n_N \rightarrow \sigma^*_{C\text{-}O}$ interaction, while electron-donating substituents weaken it. For example, the presence of nitro groups (NO_2) increases the delocalisation of the n_O electrons to the π system of the benzopyran ring, thus further weakening the C_{spiro}-O bond. Photoexcitation of the molecule by UV light irradiation leads the cleavage of the already weakened and elongated C_{spiro}-O bond.[10,22]

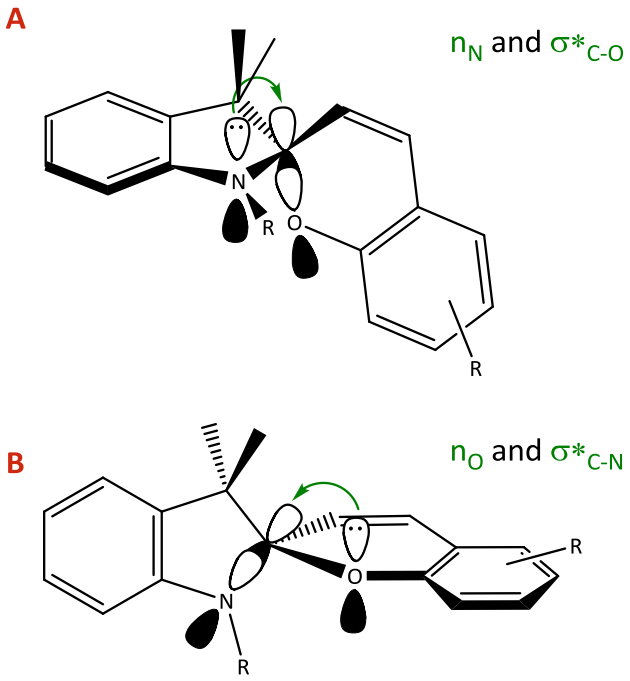

Figure 1.3 Representation of the interactions occurring between (A) the lone pair of electrons on the nitrogen atom and the vacant antibonding $\sigma^*_{C\text{-}O}$ orbital and (B) the lone pair of electrons on the oxygen atom and and $\sigma^*_{C\text{-}N}$ orbital. The interaction A is favoured compared to the interaction B, because the nitrogen atom, being less electronegative than oxygen, is a richer electron donor and the energy level gap between its lone electron pair and $\sigma^*_{C\text{-}O}$ is smaller than $n_N \rightarrow \sigma^*_{C\text{-}O}$.

1.1.2 Dynamic of the SP conversion to the MC form

The initial step of the ring-opening reaction is the C_{spiro}-O heterolytic bond cleavage to form a cisoid open intermediate which can be described in general as a resonance hybrid between a quinonic (Q) and a dipolar zwitterionic (Z) form (**Figure 1.4**).[1] The mechanism involved in the first step of SP-MC photoisomerization is strongly influenced by solvent polarity: in polar solvents the C_{spiro}-O cleavage occurs with anchimeric assistance by the indoline nitrogen (**Figure 1.5**, top), leading to a zwitterionic intermediate (Z), while a nonpolar electrocyclic ring opening mechanism with no anchimeric assistance from the indoline nitrogen occurs in nonpolar solvent (**Figure 1.5**, bottom), leading to a quinoidal intermediate (Q).[12,23]

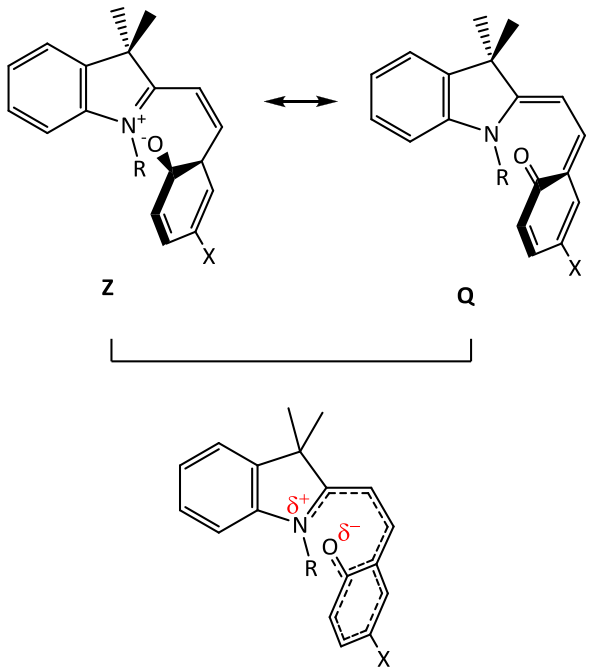

Figure 1.4 Representations of the cisoid isomer formed with the C_{spiro}-O heterolytic bond cleavage of SP. This isomer can be represented as different resonance forms with zwitterionic (Z) or quinoidal (Q) structures.

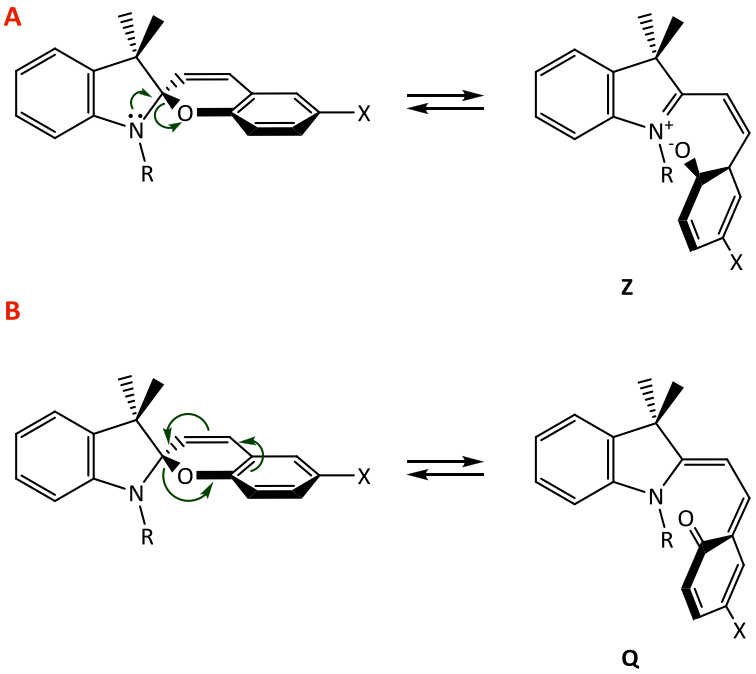

Figure 1.5 Competing mechanisms involved in the first step of SP-MC photoisomerization. (A) In polar solvents the heterolytic C_{spiro}-O bond cleavage is anchimeric assisted by the indoline nitrogen, leading to the zwitterionic intermediate Z; (B) In nonpolar solvent the heterolytic C_{spiro}-O bond cleavage occurs in a 6π electrocyclic ring opening nonpolar mechanism, leading to the quinoidal intermediate Q.

The cisoid open intermediate formed is sterically strained as the two halves of the molecule are still orthogonal to each other, and through geometrical rearrangements rapidly converts to planar MC isomers (**Figure 1.6**).[10,24] These MC isomers differ in the geometrical arrangements along the central chain of the three partial C-C double bonds and they are labeled by a sequence of three C or T letters, indicating their cis or trans configuration, respectively. The only stable MC isomers have a trans configuration of the central C-C partial double bond, the corresponding cis isomer are at relatively higher energy due to internal steric hindrance.[25] The presence of different MC isomers in solution of SP has been widely reported in the literature and has been shown in several studies, using various techniques including transient spectroscopy and low temperature NMR experiments.[10,25-27] According to theoretical modeling calculations, the structure of the most stable MC isomers in solution are TTC and CTC conformers.[10,25] The presence of electron-withdrawing substituents on the benzene ring of the pyran fragment stabilizes the MC form, increasing the delocalisation by resonance of the partial negative charge on the

oxygen.[1,22] The position of the electron accepting substituents is crucial: only *para* and *ortho* substituted are able to stabilize the MC form through their mesomeric effect.

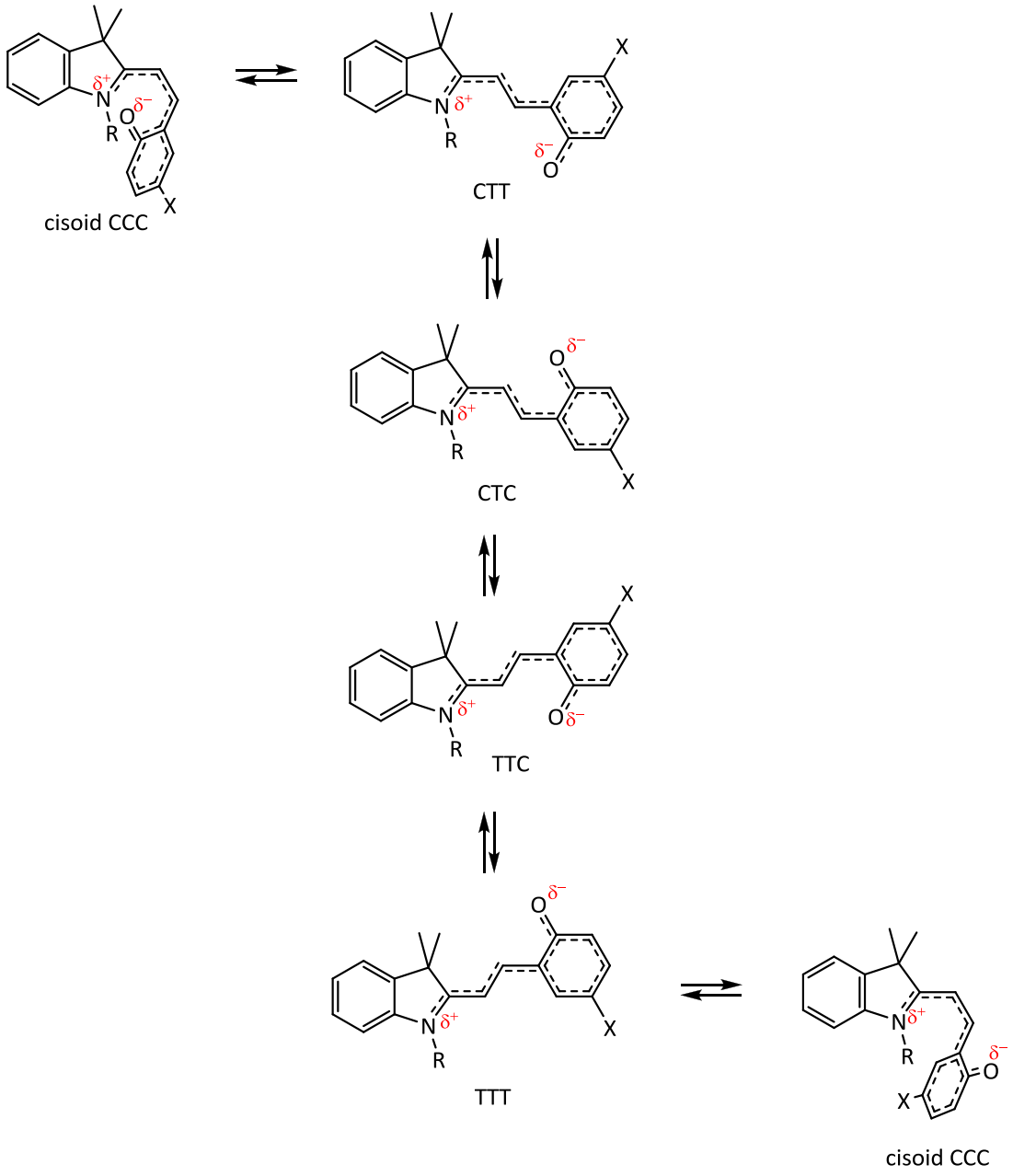

Figure 1.6 Representation of different possible MC isomers induced by photoexcitation of the closed SP form. The sterically strained cisoid intermediate Q undergoes to geometrical rearrangements to form planar MC isomers. The MC isomers are labelled by a sequence of three C or T letters, indicating respectively the cis or trans configuration of the three partial C-C double bonds along the central chain. The isomers with cis configuration of the central C-C double bond are excluded from this scheme because they are significantly higher in energy than their corresponding trans isomers.[10]

1.1.3 Excited-state ring-opening Reaction

The initial step of the photoisomerization is the dissociation of a C_{spiro}-O bond in an electronic excited state. The nature and details of the mechanism that allows such interconversion is far from being fully understood.[28] It has been reported that the nature of the excited state is significantly substituent dependent.[10,24] For example, the ring-opening reaction of unsubstituted SP involves only singlet states,[25] while for its NO_2-subtituted derivative a triplet state is found to play a role in the reaction.[4,24] The photochromic SP-MC interconversion is a very complex reaction but it is generally accepted that the excitation induces the formation of an open MC-cis that relaxes to the merocyanine ground state MC (figure). The cisoid form corresponds to the reaction intermediates previously mentioned (cisoid CCC, **Figure 1.6**). A fraction of the ring-opened product molecules can be closed back to SP.[10,29]

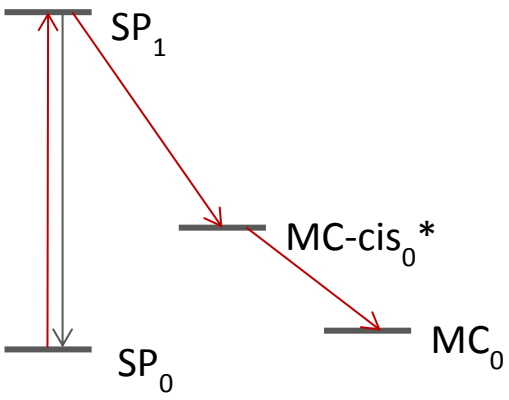

Figure 1.7 Schematic representation of the energy levels probably involved photoisomerization of the SP-MC. The ring-opening pathway is depicted by the red arrows, while the black arrow shows that a the SP is partially reformed. The subscripts indicate the state of the molecule: 0 for the ground state and 1 for the excuted state. * represents a vibrationally excited state.

1.1.4 Synthesis of spiropyrans

From the synthetic point of view, SP are relatively easy to prepare as their synthesis may be performed in three stages. The starting material, the indolenine derivative (**1**), is alkylated on the nitrogen atom to give the indoleninium salt (**2**). The quaternary salt in basic conditions forms the corresponding methylene base (**3**), which subsequently reacts with the salicylaldehyde (**4**) in ethanol (EtOH) by condensation to lead to the SP formation (**Scheme 1.4**).[30,31]

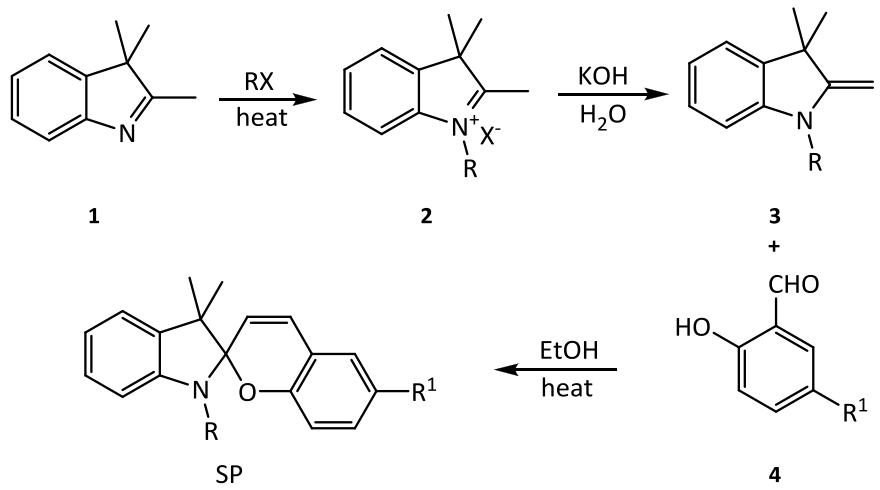

Scheme 1.4 General reaction scheme for the three-step synthesis of SP.

The most probable mechanism for the last step involves the nucleophilic addition of the methylenic carbon atom in **3** on the carbonilic carbon of the aldehyde **4** and the consequent formation of the tetrahedral intermediate **5,** which, through a proton exchange, generates a phenolate function (**6**). The intramolecular addition of the phenolate group onto the electrophilic carbon and the dehydration leads to the SP formation (**Scheme 1.5**). The pyran segment of the SP is usually a benzopyran because the synthetic intermediates, such as substituded salicylic aldehyde, are easily available. The class of spiropyran with a benzopyran ring is named benzospiropyran (BSP) and the corresponding MC form is called benzomerocyanine (BMC).[1,6,31]

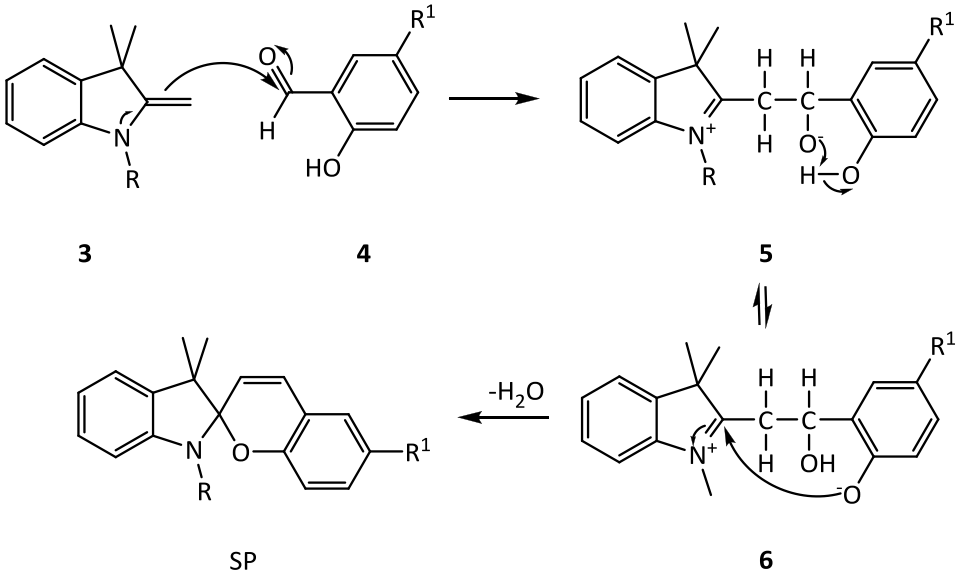

Scheme 1.5 Schematic representation of the reaction mechanism involving the condensation of the salicylaldehyde 4 onto methylene base 3.

1.1.5 Solvatochromism of BSP

Solvatochromism is the ability of a chemical substance to change color on variations in the polarity of the solvent medium, which typically involves a change in the position and intensity of the UV-Vis absorption band of the molecule when measured in different solvents. This change is due to intermolecular interactions between the solute and the solvent that modify the energy gap between the ground and the excited state of the absorbing species.[1,10] The family of BSP undergoes solvatochromism.[1,10,32] The BMC form is strongly polar because its zwitterionic resonance form strongly contributes to the electronic distribution of the ground state. Therefore, BMC is stabilized by polar solvents. The colour of the BMC in solution depends on the difference in polarity between the photoexcited BMC form and the corresponding ground state. In polar solvents, the ground state of the BMC is stabilized compared to its excited state, leading to a higher energy gap between the two states which results in a shift to shorter wavelengths (blue shift) of the corresponding absorption band. In nonpolar solvents, the energy difference between the ground and the excited states is much slower, resulting in a shift to longer wavelengths (red shift) of the related absorbance band (**Figure 1.8**).[1]

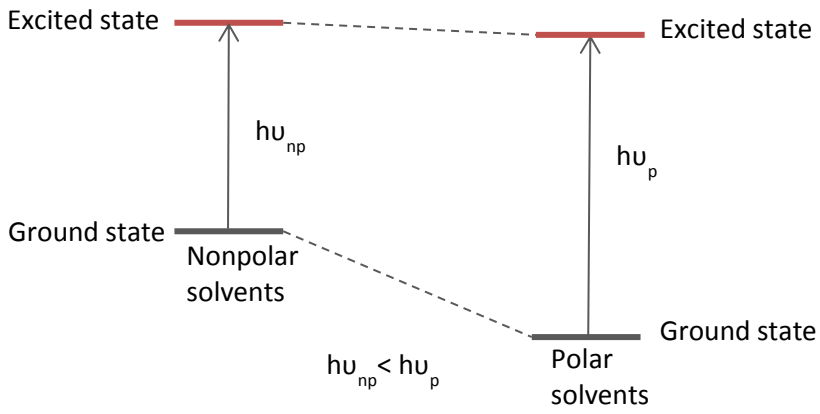

Figure 1.8 Schematic representation of the energy difference between the ground and the excited state of the BMC form in polar and nonpolar solvents.

1.1.6 Metal ion Complexation of BSP

In contrast to the BSP isomer, the open BMC form has ion-binding characteristics. The negatively charged phenolate oxygen of the BMC isomer can bind transitions metal cations, including Cu^{2+} and Co^{2+}, and this reversible process can be controlled optically. Since the binding occurs through the phenolate site, two units of the BMC isomer are required for complexation with bivalent cations (**Figure 1.9**). The complex formation results in a change in the absorbtion spectrum, which corresponds to a color change of the solution.[11-13,33]

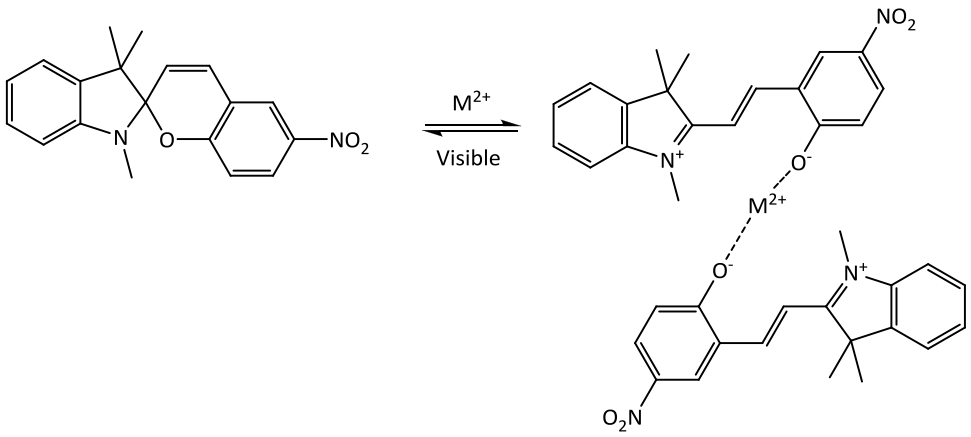

Figure 1.9 Representation of BSP complex formation. The BMC isomer can bind metal ions through the phenolate site. The guest can be expelled by irradiation with visible light, reverting the BSP to the closed form.

1.1.7 Acidochromism of BSP

In addition to metal ion interactions the phenolate anion of the BMC isomer can bind protons. The protonation of BMC can be detected by a change in the absorption spectrum: protonated BMC (BMCH) typically absorbs at around 400-450 nm while BMC isomer absorbs around 500-600 nm. The process is accompanied by a variation in color. When the BMC binds protons, the solution turns yellow.[15,16,21,34] Addition of base to the yellowish solution of protonated BMC leads to the formation of BMC isomer (**Figure 1.10**).[21,35]

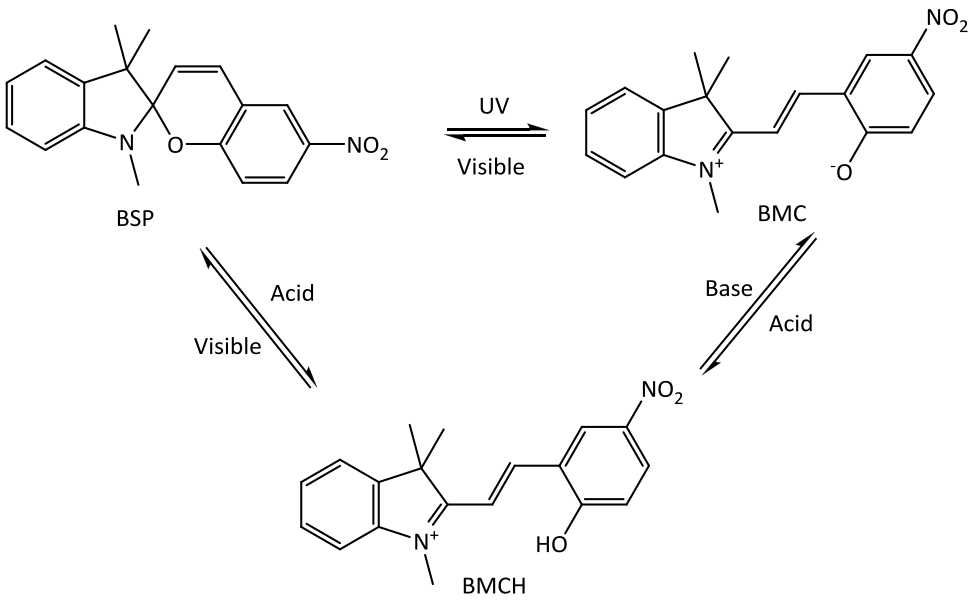

Figure 1.10 Acidochromism of BSP. Reversible transformations between BSP, BMC and its protonated form BMCH.[21]

1.1.8 Photodegradation of BSP

Photodegradation or 'fatigue' is a gradual degradation occurring when a photochromic compound is switched repeatedly between two forms over a certain number of times.[36,37] In principle photoisomerisation of BSP is a nondestructive process but side reactions leading to non-desirable by-products might occur. In the literature it has been reported that the main cause of BSP photodegradation is via a biomolecular pathway. Therefore, fatigue of BSP depends on BSP molecules concentration and their freedom, reducing the degree of motion of BSP through covalent attachment increases its photostability.[12,38]

1.2 Benzospiropyran and polymers

The interest in BSP has been widely discussed and the incorporation of this moiety into a material system extends the possible applications in nanoscience and nanotechnology,[39] in biomedical and drug delivery[17] and diagnostic imaging.[40] Polymeric systems with incorporated BSP moieties alter their physical and chemical properties, such as structure, conformation and solvation, when irradiated with the appropriate light wavelength. These alterations derive directly from the interactions between the photochromic groups, the polymeric system and their environment. Thus, within a polymer matrix photochromic isomerization can be stimulated by light to reversibly modulate the material properties.[2,41] Photo-responsive BSP polymers have been greatly exploited for the development of smart materials, devices and sensors.[2,11,42] For example Davis *et al.*[43] developed BSP mechanoresponsive polymers (**Figure 1.11**) that can provide visible detection and mapping of mechanical stresses. An external force applied to these synthetic materials induces the BSP isomerization, resulting in a strong coloration of the polymer. Therefore this system can function as a molecular force probe.[43,44]

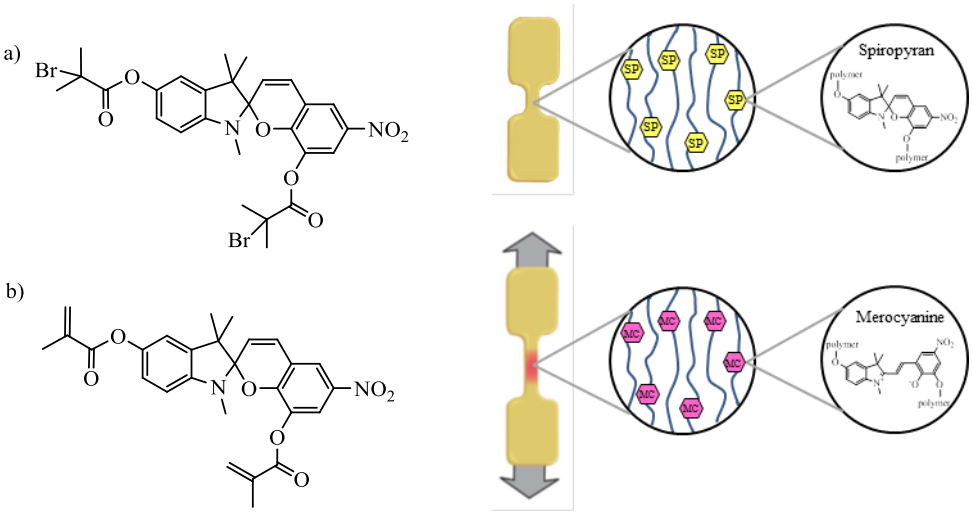

Figure 1.11 (Left) a) BSP functionalized with α-bromo esters used to initiate polymerization and incorporate a single BSP in the middle of the polymer chain. b) BSP functionalized with methacryloyl esters used to copolymerize with methyl methacrylate to form beads incorporating BSP. (Right) Schematic diagram of 'dog bone' specimens. Upon application of tensile force, a hypothesized conversion between the colourless BSP and coloured BMC forms of the mechanophore occurs. Exposure to visible light reverses the conversion back to the original BSP form.[43]

In the literature, several elegant examples were presented showing that with the help of controlled polymerization techniques the defined positioning of BSP units in the polymer can result in interesting effects.[45] For example, BSP-methacrylate (BSPMA) was copolymerized with methyl methacrylate (MMA) by atom transfer radical polymerization (ATRP) from silica surfaces by Locklin to create light sensitive polymer brushes (**Figure 1.12**).[46,47] The hydrophilicity of the brushes could reversible be switched by irradiation with light as was shown by the change of water contact angles. Similar results were reported for the surface initiated ring opening metathesis polymerization of norbonene-based BSP.[48]

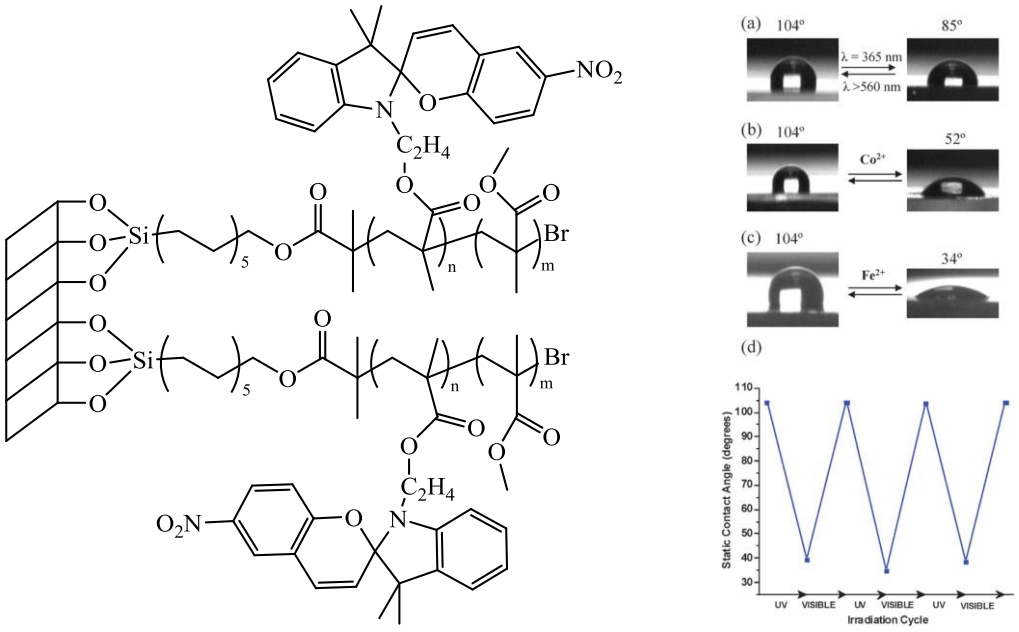

Figure 1.12 (Left) Surface initiated copolymerization of a BSP methacrylate derivative (BSPMA) and methyl methacrylate (MMA). (Right) Reversible contact angle changes. (a) Film irradiated in DMF, (b) 1×10^{-3} M Co^{2+}, (c) 1×10^{-3} M Fe^{2+}, (d) plot of reversible contact angle changes for SP film irradiated in Fe^{2+}.[46]

Another area of interest is light responsive random and block copolymer.[49,50] Matyjaszewski reported the synthesis of a BSP containing block copolymer by ATRP macroinitiation from poly(ethylene oxide) (PEO).[51] The micelles formed by this amphiphilic block copolymer were disrupted by irradiation with UV light, which converted the BSP into its BMC form rendering the amphiphilicity of the block copolymer. The process was fully reversible and could be used to encapsulate and release a payload (**Figure 1.13**).

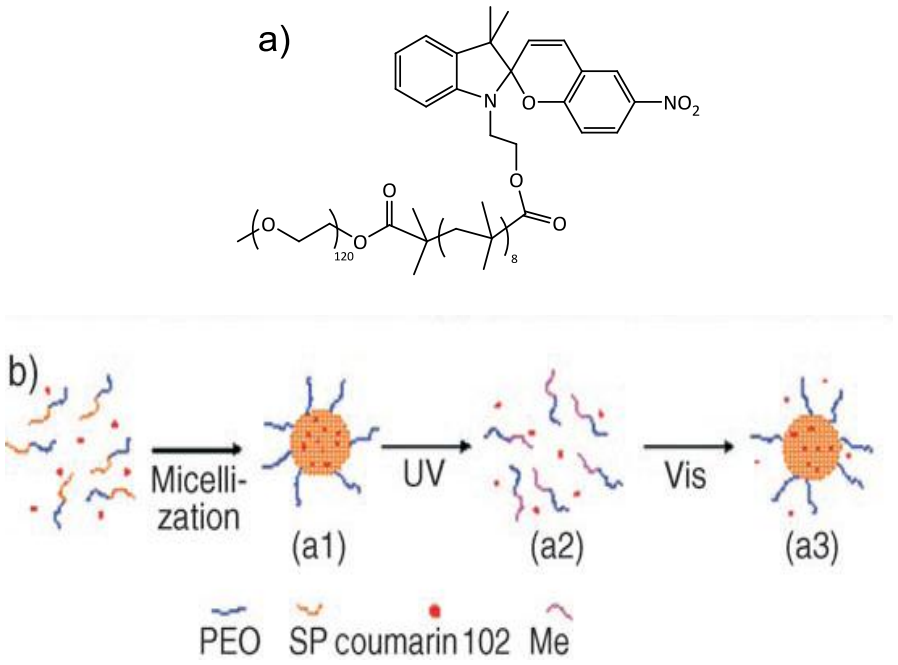

Figure 1.13 a) PEO-b-BSP diblock copolymer. b) Schematic representation of encapsulation of a dye within the hydrophobic core of a polymeric micelle on micellization (a1), release of dye on disruption of micellar structure by UV irradiation (a2), and re-encapsulation of a portion of the released dye on regeneration of the micelles by irradiation with visible light (a3).[51]

1.3 ATRP

Atom transfer radical polymerization (ATRP), a controlled/living radical polymerization (CRP) process, is one of the most successful techniques for the synthesis of well-defined polymers with designed molecular weights and narrow molecular weight distributions. ATRP is a simple and versatile method to prepare polymers with several functionalities, defined composition, very specific molecular architecture and properties.[52-54] ATRP is based on a transition metal complex able to catalyze a reversible redox process generating radicals (**Scheme 1.6**).

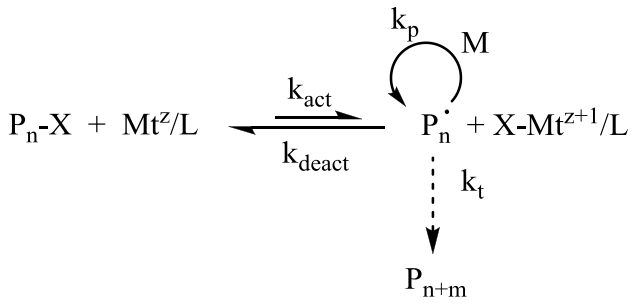

Scheme 1.6 Mechanistic scheme of the ATRP equilibrium.

The transition metal Mt presents two different oxidation states. The lower oxidation state metal complex Mt^z/L (L is a ligand and z is the oxidation state of the metal species; the charges of ionic species are omitted for simplicity) is the process activator. Its reaction with an alkyl halide initiators (RX), called dormant species, forms a propagating radical $P_n^{\bullet}$(with rate constant k_{act}). Specifically the lower oxidation state metal complex Mt^z/L is converted in the corresponding higher oxidation state metal complex with a coordinated halide anion X-Mt^{z+1}/L (deactivator), through a one-electron oxidation and a concomitant abstraction of an halogen atom, X, from the dormant species.[53,55] The reaction established by the catalyst complex is a dynamic equilibrium strongly shifted to the side of dormant species, resulting in an intermittently masking of the radical as a dormant species. Basically, the radicals generated during the process can react with the monomer and grow the polymer (with rate constant k_p), with each other and terminate the polymer (with rate constant k_t), or with X-Mt_{z+1}/L and deactivate the process (with rate constant k_{deact}). If the deactivation is efficient (i. e. high value of k_{deact}) the radical adds monomer and is deactivated into the dormant species, allowing the

homogeneous growing of the chains because they grow at the same pace, avoiding termination reactions. Moreover, if all polymer chains are initiated within a short period, the resulting polymer will be characterized by a narrow molecular weight distribution.[52,53] The so-generate well-defined polymer can also be reactivated and a second monomer can be added leading to the formation of well-defined block copolymers. Indeed, as previously discussed, ATRP allows the control of polymer molecular architecture, in terms of composition, topology, and functionality.

The rate constants k_{act} and k_{deact} depend on both the transition metal and the ligand, therefore the control of the propagating process strongly depends on the catalyst complex selected. Various metals, such as Cu, Ru, Fe, Mo, Os,[56] and ligands have been successfully employed as catalysts in ATRP but the most efficient transition metal complex is copper halide/nitrogen-based ligands where the two metal oxidation states are Cu(I) and Cu(II).[52,53,57]

As already mentioned, a fast initiation is crucial to obtain well-defined polymers, therefore the selection of the appropriate initiator is one of the main points in ATRP. The most commonly employed initiators are halogenesters, halogenalkylbenzenes, sulfonylhalogenides. If these compounds contain another functional group, such as an alcohol, ester or epoxide, they generate polymers with this functional moiety at the end of the chain. Another method to functionalize polymer chain end is the nucleophilic substitution of the halogen group. The polymer architecture can be varied from linear, star-like and brush-like, according to the structure and the number of halogens of the initiator (**Figure 1.14**).

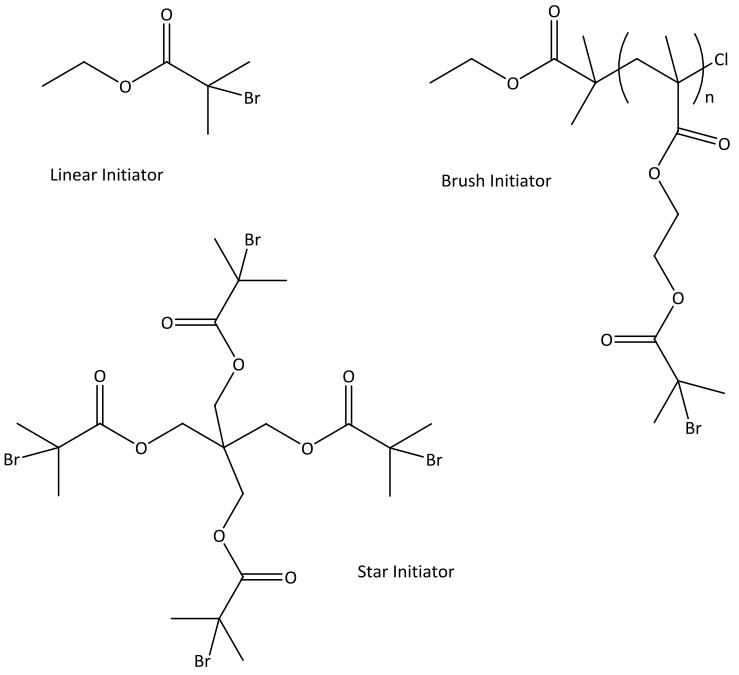

Figure 1.14 ATRP initiators for the synthesis of linear and multi-arm polymer.

ATRP has allowed a variety of conjugated monomers to be polymerized into well-defined polymers of controlled molecular weights. Typical monomers include acrylates, methacrylates, acrylonitrile, styrenes, acrylamides etc (**Figure 1.15**). Each monomer has its own unique atom transfer equilibrium constant for its active and dormant species ($K_{eq}=k_{act}/k_{deact}$) and consequently its own intrinsic radical propagation rate, even under the same conditions. Thus, to control the polymerization of a specific monomer, adjusting the concentration of the active species is crucial.[55]

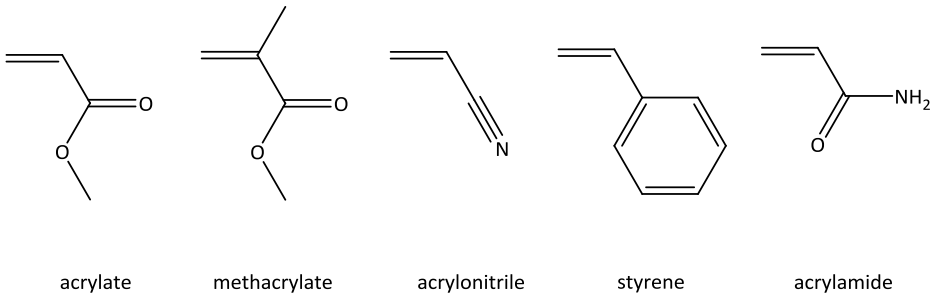

Figure 1.15 Examples of functional monomers for ATRP.

1.4 Click Chemistry

The modification of polymer after a successful polymerization is a useful method to develop new polymeric materials. To be suitable and applicable in polymer synthesis, a post-modification reaction requires high selectivity and efficiency. A wide class of reactions, termed 'Click Chemistry', meets these requisites. Click Chemistry reactions, indeed, proceed with high fidelity and tolerance in the presence of a wide variety of functional groups and solvents, in quantitative yields (usually above 95%), under mild conditions and with a simple product isolation.[58-60]

One of the most exploited class of Click Chemistry reactions for polymer synthesis is the cycloaddition of unsaturated species, in particular the copper(I) catalyzed azide/alkyne reaction (a variation of the Huisgen 1,3-dipolar cycloaddition reaction between terminal acetylenes and azides).[61] The mechanism of this reaction is a stepwise process that begins with the coordination of the alkyne to the Cu(I) species **1**, by displacing one of the ligands and forming the π-complex **1b**. This coordination, lowering the p*K*a of alkyne C-*H* by up to 9.8 units, facilitates the following deprotonation and therefore the copper(I) acetylides **2** formation (**Scheme 1.7**).[62]

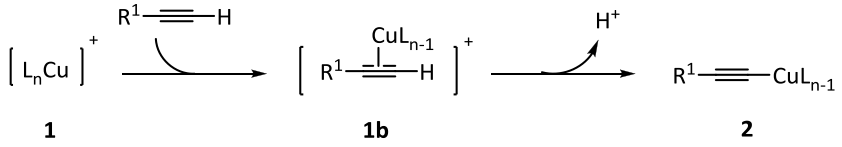

Scheme 1.7 Formation of the Copper(I) Acetylide. **62**

In the next step the nitrogen proximal to carbon in the azide coordinates copper, replacing one of the ligands and generating the copper acetylide-azide complex **3**. This complexation activates the azide toward nucleophilic attack of the C-2 acetylide carbon at the distal nitrogen, forming the Cu(III) metallocycle **4**. The following step is a ring contraction by a transannular association of the nitrogen proximal to carbon in the azide with the C-1 acetylide carbon, generating the triazole-copper(I) derivative **5**. Protonation of the latter intermediate **5**, following by dissociation of the 1,2,3-triazole, terminates the reaction regenerating the catalyst (**Scheme 1.8**).[62,63]

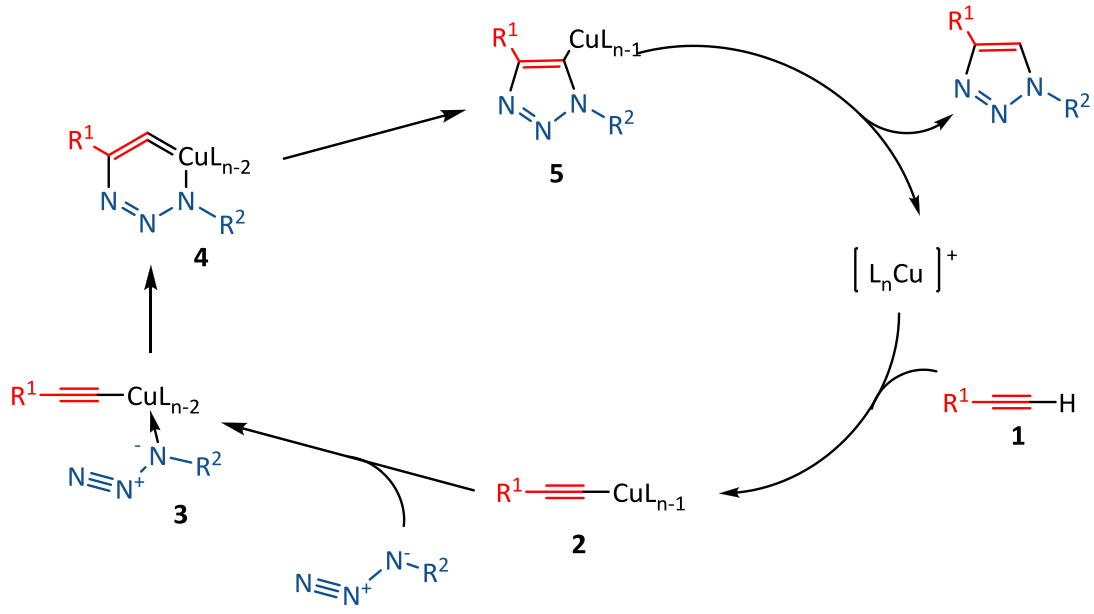

Scheme 1.8 Proposed mechanism for azide/alkyne reaction.[62]

The ligand plays a significant role in this process, influencing considerably the catalytic activity of the copper center. For this reason the ligand choice is extremely important. A wide range of compounds, such as pyridines, amines, triazoles and phosphines, has been successfully employed as ligands in this reaction and it has been proven that the aliphatic amines are the most efficient ones (**Figure 1.16**).[59]

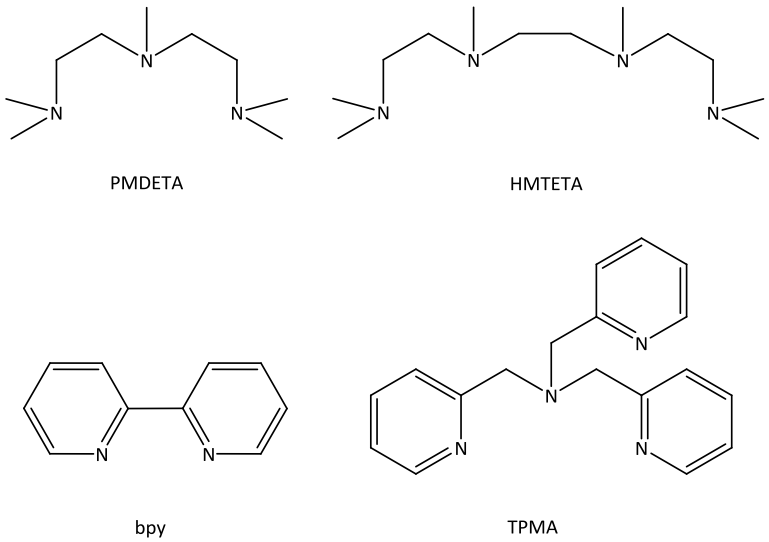

Figure 1.16 Examples of ligands for click chemstry. *N*,*N*,*N*′,*N*′′,*N*′′–pentamethyldiethylenetriamine (PMDETA), 1,1,4,7,10,10–hexamethyltriethylenetetraamine (HMTETA), 2,2′-bipyridine (bpy) and tris[(2-pyridyl)methyl]amine (TPMA).

In 2004 Wu et al. exploited the copper-catalyzed azide-alkyne 1,3-dipolar cycloaddition (CuAAC) to synthetize several dendritic structures of high purity and in excellent yield.[64] This work reports for the first time the use of CuAAC as conjugation tool in material science and represents the precursor of numerous original papers. From this point onwards hundreds of articles have been published in the context of click chemistry and polymer science.[65] CuAAC can be applied in polymer synthesis in several manners, such as connection of polymer fragments to generate linear, star or branched polymers, synthesis of cross-linked polymers with well-defined structures and functionalization of polymer sites with bioprobes, labels etc.[66] An example of the latter type of application is the recent work of Bertoldo et al. In 2011 they synthetized a new light responsive polysaccharide, derivatizing through CuAAC a N_3-functionalyzed chitosan with a propyne BSP compound (**Scheme 1.9**).[67]

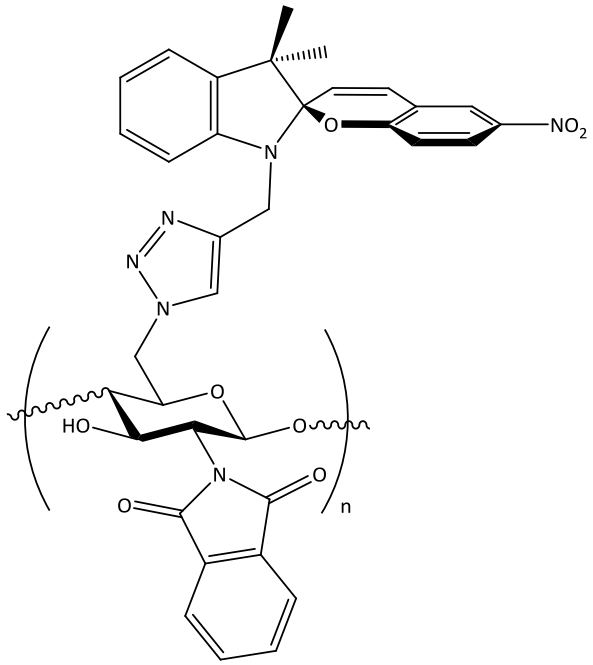

Scheme 1.9 Rappresentation of the structure of the propyne BSP compound.[67]

1.5 Click Chemistry and ATRP

Of particular interest for macromolecular engineering is the combination of CuAAC with ATRP. As already mentioned, ATRP is one of the most powerful polymerization techniques for designing polymers with complex architectures. Using the CuAAC in conjunction with ATRP expands considerably the range of producible materials, increases the possibilities of polymer architecture variations and therefore widens the applications in macromolecular engineering.[59]

There are three different strategies to combine ATRP and CuAAC: the *initiator approach*, the *Br^-/N_3^- approach* and the *Side-chain modified polymers*. The first approach consists of using an ATRP initiator containing an alkyne or azide moiety. These moieties are compatible with the ATRP process and can be exploited afterwards for click chemistry reactions (**Scheme 1.10**).[65,68]

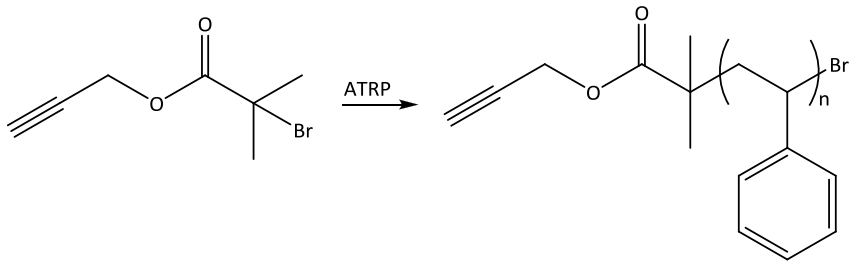

Scheme 1.10 Synthesis of clickable polymers through ATRP, exploiting an appropriate initiator.

The second approach relies on the terminal bromine group at the end of the polymer chain, easily convertible in azide through nucleophilic substitution. The full conversion has been widely demonstrated but seems to be very dependent on the polymer structure and reaction conditions (**Scheme 1.11**).[65,68]

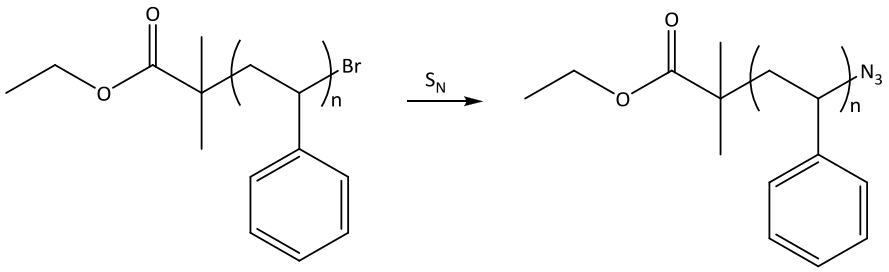

Scheme 1.11 Synthesis of clickable polymers through conversion of bromine functions in azide moieties.

The third method for combining ATRP and CuAAC involves the ATRP polymerization of appropriate monomers, bearing an azide or an alkyne group. As already mentioned in the first approach, these moieties are compatible with the ATRP process and they can be used for a subsequent CuAAC reaction. This approach leads to a high degree of clickable functionality (**Scheme 1.12**).[65,68]

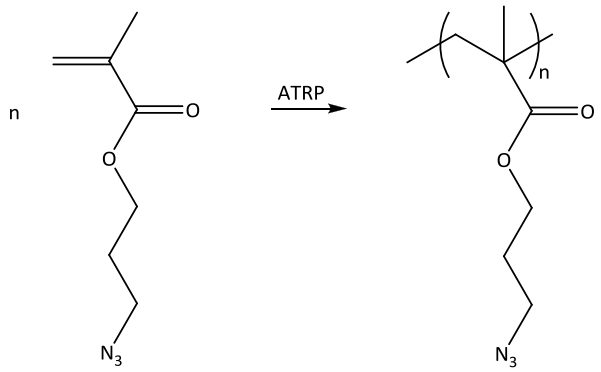

Scheme 1.12 Synthesis of clickable polymers through ATRP, exploiting an appropriate monomer.

Therefore the combination of ATRP and CuAAC enables the synthesis of all types of chain-end, head-end and side-chain modified polymers.

1.6 References

1. Dürr H., Bouas L.H. *Photochromism: molecules and systems*. Boston: Elsevier; **2003**.
2. Ercole F., Davis T.P., Evans R.A. *Polym. Chem.* **2010**, *1*, 37.
3. Fischer E., Hirshberg Y. *J. Chem. Soc.* **1952**, 4522.
4. Berkovic G., Krongauz V., Weiss V. *Chem. Rev.* **2000**, *100*, 1741.
5. Song Y., Xu C., Wei W., Rena J., Qu X. *Chem. Commun.* **2011**, *47*, 9083.
6. Celani P., Bernardi F., Olivucci M., Robb M.A. *J. Am. Chem. Soc.* **1997**, *119*, 10815.
7. Byrne R., Diamond D. *Nature Mater.* **2006**, *5*, 421.
8. Liu D., Chen W., Sun K., Deng K., Zhang W., Wang Z., Jiang X. *Angew. Chem. Int. Ed.* **2011**, *50*, 4103.
9. Crano J.C., Flood T., Knowles D., Kumar A., Van Gemert B. *Pure Appl. Chem.* **1996**, *68*, 1395.
10. Minkin V.I. *Chem. Rev.* **2004**, *104*, 2751.
11. Byrne R., Ventura C., Lopez F.B., Walther A., Heise A., Diamond D. *Biosens. Bioelectron.* **2010**, *26*, 1392.
12. Klajn R. *Chem. Soc. Rev.* **2013**, DOI:10.1039/c3cs60181a.
13. Gorner H., Chibisov A.K. *J. Chem. Soc., Faraday Trans.* **1998**, *94*, 2557.
14. Scarmagnani S., Walsh Z., Slater C., Alhashimy N., Paull B., Macka M., Diamond D. *J. Mater. Chem.* **2008**, *18*, 5063.
15. Radu A., Byrne R., Alhashimy N., Fussaro M., Scarmagnani S., Diamond D. *J. Photochem. Photobiol., A* **2009**, *206*, 109.
16. Raymo F.M. *Adv. Mater.* **2002**, *14*, 401.
17. Ipe B.I., Mahima S., Thomas K.G. *J. Am. Chem. Soc.* **2003**, *125*, 7174.
18. Shao N., Jin J., Wang H., Zheng J., Yang R. *J. Am. Chem. Soc.* **2010**, *132*, 725.
19. Andersson J., Li S., Lincoln P., Andreasson J. *J. Am. Chem. Soc.* **2008**, *130*, 11836.
20. Jiang G., Song Y., Guo X. *Adv. Mater.* **2008**, *20*, 2888.
21. Raymo F.M., Giordani S. *J. Am. Chem. Soc.* **2001**, *123*, 4651.

22. Aldoshin S.M., Chuev L.L., Filipenko O.S., Utenyshev A.N., Lokshin V., Laregenie P., Samat A., Guglielmetti R. *Russ. Chem. Bull.* **1998**, *47*, 1089.

23. Swansburg S., Buncel E., Lemieux R.P. *J. Am. Chem. Soc.* **2000**, *122*, 6594.

24. Liu F., Morokuma K. *J. Am. Chem. Soc.* **2013**, *135*, 10702.

25. Emsting N.P., Arthen-Engeland T. *J. Phys. Chem.* **1991**, *95*, 5502.

26. Chibisov A.K., Gorner H. *Chem. Phys.* **1998**, *237*, 425.

27. Li Y., Zhou J., Wang Y., Zhang F., Song X. *J. Photochem. Photobiol. A* **1998**, *113*, 65.

28. Sanchez-Lozano M., Estèvez C.M., Hermida-Ramòn J., Serrano-Andres L. *J. Phys. Chem. A* **2011**, *115*, 9128.

29. Buback J., Kullmann M., Langhojer F., Nuernberger P., Schmidt R., Würthner F., Brixner T. *J. Am. Chem. Soc.* **2010**, *132*, 16510.

30. Guglielmetti R., Meyer R., Dupuy C. *J. Chem. Educ.* **1973**, *50*, 413.

31. Guglielmetti R.J., Crano J.C. *Organic Photochromic and Thermochromic Compounds*. New York: Plenum Publishers; **1999**.

32. Reichardt C., Welton T. *Solvents and solvent effects in organic chemistry.* Weinheim, Germany: Wiley-VCH; **2010**.

33. Byrne R., Stitzel S.E., Diamond D. *J. Mater. Chem.* **2006**, *16*, 1332.

34. Wojtyk J.TC., Wasey A., Xiao N.N., Kazmaier P.M., Hoz S., Yu C., Lemieux R.P., Buncel E. *J. Phys. Chem. A* **2007**, *111*, 2511.

35. Raymo F.M., Giordani S. *Org. Lett.* **2001**, *3*, 1833.

36. Li X., Li J., Wang Y., Matsuura T., Meng J. *J. Photochem. Photobiol. A* **2004**, *161*, 201.

37. Bilski P., McDevitt T., Chignell C.F. *Photochem. and Photobiol.* **1999**, *69*, 671.

38. Tork A., Boudreault F., Roberge M., Ritcey A.M., Lessard R.A., Galstian T.V. *Appl. Optics* **2001**, *40*, 1180.

39. Yildiz I., Impellizzeri S., Deniz E., McCaughan B., Callan J.F., Raymo F.M. *J. Am. Chem. Soc.* **2011**, *133*, 871.

40. Huang CQ., Wang Y., Hong CY., Pan CY. *Macromol. Rapid Commun.* **2011**, *32*, 1174.

41. Bell N.S., Piech M. *Langmuir* **2006**, *22*, 1420.

42. Roy D., Cambre J.N., Sumerlin B.S. *Prog. Polym. Sci.* **2010**, *35*, 278.

43. Davis D.A., Hamilton A., Yang J., Cremar L.D., Van Gough D., Potisek S.L. *Nature* **2009**, *459*, 68.

44. Lee C.K., Davis D.A., White S.R., Moore J.S. *J. Am. Chem. Soc.* **2010**, *132*, 16107.

45. Ventura C., Byrne R., Audouin F., Heise A. *J. Polym. Sci. A: Polym Chem* **2011**, *49*, 3455.

46. Fries K., Samanta S., Orski S., Locklin J. *Chem. Commun.* **2008**, 6288.

47. Fries K.H., Driskell J.D., Samanta S., Locklin J. *Anal. Chem.* **2010**, *82*, 3306.

48. Samanta S., Locklin J. *Langmuir* **2008**, *24*, 9558.

49. Schumer JM., Fustin CA., Gohy JF. *Macromol. Rapid Commun.* **2010**, *31*, 1588.

50. Zhao Y. *J. Mater. Chem.* **2009**, *19*, 4887.

51. Lee H., Wu W., Oh J.K., Mueller L., Sherwood G., Peteanu L., Kowalewski T., Matyjaszewski K. *Angew. Chem. Int. Ed.* **2007**, *46*, 2453.

52. Coessens V.MC., Matyjaszewski K. *J. Chem. Educ.* **2010**, *87*, 916.

53. Jakubowski W., Tsarevsky N.V., McCarthy P., Matyjaszewski K. *Material Matters* **2010**, *5*.

54. Matyjaszewsky K., Tsarevsky N.V. *Nat. Chem.* **2009**, *1*, 276.

55. Matyjaszewski K., Xia J. *Chem. Rev.* **2001**, *101*, 2921.

56. Tsarevsky N.V., Braunecker W.A., Matyjaszewski K. *J. Organomet. Chem.* **2007**, *692*, 3212.

57. Coessens V., Pintauer T., Matyjaszewski K. *Prog. Polym. Sci.* **2001**, *26*, 337.

58. Kolb H.C., Finn M.G., Sharpless K.B. *Angew. Chem. Int. Ed.* **2001**, *40*, 2004.

59. Golas P.L., Matyjaszewski K. *QSAR Comb. Sci.* **2007**, *26*, 1116.

60. Hawker C.J., Wooley K.L. *Science* **2005**, *309*, 1200.

61. Binder W.H., Sachsenhofer R. *Macromol. Rapid Commun.* **2007**, *28*, 15.

62. Himo F., Lovell T., Hilgraf R., Rostovtsev V.V. *J. Am. Chem. Soc.* **2005**, *127*, 210.

63. Bock V.D., Hiemstra H., van Maarseveen J.H. *Eur. J. Org. Chem.* **2006**, 51.

64. Wu P., Feldman A.K., Nugent A.K., Hawker C.J., Scheel A., Voit B., Pyun J., Fréchet J.MJ., Sharpless K.B., Fokin V.V. *Angew. Chem. Int. Ed.* **2004**, *43*, 3928.

65. Binder W.H., Sachsenhofer R. *Macromol. Rapid Commun.* **2008**, *29*, 952.

66. Meldal M. *Macromol. Rapid Commun.* **2008**, *29*, 1016.

67. Bertoldo M., Nazzia S., Zampanob G., Ciardelli F. *Carbohydr. Polym.* **2011**, *85*, 401.

68. Tsarevsky N.V., Sumerlin B.S., Matyjaszewski K. *Macromolecules* **2005**, *38*, 3558.

Chapter 2

Aim of work

The general aim of this work is the synthesis of light-responsive spiropyran-based polymers and the investigation of their properties. In order to obtain valuable information on the structure-property relationships, the synthesis of well-defined polymers with BSP in particular position is proposed. Synthetically this will be achieved by the combination of controlled polymerization techniques like ATRP using BSP initiators as well as polymer post modification by 'click chemistry'. Ultimately the goal is the synthesis of novel light-responsive polymers and an understanding of the synthetic scope beyond the current state of the art.

Chapter 3

ATRP with BSP initiators

This work was published in *Journal of Polymer Science Part A: Polymer Chemistry* **2011**, *49*, 3455 and in parts in *Biosensors and Bioelectronics* **2010**, *26*, 1392.

3.1 Introduction

Stimuli responsive polymers have been investigated intensively as important elements for the development of smart materials and devices. The ability of these materials to respond with a property transformation triggered by an environmental change can be utilized specifically in biomedical applications such as targeted drug delivery and sensing. A variety of external triggers have been investigated in responsive polymers in the past including temperature, pH, biomolecule interaction, ultrasound, among others and were highlighted in extensive reviews recently.[1,2] We are specifically interested in photoresponsive polymers to modulate sensing interfaces and sensor response. Light is an attractive stimuli in sensor applications, because it can be localized, and if the response is reversible, it can be conveniently switched on and off. Photoresponsive polymers have been reported in the literature using various chromophores.[3-6] Our interest is in polymers functionalized with BSP, a well-known photochromic molecule that undergoes a heterocyclic ring cleavage at the C–O spiro bond to form a planar and highly conjugated chromophore (**Scheme 1.2**).[7-9] The BMC isomer absorbs strongly in the visible region and binds divalent metal ions,[10] H^+,[11] amino acids,[12] and DNA[13,14] resulting in a shift of the absorbance spectrum, associated with a color change. Illumination with green or white light decouples the guest from the BMC, which reverts to the BSP. Of particular interest is to determine the minimum number of BSP units required in a polymer to trigger a measurable response. This also relates to the question of positioning of the BSP units in the polymer. In the literature, several elegant examples were presented showing that with the help of controlled polymerization techniques the defined positioning of BSP units in the polymer can result in interesting effects. For example, BSP-methacrylate was copolymerized with MMA by ATRP from silica surfaces by Locklin to create light sensitive polymer brushes (**Figure 1.3**).[15,16] The hydrophilicity of the brushes could reversible be switched by irradiation with light as was shown by the change of water contact angles. Similar results were reported for the surface initiated ring opening metathesis polymerization of norbonene-based BSP.[17] Another area of interest is light responsive random and block copolymer.[4,18] Matyjaszewski reported the synthesis of a BSP containing block copolymer by ATRP macroinitiation from

poly(ethylene oxide).[19] The micelles formed by this amphiphilic block copolymer were disrupted by irradiation with UV light, which converted the BSP into its BMC form rendering the amphiphilicity of the block copolymer. The process was fully reversible and could be used to encapsulate and release a payload (**Figure 1.4**). Block copolymers comprising a BSP functionalized block were synthesized using reversible addition fragmentation chain transfer (RAFT) by Moller.[20] Recently, Vamvakaki reported the synthesis of multireponsive (pH and light) polymers by ATRP copolymerization of 2-(dimethylamino)ethyl methacrylate with BSP-methacrylate in different ratios and molecular weights.[21] All these materials have in common that they use polymers with multiple BSP units. Polymers with a single photochromic group were investigated by Evans and Davis for applications in polymer matrixes (optical lenses).[22,23] For example, spirooxazine and naphthopyran (**Figure 3.1**) end-functionalized polymers were synthesized by ATRP and RAFT polymerization from respective functional initiators.[24-28] The photochromic behavior of the polymers was investigated in the solid state (rigid polymer matrix), and a dependence on the polymer nature and molecular weight was found. In a very recent paper, the same authors presented an investigation on the effect of the polymer architecture and position of the single photochromic group with respect to the switching behavior in a polymer matrix.[29]

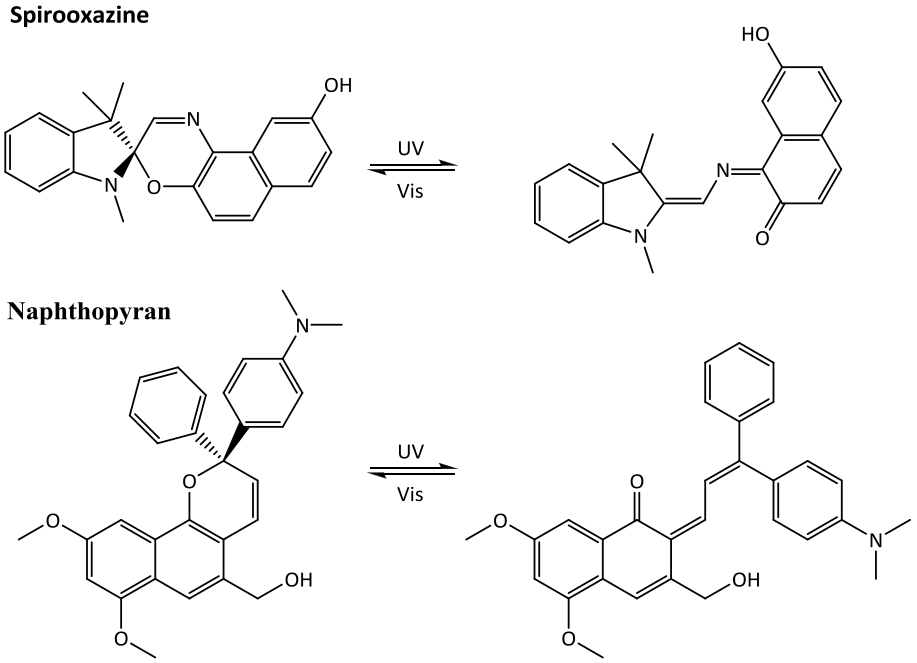

Figure 3.1 Transition between colorless to colored forms in a spirooxazine and naphthopyran photochromic dye, showing redistribution of double bonds and intramolecular rotation.

In this work, we report the synthesis of poly(methyl methacrylate) (PMMA) with a single BSP terminal unit and the investigation of their light responsive solution properties. Two BSP derivatives bearing an OH group have been selected for these studies (**Scheme 3.1**). These compounds, exploiting the OH function, can be converted in α-bromo esters to obtain BSP initiators suitable for ATRP. From the synthetic point of view the OH group in the two derivatives has a different nature: BSP-OH-1 is an alcohol while BSP-OH-2 is a phenol. These two BSP compounds differ also in their photochromic properties: the 6-nitro substitued molecule (BSP-OH-1; **Scheme 3.1**) shows an higher ring opening efficiency, a more rapid switching, a better ability of its merocyanine to bind metal ion and a dramatic colour change induced by UV irradiation. Indeed the nitro electron withdrawing group on the BSP ring has the ability to conjugate with the extended π system generated in the BMC form, resulting in a strong coloration.[10,30,31]

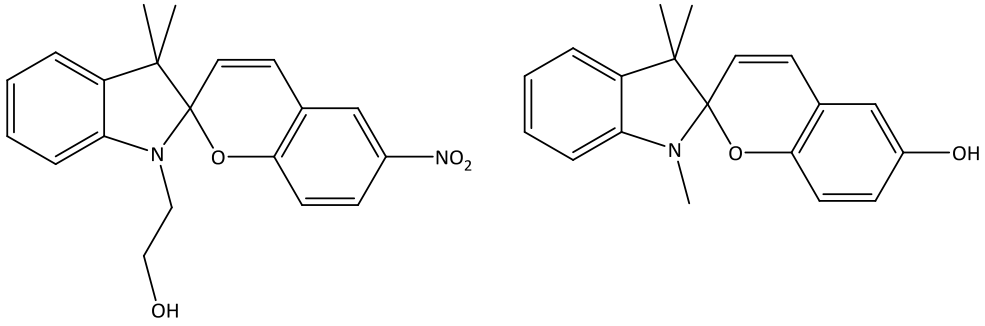

BSP-OH-1 BSP-OH-2

Scheme 3.1 Structures of the two BSP derivatives bearing an OH group selected for our studies.

The aims of our investigation were: (1) studing the reactivity of these BSP compounds in the esterification reaction to form the ATRP initiator, (2) examining the reactivity of the so-generated BSP α-bromo esters in the polymerization process and (3) investigating the photochromic properties of the BSP based polymers obtained.

3.2 Results and Discussion on BSP-OH-2

ATRP was chosen for the synthesis of BSP functional PMMA because of the high end-group fidelity of this technique. A BSP functional ATRP initiator (BSP-Br-2) was synthesized by the reaction of 2-bromoisobutyryl bromide with an OH functional BSP (BSP-OH-2; **Scheme 3.2**) as a dark brown solid with a melting point of 77-80 °C, without further purification.

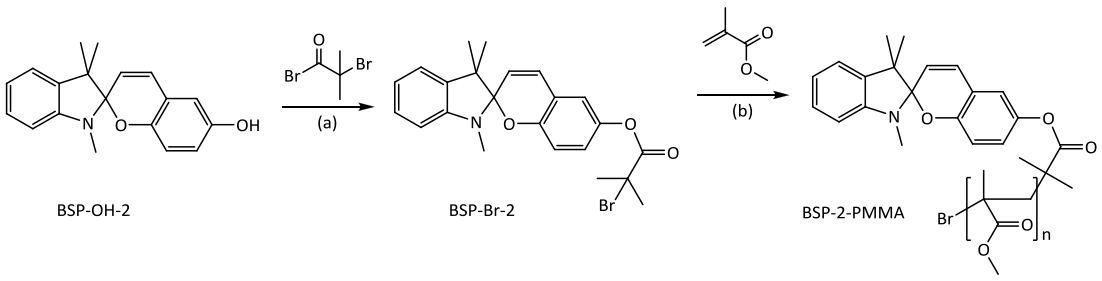

Scheme 3.2 Synthesis of BSP ATRP initiator (BSP-Br-2) and BSP functionalized poly(methyl methacrylate (BSP-2-PMMA). Reaction conditions: (a) Et_3N (1 equiv), N_2, DCM, 0 °C, 18 h and (b) $CuCl/CuCl_2$ (0.8/0.2 equiv), HMTETA (2 equiv), THF, 60 °C, 3h.

The structure of the initiator was confirmed by ^{13}C and ^{1}H NMR. Characteristic peaks can be assigned to the aromatic part of the BSP unit ranging from 6.53 to 7.20 ppm, the singlet of the methyl group adjacent to the nitrogen at 2.72 ppm and singlets of the methyl groups of the ATRP initiator at 2.05 ppm. The polymerizations were carried out using the BSP-Br-2 initiator and MMA monomer at 60 °C in THF in the presence of the heterogeneous ATRP catalytic system Cu(I)Cl/Cu(II)Cl/HMTETA (**Scheme 3.2**). The reaction was allowed to proceed for 40 min. or 4 h, respectively, depending on the desired polymer molecular weight. The polymers obtained were characterized by gel permeation chromatography (GPC), the resulting number-average molecular weights (M_n) of BSP-2-PMMA1 and BSP-2-PMMA2 were 9,800 and 28,000 g/mol, respectively, with polydispersities indices (PDI) of 1.3 and 1.2 (**Figure 3.2**). Size exclusion chromatograms (SEC) graphs in **Figure 3.2** shows a bimodal distribution for both polymers. The reason for this is unknown and the reaction were not further optimized.

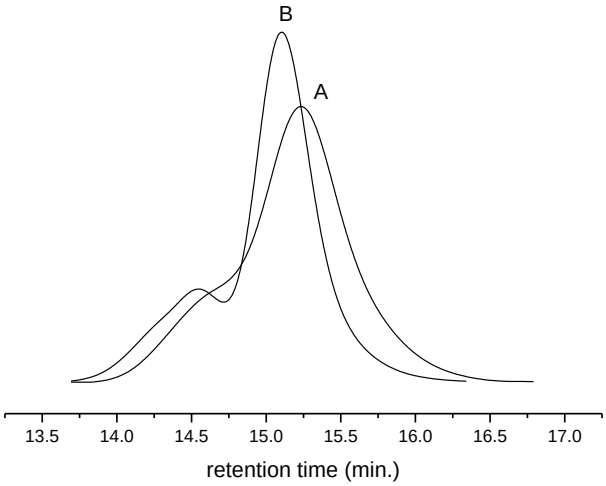

Figure 3.2 Size exclusion chromatograms of (A) BSP-2-PMMA1 (9800 g/mol, PDI: 1.3) and (B) BSP-2-PMMA2 (28,000 g/mol, PDI: 1.2).

3.2.1 Cation Complexation

As mentioned previously, the ability to manipulate the physical and chemical properties of a material using an external stimulus forms the basis for several attractive applications. Metal complexation is one of the exploitable stimuli. The MC isomer of BSP has a phenolate site to which transitions metal cations can bind, such as Cu^{2+} and Co^{2+}, and this reversible process can be controlled optically. Fries et al.[16] recently published a chemo-responsive co-polymer of PMMA and BSP methyl methacrylate. They demonstrated that different metal ions gives rise to unique colorimetric responses that are dependent on the amount of BSP co-monomer contained in the polymer backbone. The chemo-responsive behavior of BSP-2-PMMA-1 and -2 upon the addition of certain guest ions (Cu^{2+}) was studied to investigate the influence of the polymer chain on the single BSP terminal unit. As shown in **Figure 3.3**, the binding of a transition metal ion such as Cu^{2+}, requires two units of the BMC isomer to form the most thermodynamically stable BMC_2–metal ion complex.[30,32] In BSP-2-PMMA-1 and -2 each polymer chain contains only one unit of BSP, and consequently, if the metal ion complex is to form, two polymer chains must come together to chelate the metal ion (**Figure 3.3**).

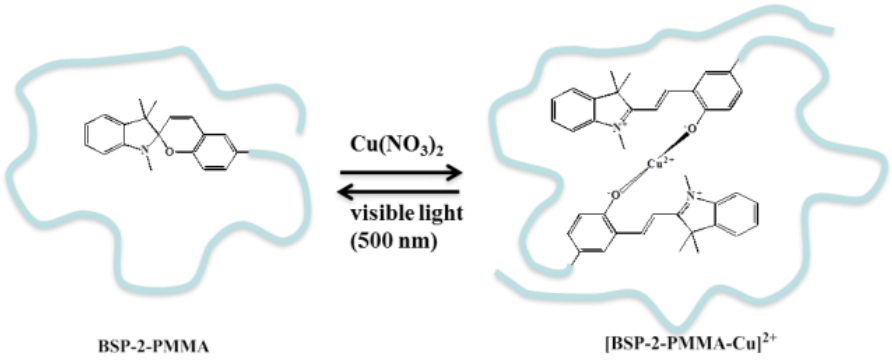

Figure 3.3 Cartoon representation of the BSP-2-PMMA and Cu^{2+} complex formation and its reversibility with visible light.

Figure 3.4 shows the kinetic monitoring of the BSP-2-PMMA-1 and Cu^{2+} complex formation in acetonitrile. Upon addition of the Cu^{2+} ions, the emergence of a new absorption band at 510 nm was observed. After 80 s another distinct absorption band located at 434 nm emerged.

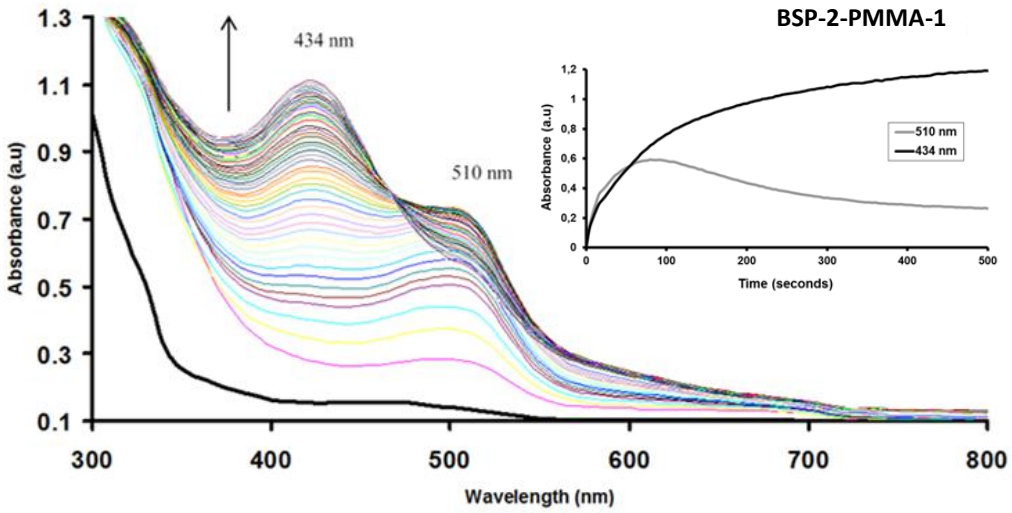

Figure 3.4 UV-vis spectra of 1×10^{-4} M BSP-2-PMMA-1 after the addition of 1×10^{-4} M $Cu(NO_3)_2$. (Inset) Absorbance change at 510 nm and 434 nm versus time. Measurements taken every 25 s in acetonitrile at 25 °C.

As time progresses to 500 s, the absorption band intensity at 510 nm steadily decreases, whereas the band at 434 nm steadily rises to become the only absorption band in the visible region. This process contains an isobestic point at 480 nm. From the literature it is known that the absorption band at 434 nm corresponds to the BMC_2–Cu^{2+} complex.[16,31] The absorption band at 510 nm has not

encountered before in similar Cu^{2+} experiments with the single BSP molecule in acetonitrile, but rather it appears in the same region of the spectrum as the ring-opened MC isomer. Zhou describes the metal chelation mechanism formation and disassociation as follows: BSP + BMC + $Cu^{2+} \rightarrow BMC_2–Cu^{2+}$.[33] The BMC isomer complexes readily with the Cu^{2+} ions as it is formed thermally from BSP and this formation process is the rate-determining step in the reaction sequence with the Cu^{2+} ion concentration having little effect on the reaction rate. This proposed mechanism would appear to hold true in this instance as shown in **Figure 3.4**, if the absorption species at 510 nm is responsible for the BMC isomer then it behaves as the rate-determining step. The concentration of the species at 510 nm builds up to a maximum point at 80 s, thereafter decreasing as the $BMC_2–Cu^{2+}$ species (434 nm) starts to increase more rapidly. As the BSP-2-PMMA-1 polymer has a molecular weight of 9,800 g/mol, it was decided to synthesize a larger polymer containing BSP for comparison. BSP-2-PMMA-2 (28,000 g/mol) due to its larger polymer chain should have a slower rate of complex formation due to the increased methacrylate chain density. **Figure 3.5** shows the kinetic monitoring of the BSP-2-PMMA-2 and Cu^{2+} complex formation. Upon addition of the Cu^{2+} ions, the emergence of a new absorption band at 500 nm was seen, and after 122 s, another distinct absorption band located at 410 nm was observed.

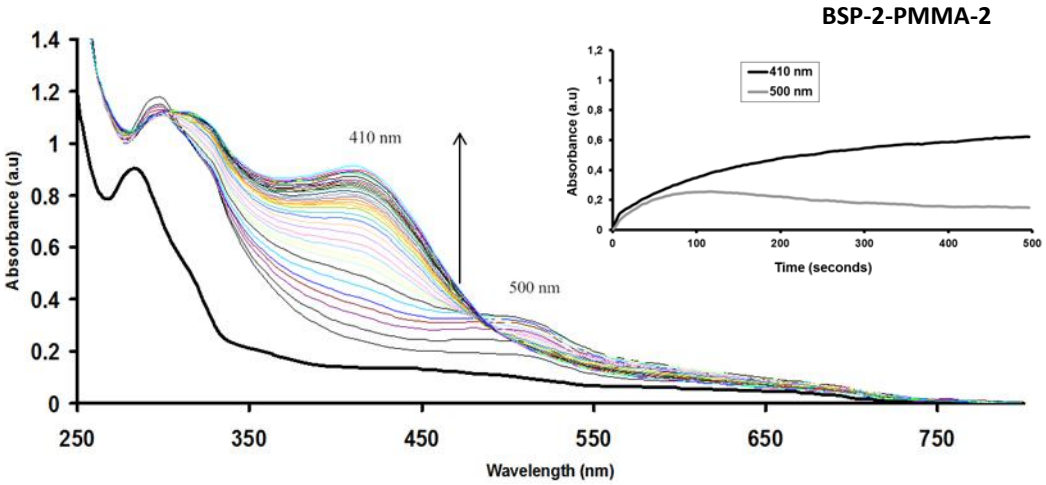

Figure 3.5 UV-vis spectra of 1×10^{-4} M BSP-2-PMMA-2 after the addition of 1×10^{-4} M $Cu(NO_3)_2$. (Inset) Absorbance change at 500 nm and 410 nm versus time. Measurements taken every 25 s in acetonitrile at 25 °C.

This occurs at a significantly longer time (approximately 40%) compared to the BSP-2-PMMA-1 and Cu^{2+} complex formation. As time progresses to 500 s, the absorption band intensity at 510 nm steadily decreases, whereas the band at 434 nm steadily rises to become the only absorption band in the visible region. The spectra also have a clear isobestic point at 480 nm. This process is completely photo-reversible, i. e. when $[BMC\text{-}2\text{-}PMMA\text{-}2]_2$–$Cu^{2+}$ is irradiated with white light, the BMC photo-isomerizes back to the closed BSP isomer, ejecting the Cu^{2+} ion (**Figure 3.6**).

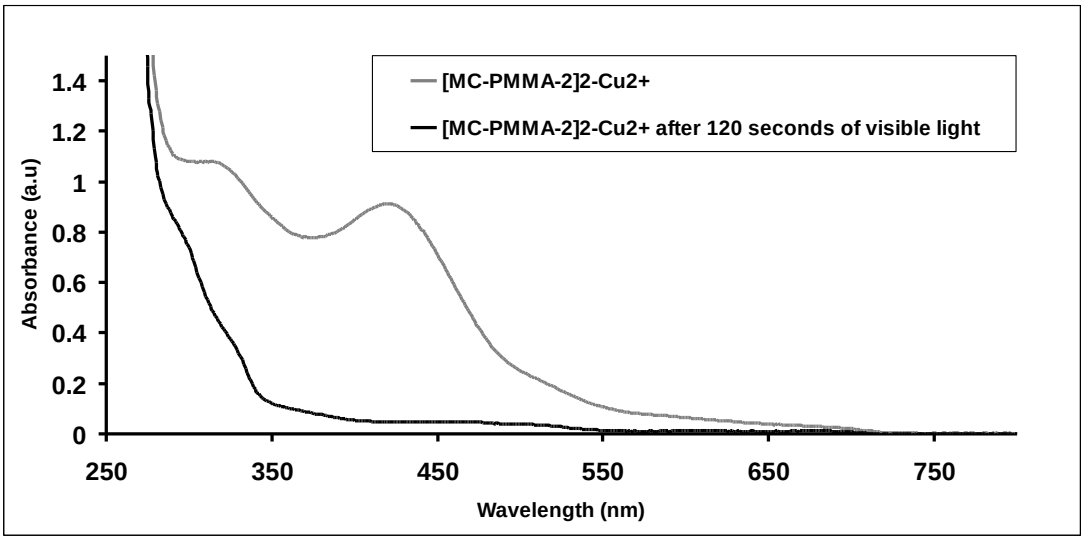

Figure 3.6 Photo-disassociation of $[BMC\text{-}2\text{-}PMMA\text{-}2]_2$-$Cu^{2+}$ complex using visible light.

The ability to control the properties of a surface has become a goal of many biomimetic researchers, especially the wettability of a solid surface, due to its importance in many aspects of nature. The modification of surfaces with photochromic molecules to produces surfaces with switchable wettability holds much promise and there are some very interesting examples using SP in the literature.[34,35] Polymeric films of BSP-2-PMMA- 2 were prepared by dip coating glass slides into an acetonitrile solution of the polymer. When BSP-2-PMMA- 2 and $Cu(NO_3)_2$ are mixed together the formation of the corresponding complex was observed. Due to the size of the polymer chain connected to the BSP fragment, significant rearrangement of the polymer chains must happen, affecting the physical and chemical properties of the system as the BSP fragments coordinate the Cu^{2+}. The wettability of the BSP-2-PMMA-2 and $[BSP\text{-}2\text{-}PMMA\text{-}2]_2$–$Cu^{2+}$ has been investigated using the contact angle measurement of a droplet of water. A

significant difference in contact angle was observed between the BSP-2-PMMA-2 (77.3°) and $[BSP\text{-}PMMA\text{-}2]_2$–$Cu^{2+}$ (32.12°) (**Figure 3.7**).

The Cu^{2+} coordination induces a 45.2° change on BSP-2-PMMA-2, whereas the PMMA polymer with no BSP moiety, we only observe a 4.0° change upon addition of Cu^{2+}. It is believed that the Cu^{2+} ions are retained in the BSP-2-PMMA-2 polymer film due to coordination whereas in the PMMA film, the Cu^{2+} ions are removed when washing with deionised water. This change in surface wettability utilizing the chelating properties of BSP is an improvement of over 10° on the recent work reported.[17] This considerable response has been achieved with a very simple polymeric system bearing only one BSP unit.

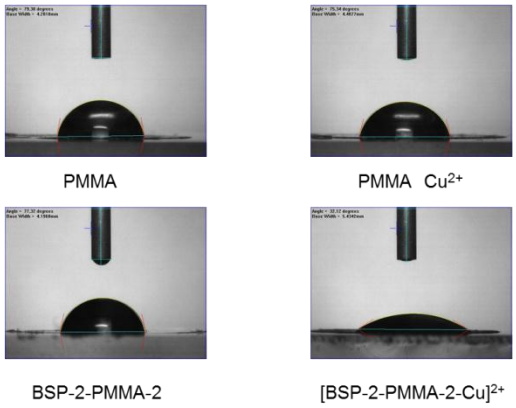

Figure 3.7 Contact angle measurement of water on PMMA and BSP-2-PMMA films and the effect Cu^{2+} ions have on the polymeric films. Measurements taken at 20 °C.

3.3 Results and Discussion on BSP-OH-1

In order to investigate photochromic properties of BSP based polymers in solution our attention was focused on the 6-nitro BSP derivative, because of its better photochromic response. BSP-OH-1 is more promising from the photochromic point of view than BSP-OH-2 (**Scheme 3.1**). Following the same synthetic strategy as for the previous work (**Scheme 3.3**) and using BSP-OH-1, PMMA containing a single BSP unit located at the end of the polymer chain have been obtained.

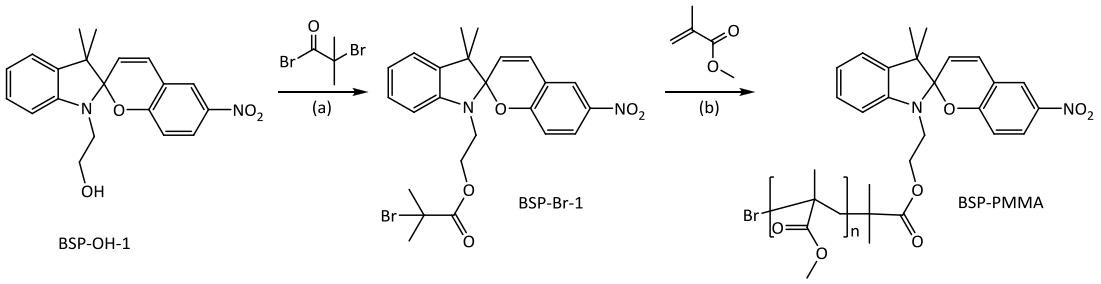

Scheme 3.3 Synthesis of BSP ATRP initiator (BSP-Br-1) and BSP functionalized poly(methyl methacrylate) (BSP-PMMA). Reaction conditions: (a) Et_3N (1 equiv), N_2, DCM, 0 °C, 18 h and (b) $CuCl/CuCl_2$ (0.8/0.2 equiv), HMTETA (2 equiv), THF, 60 °C, 3h.

A BSP functional ATRP initiator (BSP-Br-1) was first synthesized by the reaction of 2-bromoisobutyryl bromide with an OH functional BSP (BSP-OH-1; Scheme 2.3). The initiator was obtained in 55% yield as a pale yellow solid with a melting point of 124 °C. The structure of the initiator was confirmed by Fourier transform infrared spectroscopy (FT-IR), ^{13}C and ^{1}H NMR, as shown in **Figure 3.8**. Characteristic peaks can be assigned to the methyl groups of the ATRP initiator at 1.90 ppm (f), the multiplets of the methylene groups adjacent to the nitrogen and oxygen atom centered at 3.5 (d), and 4.3 ppm (e), respectively. The latter experienced a shift from 3.77 ppm upon esterification with 2-bromo-2-methylpropionyl bromide. Moreover, the series of peaks ranging from 5.99 to 8.03 ppm (a, g, h, and j) can be assigned to the BSP unit.

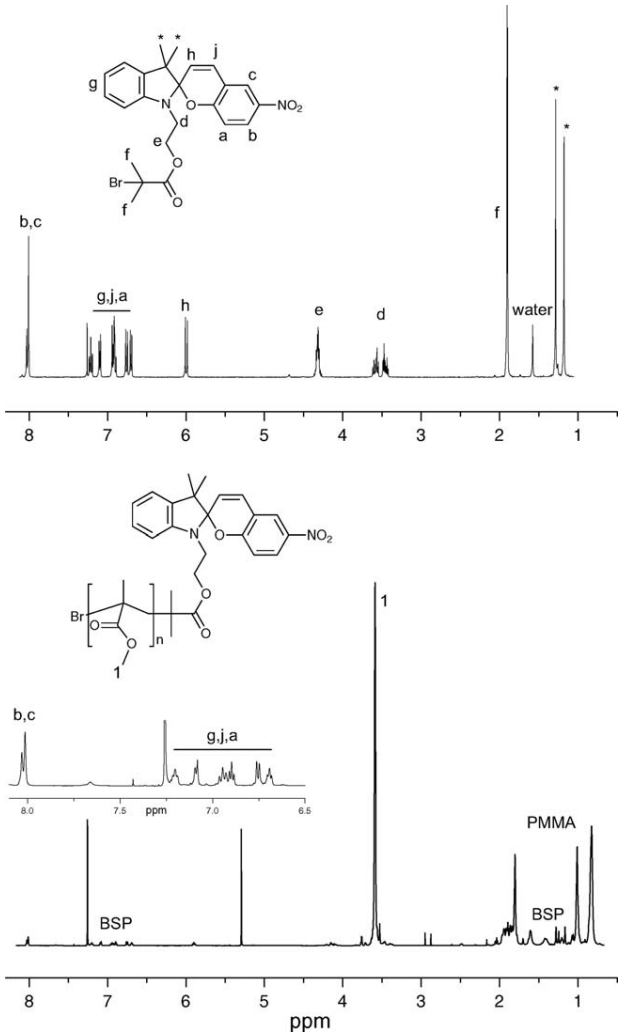

Figure 3.8 ^{1}H NMR spectra of BSP functionalized ATRP initiator (BSP-Br-1; top spectrum) and BSP-PMMA (Mn, 3600 g/mol) obtained from the initiator by ATRP (bottom spectrum).

The polymerizations were carried out using the BSP-Br-1 initiator and MMA monomer at two different ratios at 60 °C in THF in the presence of the heterogeneous ATRP catalytic system Cu(I)Cl/Cu(II)Cl/HMTETA (Scheme 4). Both polymerizations were stopped after 3 h and not further optimized. The resulting M_n of BSP-PMMA1 and BSP-PMMA2 were 3,600 and 23,800 g/mol, respectively, with PDI of 1.3 and 1.1 (**Figure 3.9**).

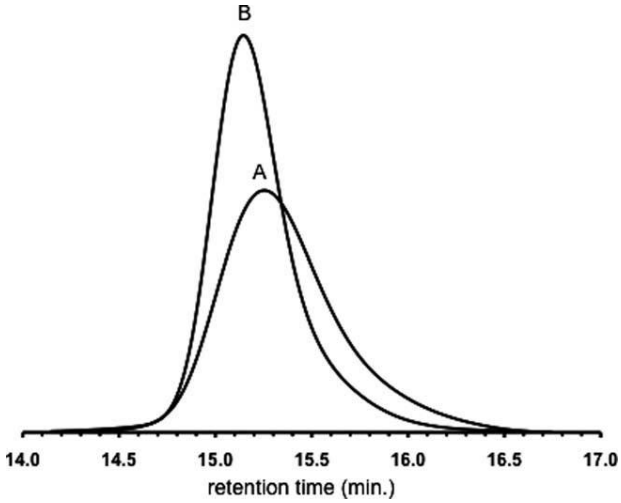

Figure 3.9 SEC of (A) BSP-PMMA1 (3600 g/mol, PDI: 1.3) and (B) BSP-PMMA2 (23,800 g/mol, PDI: 1.1).

Confirmation for the presence of the BSP end-group was obtained from ^{1}H NMR spectroscopy, where signals of the BSP (a–c, g, h, and j) and PMMA can clearly be observed in the spectrum of the polymer with lower molecular weight, BSP-PMMA1 (**Figure 3.8**). Matrix-assisted laser desorption/ionitiation time of flight-mass spectroscopy (MALDI-ToF) analysis of the same polymer reveals several peak series' with a peak distance corresponding to the MMA repeating unit (**Figure 3.10**).

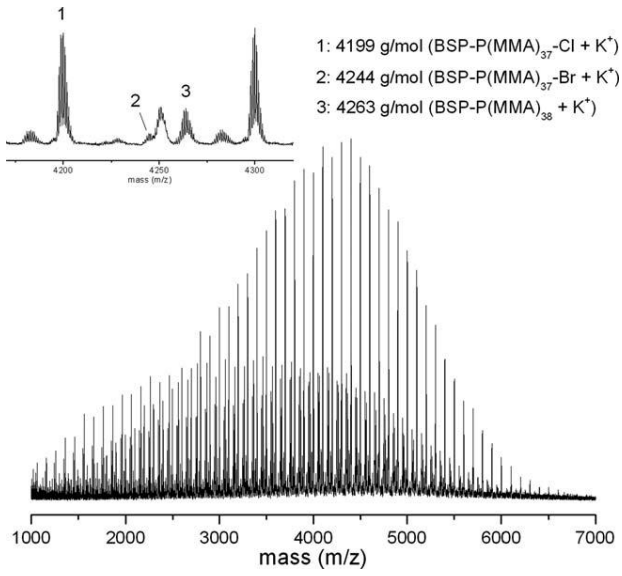

Figure 3.10 MALDI-ToF spectrum of BSP-PMMA1 with peak assignment. Nonassigned peaks are caused by fragmentation of the BSP end-group during laser desorption.

The most prominent peak series could be assigned to the polymer structure with BSP and a Cl end-groups because of the halogen exchange with CuCl in the ATRP in

addition to a minor series with BSP and Br end-groups. Moreover, several peaks caused by end-group fragmentation are present in the spectrum, the most straightforward one being caused by halogen abstraction. Fragmentation of the BSP group under the laser desorption process produces several complex small peaks, which cannot be assigned to the exact end-group structures. Both NMR and MALDI-ToF results confirm the near quantitative presence of the BSP end-group on the synthesized polymers.

3.3.1 Photophysical Characterization

Spiropyran has the ability to switch from an uncharged, colorless form, to a zwitterionic, planar, and highly colored merocyanine form upon illumination with UV light (**Scheme 1.2**).[9] The photoisomerism and subsequent physical behavior of BSP-Br-1, BSP-PMMA1, and BSP-PMMA2 upon exposure to UV light was characterized to investigate the influence of the polymer chain on the single BSP terminal unit. The photoisomerization of SPs to merocyanines is typically characterized by the appearance of a strong, long-wavelength absorption band, resulting from an increase in conjugation between the two heterocycles in the BMC isomer.[36] The BMC isomer thermally reverts back to the BSP isomer following first-order kinetics. The BSP-BMC isomerization also exhibits properties similar to a molecular probe, as it reveals a significant amount of information about its surrounding molecular environment:[37-39] (i) at equilibrium, an estimate of local polarity can be obtained from the value K_e, the population of nonpolar BSP versus the highly polar BMC, (ii) the BMC isomer exhibits a large negative solvatochromic shift with increasing polarity, (iii) the BMC isomer possesses a large polarizable π-electron system, suitable for observing dispersion interactions, (iv) the phenolate oxygen on the BMC possesses a highly basic, electron pair donor, suitable for interaction with hydrogen bond donors, and Lewis acids (e.g. the coordination with the cations like Co^{2+} and H^{+}), and also (v) the thermal reversion of BMC to BSP is dependent on all of the above. For example, the interactions with certain zwitterionic amino acids at the complementary binding sites on the BMC inhibit the thermal back reaction.[13, 40]

The absorption spectra of BSP-Br-1, BSP-PMMA1 and BSP-PMMA2 were measured in acetonitrile as one of the most common solvents to study the photophysical properties of BSP before and after UV irradiation [*Note*: all polymer concentrations for the photophysical measurements were calculated based on the polymer M_n from SEC (PMMA standards)]. Photochromism was observed for BSP initiator and polymers, upon irradiation of UV light, a strong long-wavelength absorption band was observed at 568 nm for all BSP derivatives, this being associated with a change from a colorless (BSP) to a purple solution (BMC; **Figure 3.11**).

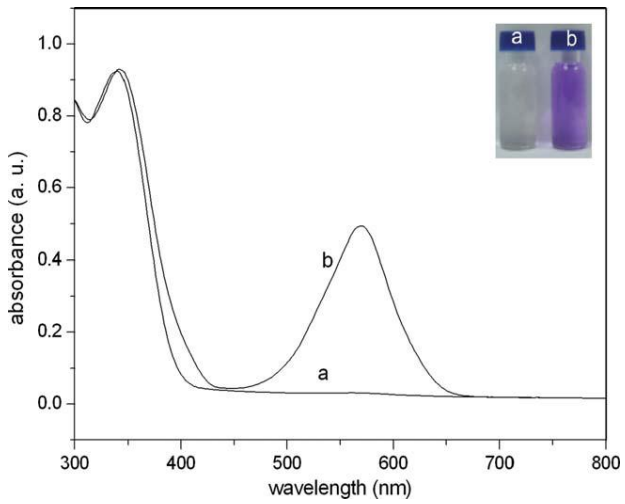

Figure 3.11 UV–vis spectra of BSP-PMMA1 (1×10^{-4} M in acetonitrile) before (a) and after (b) 60 s of UV (365 nm) irradiation.

The measured absorption maximum represents a significantly red-shift compared with the individual BMC molecule in acetonitrile, which typically shows a maximum at 555 nm,[38] this can be explained by electronic effects because of the modification of the indoline section of BMC. Also, both polymers reveal solid-state photochromism with a long-wavelength absorption band at 597 nm. This suggests that in the absence of acetonitrile, the BMC end-group is located in the nonpolar environment of the random coil of the PMMA, in a state of low solvation.

The ring-closure of the BMC to the BSP form is thermally induced upon removal of the UV light source or by irradiation with visible light. Kinetic studies were performed to monitor how the length of the polymer chain affects the ring closing kinetic of the BMC, which is known to follow first-order kinetic.[41] This is involved in inducing the formation of the BMC-PMMA by exposure to the UV light for 1 min and

recording the absorbance value of the BMC-PMMA at the λ_{max} upon removal of the UV light source. Samples were placed in a thermostatically controlled UV–vis spectrometer, were irradiated *in situ* using a Light-emitting diode (LED) array and kept in the dark during the measurement to avoid the influence of the ambient light on the reconversion to BSP-PMMA isomer.[42] **Figure 3.12** shows the reduction of the absorbance at the λ_{max} for the transition from BMC-PMMA1 to BSP-PMMA1 at different temperatures.

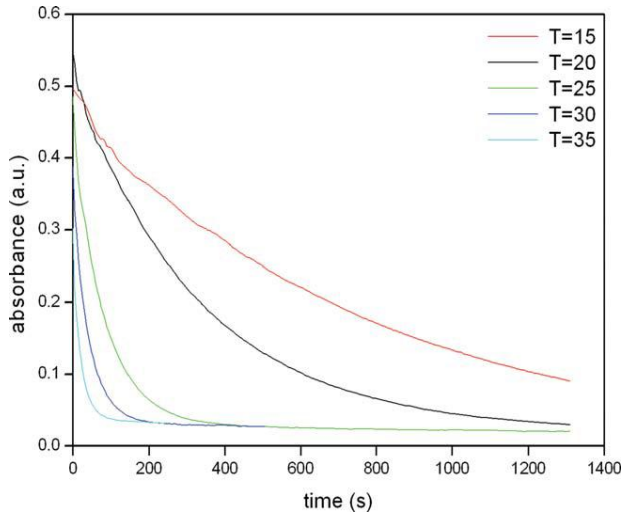

Figure 3.12 Absorbance decrease at the λ_{max} (568 nm) in acetonitrile as a function of time for the transition of BMC-PMMA1 to BSP-PMMA1 after removing the UV light source at different temperatures.

From these measurements, the first-order rate constants *k* for the transition BMC-PMMA to BSP-PMMA were determined by plotting $\ln(A_t/A_0)$ versus time. A linear correlation between BMC-PMMA (λ_{max}) and its thermal relaxation rate constant (*k*) was found for both polymers (**Table 1**).

Table 1 Values of the relaxation rate constants *k* of BSP-Br, BSP-PMMA1 (3600 g/mol, PDI: 1.3), and BSP-PMMA2 (23,800 g/mol, PDI: 1.1) in acetonitrile at various temperatures (λ_{max} 568 nm), standard deviation in parentheses.

	15°C	**20°C**	**25°C**	**30°C**	**35°C**
BSP-Br-1 *k* (s^{-1})	2.76×10^{-3} (5.07×10^{-5})	5.73×10^{-3} (5.77×10^{-5})	1.06×10^{-2} (1.15×10^{-4})	1.79×10^{-2} (1.47×10^{-3})	2.33×10^{-2} (6.5×10^{-3})
BSP-PMMA1 *k* (s^{-1})	2.67×10^{-3} (5.77×10^{-5})	6.2×10^{-3} (1×10^{-4})	9.73×10^{-3} (5.77×10^{-5})	1.94×10^{-2} (3.06×10^{-4})	3.26×10^{-2} (7×10^{-4})
BSP-PMMA2 *k* (s^{-1})	3.03×10^{-3} (5.7×10^{-5})	6.3×10^{-3} (8.23×10^{-6})	1.3×10^{-2} (3.46×10^{-4})	2.61×10^{-2} (5.77×10^{-5})	5.21×10^{-2} (1.34×10^{-3})

At low temperatures, the rate constants have nearly the same values for both polymers, and both increase with temperature as expected. However, with increasing temperature, the values for the two polymers become strongly different showing a larger increase in the rates of relaxation, as the molecular weight of the polymer increases. This means that at high temperature, ring-closure from the BMC to the BSP end-group occurs significantly faster for the longer polymer. The relaxation rate of BMC can be influenced by several factors. As the BMC to BSP transition requires an ~90° rotation of half of the molecule, the mobility of the surrounding molecules affects the relaxation.[23] This was shown to be highly relevant in polymer matrixes but might not play a major role in solution.[27] Two other factors are more electronic in nature and relate to the electronic environment of the BMC molecule, for example, by substituents and the polarity of the environment, for example, by the choice of solvent.[6,37] As the substitution of the BMC in these samples is identical for both polymers, the observed difference in the ring-closure kinetic must be due to the polarity of the medium surrounding the BMC end-group, which is determined by the solvent and the polymer chain. The thermal relaxation of BMC-Br-1 was also studied for reference; it is quite clear that without the PMMA chain extension, the thermal relaxation process is significantly slower at higher temperatures. The thermal relaxation for BMC-Br-1 at 35 °C is 42.9 s, whereas BMC-PMMA2 is 19.19 s. To analyze the thermodynamic contributions, the dependence of the rate of thermal relaxation with temperature was examined. Processing the sets

of kinetic data collected at various temperatures using the Arrhenius equation (eq 1) the activation energy (*E*a) for both polymers was determined by plotting ln *k* against 1/*T* (**Figure 3.13**).

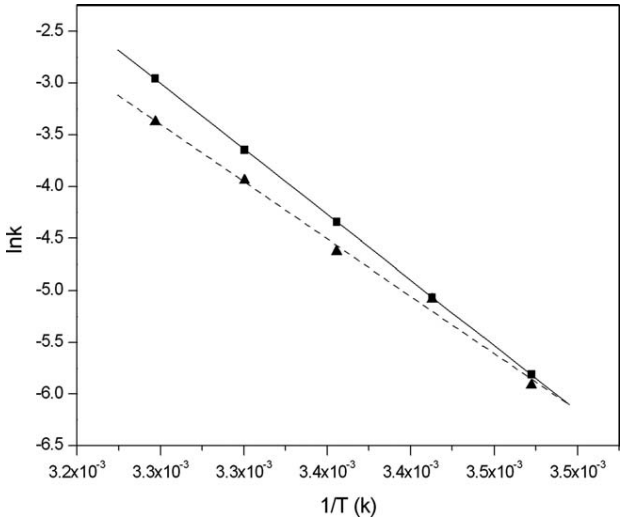

Figure 3.13 Arrhenius plots of thermal relaxation of BMC-PMMA1 (▲; correlation coefficient 0.995) and BMC-PMMA2 (■; correlation coefficient > 0.999) in acetonitrile.

The values of activation energy and the pre-exponential factor derived by the linear Arrhenius dependences are gathered in **Table 2**.

Table 2 Physicochemical properties of BSP-Br-1, BSP-PMMA1 (3600 g/mol, PDI: 1.3), and BSP-PMMA2 (23,800 g/mol, PDI: 1.1) at 10^{-4} M in acetonitrile.

	E_a (kJ mol^{-1})	A (s^{-1})	$\Delta H^{\pm}$ (kJ mol^{-1})	$\Delta S^{\pm}$ (J K^{-1} mol^{-1})	$\Delta G^{\pm}_{25}$ (kJ mol^{-1})
BMC-Br-1	78.52	5.73×10^{11}	76.04	-28.65	84.58
BMC-PMMA1	91.78	1.2×10^{14}	89.31	16.80	84.30
BMC-PMMA2	105.13	3.49×10^{16}	102.66	63.47	83.74

Using Eyring's transition state theory (eq 2), it is possible to derive activation thermodynamic parameters for the thermal relaxation of BMC-PMMA1 and BMC-PMMA2 such as enthalpy of activation values ($\Delta H^{\pm}$) by plotting ln(k/T) against 1/T. These values were used to extract entropy of activation values ($\Delta S^{\pm}$) and the Gibbs energy of activation ($\Delta G^{\pm}$) using the Gibbs fundamental equation for constant temperature (eq 3). All data are collected in **Table 2**.

$$\ln k = E_a/RT + \ln A \quad (1)$$

$$\ln(k/T) = -\Delta H^{\pm}/RT + \ln(k_B/h) + \Delta S^{\pm}/R \quad (2)$$

$$\Delta G^{\pm} = \Delta H^{\pm} - T \cdot \Delta S^{\pm} \quad (3)$$

where R = gas constant, h = Planck constant, and k_B = Boltzmann constant.

The entropy of activation $\Delta S^{\pm}$ is a measure of the amount of reorientation of the system during the thermal relaxation from BMC-PMMA to BSP-PMMA and is related to degrees of freedom lost or gained from the aforementioned system. The positive $\Delta S^{\pm}$ values for both polymers indicate that when the BMC end-group reverts to the BSP form, it gains degrees of freedom, for example, by solvation.[43] The higher $\Delta S^{\pm}$ value of 63.47 J K^{-1}/mol for the higher molecular weight polymer indicates a more significant gain for this polymer (**Figure 3.14**).

Figure 3.14 Cartoon representation of the BSP-PMMA and BMC-PMMA behavior in acetonitrile.

We hypothesize that the observed higher ring-closure kinetic and higher entropy of activation $\Delta S^{\pm}$ for this process is a direct consequence of the hydrophobic/hydrophilic balance of the environment surrounding the BSP or BMC end-group, which is strongly affected by the polymer molecular weight. Assuming that the shape and hydrodynamic volume of the random coil of the PMMA in solution is not affected by the state of the end-group (BSP or BMC), and it is reasonable to assume that the end-group is mostly located in the nonpolar environment of the PMMA coil. When the BSP end-group is switched to the polar BMC form, the nonpolar PMMA environment is energetically unfavorable, and this can only be circumvented by either diffusion of the BMC end-group into the more polar solvent environment or by reverting back to the BSP form. For the lower

molecular weight PMMA with its smaller hydrodynamic volume, the diffusion path length is much shorter, and with increasing temperature, it becomes more likely for the end-group to diffuse into the solvent.

Another contributing factor might be that the solubility of the low molecular weight PMMA increases faster with increasing temperature allowing a better solvation of the random coil and more solvent molecules to stabilize the BMC. Analyzing the thermodynamic contributions of BMC-Br further reinforces this hypothesis, as we can see that the entropy value is negative for the ring closing process, indicating no significant change in solvation occurs for the photochromic initiator unit. This is also reflected in the lower activation energy (E_a) of the monomer in comparison to the polymers. The E_a and related parameters of activation enthalpies ($\Delta H^{\ddagger}$) were also found to increase with increasing chain length. Most likely, the environment of the photochromic end-group in the shorter chain is more polar than that of the longer chain. The polar interaction might thus lower the energy barrier of the reaction. However, the thermal relaxation process provides far greater energy gain than this energy barrier, and thus, although the enthalpy of activation increases with the polymer molecular weight, also the process rate increases. Although at room temperature there is a balance between these factors, indicated by relatively similar rate constants, at higher temperatures the entropic factor dominates.

3.3.2 Cation Complexation

The negatively charged phenolate group in the BMC form has ion-binding characteristics.[30] The binding results in a shift in absorbance, which correspond to a color change of the solution. To confirm that this property is maintained in the linear BSP end-functionalized PMMA, the optical properties and complexation behavior of BSP-PMMA1 and BSP-PMMA2 were investigated with Co^{2+}. For these experiments, 1×10^{-4} M solutions of each polymer were prepared in acetonitrile and kept in the dark, before 100 μL of 1×10^{-2} M solution of the metal nitrate in acetonitrile was added. The colorless solutions were exposed to UV light for 1 min to promote the complexation after which a pink color was observed. For both polymers, the absorption spectra show a peak at 505 nm, in addition to the peak at 568 nm that corresponds to the BMC-PMMA (**Figure 3.15**).

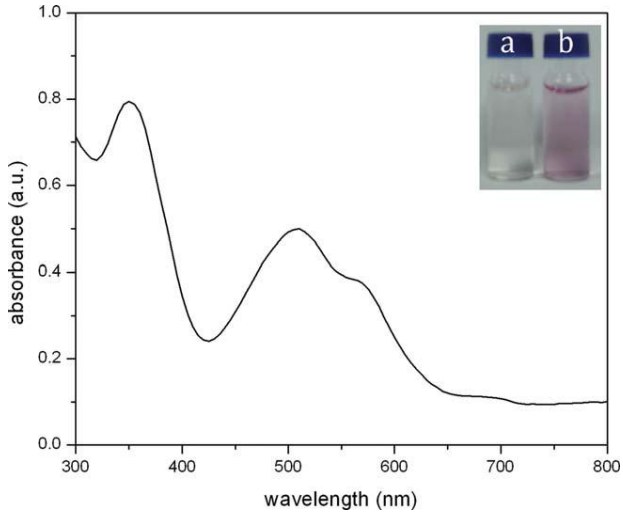

Figure 3.15 UV–vis spectrum of BSP-PMMA1 (1×10^{-4} M in acetonitrile) after addition of 100 μL of $Co(NO3)_2$ (1×10^{-2} M) and 60 s of UV irradiation (365 nm). The inset shows the sample before (a) and after UV irradiation (b).

The presence of this new peak indicates the formation of a metal complex.[44] As BMC bivalently complexes Co^{2+}, this process requires two BMC end-groups to bind to the metal ion and consequently links two linear polymer chains.[30] This process is reversible and controllable using UV and visible light. This implies a certain control on the supramolecular organization of these types of systems. In agreement with the results discussed above, the BMC end-groups of the polymer with lower molecular weight experience a longer life time and a shorter diffusion path, which possibly promotes the formation of more bivalent complexes as compared with the higher molecular weight polymer. The solution was then exposed to visible light and the color disappeared, leaving a colorless solution. The kinetic rate of thermorelaxation of the complex for the longer polymer was monitored at room temperature, and our preliminary studies show a rate constant 0.0021 s^{-1}. Comparison with the above collected data on the thermorelaxation of BSP-PMMA2 suggests that this process is slower in the presence of the metal, because the metal stabilizes the BMC form. However, these data need to be verified in a more detailed study.

3.4 Conclusion

In the first part of this work new polymeric methacrylates bearing a terminal BSP derivative with different M_n have been synthesized and analyzed. The complexation properties of the polymeric systems were shown and the photonic control of uptake and release of Cu^{2+} ions was demonstrated. Utilizing the chelating properties of BSP, considerable changing in surface wettability of their polymeric films was achieved, with an improvement of over 10° on the recent work reported.

Moreover, PMMA of two different chain lengths having a single photochromic 6-nitro BSP end-group were synthesized by ATRP. Polymer characterization confirms that using an ATRP initiator equipped with BSP, a near quantitative functionalization of the PMMA with the BSP was achieved. Both polymers exhibited conventional photochromism characterized by the UV-induced transition from BSP to BMC in acetonitrile. However, the strong dependence of the thermal relaxation of the BMC suggests a different polar (solvation) environment of the BMC in the two polymers. This is mainly manifested in a temperature-dependent faster transition for the higher molecular weight polymer. The ability of the BMC polymer end-groups to organize was shown by metal ion-binding experiments forming bivalently linked complexes. The results reported here provide further understanding of the photochromic behavior of polymers with a single chromophore. Moreover, it might open opportunities to probe molecular polymer dynamics in solution.

In conclusion, according to our studies, even if the 6-nitro BSP derivative (BSP-OH-1) is less reactive then the 6-hydroxy BSP compound (BSP-OH-2) in the esterification reaction, its α-bromo ester reacts in a better controlled manner in the ATRP polymerization and, as expected, the polymer so-generated has a considerably better photochromic behaviour than the BSP 6-hydroxy based material.

3.5 Experimental part

3.5.1 Work on BSP-OH-2

Materials

1-(methyl)-3,3-dimethylindolino-6-hydroxybenzopyrylospiran was provided from NCSR (National Centre for Sensor Research) and used as received. Triethylamine, 2-bromo-2-methylpropionyl bromide, copper(I)chloride, copper(II)chloride, HMTETA, and dichloromethane anhydrous were purchased from Sigma–Aldrich and used without further purification. Methyl methacrylate (99% purity, Sigma–Aldrich) was purified by vacuum distillation.

Methods

Molecular weight analysis of the polymers was carried out by SEC with THF as an eluent using an Agilent 1200 series isocratic pump (flow rate 1mL/min) and an Agilent 1200 series refractive index detector at 35 °C calibrated with poly(methyl methacrylate). Two PLGel 5μm Mixed-C (300 mm×7.5 mm) columns at 40 °C were used. Injections were done by an Agilent 1200 autosampler using a 50μL injection volume. BSP-2-PMMA-1 and -2 were characterised using Cary 50 UV–vis spectrophotometer. Approximately, 1×10^{-4} M solutions of each polymer were prepared in acetonitrile. For the protonation experiments, solutions of the polymers were kept in the dark for 2 h before 100μL of 1×10^{-2} M aqueous solution of hydrochloric acid was added to the colourless polymer solution. After 10 s, a strong yellow coloured was observed. The solution was then exposed to green light (500 nm), after 30 s the yellow colour disappeared, leaving a colourless solution. ^{1}H and ^{13}C NMR spectra were recorded at room temperature with a Bruker Avance 400 (400 MHz) and a Bruker Avance Ultrashield 600 (600 MHz). Deuterated Chloroform ($CDCl_3$) was used as solvent, and signals were referred to the signal of the residual protonated solvent signal.

Cation complexation with BSP polymers

For Co^{2+} and Cu^{2+} complexation experiments, 1×10^{-4} M solutions of the polymer were kept in dark before addition of equal molar equivalents of the metal salt (nitrate in both cases). The kinetic rate of formation of the coloured complex was

monitored at 25 °C. The solution was then exposed to green light (500 nm), after 30 s the colour disappeared, leaving a colourless solution.

Contact angle measurements for BSP-2-PMMA-2

Contact angle measurements were carried out using a FTÅ200 dynamic contact angle analyser. Polymeric films were prepared by dip coating glass slides into an acetonitrile solution of the polymer (5 mg/mL). For the BSP-2-PMMA-2–Cu^{2+} complex containing films, equal molar equivalents of the metal salt were added to the solution before dip coating the glass slide. For the control experiment, 5mg/mL PMMA was used instead of the BSP-2-PMMA-2. Polymer solutions containing the $Cu(NO_3)_2$ were allowed to equilibrate for more than 500 s. Slides were then washed with deionised water and placed in vacuum oven for 30 min before contact angle measurement. This procedure was repeated three times.

Synthesis of 1',3',3'-trimethyl-6-(2-bromoisobutyryloxy)spiro[2H-1-benzopyran-2,2'-indoline] (BSP-Br-2)

A solution of 1′,3′,3′-trimethyl-6-hydroxyspiro[2*H*-1-benzopyran-2,2′-(2*H*)-indole] (BSP-OH-1) (293 mg, 1 mmol) and triethylamine (0.139 mL, 1 mmol) in 2.5 mL of dry DCM was stirred at 0 °C under N_2 atmosphere for 1 hour. 2-bromoisobutyryl bromide (0.136 mL, 1.1 mmol) was added dropwise to the mixture. The resulting solution was stirred at 25°C overnight. After evaporation of the solvent, the residue was dissolved in diethyl ether. The solution was then extracted with 2N hydrochloride. The organic phase was dried over $MgSO_4$ and filtered. The solvent was removed under reduced pressure to leave the product as a dark brown solid. The crude product contained traces of triethylamine hydrobromide and was used without further purification. Mp 77-80 °C; ^{1}H-NMR (400 MHz, $CDCl_3$, δ, ppm) 1.16 (3H, s, 3'-CH_3), 1.30 (3H, s, 3'-CH_3), 2.05 (6H, s, $(CH_3)_2CBr$), 2.72 (3H, s, CH_3N), 5.73 (1H, d, *J* = 10.7 Hz, 2-CCH=CH), 6.53 (1H, d, *J* = 7.6 Hz, ArH), 6.71 (1H, d, *J* = 8.3, ArH), 6.81 (1H, d, *J* = 8.3, ArH), 6.82-6.87 (3H, m, ArH, 2-CCH=CH), 7.07 (1H, d, *J* = 7.4, ArH), 7.15-7.20 (1H, t, *J* = 7.6). ^{13}C-NMR (400 MHz, $CDCl_3$, δ, ppm) 20.18, 25.84, 28.96, 29.68, 51.85, 55.45, 104.46, 106.86, 115.67, 118.68, 119.23, 120.51, 121.51, 121.82, 127.64, 128.78, 136.62, 143.09, 152.27, 170.69.

Polymerization procedures BSP-2-PMMA

ATRP was applied for the synthesis of the polymers. All polymerization reactions were carried out in a moisture and oxygen-free glass tube. MMA (2.49 g, 24.8 mmol), BSP-Br-2 (44.3 mg, 0.1mmol), CuCl (7.9 mg, 0.08mmol), $CuCl_2$ (2.7 mg, 0.02 mmol), and HMTETA (46.1 mg, 0.2 mmol) were mixed at a 25:1:0.8:0.2:2 molar ratio. THF (0.3 mL) was added to the mixture and it was stirred and placed in a thermostated oil bath kept at 60 °C. The reaction was allowed to proceed for 40 min. or 4 hours, respectively, depending on the desired polymer molecular weight. The resultant dark brown mixture was cooled at room temperature, dissolved in DCM and then filtered through a short column of alumina (Al_2O_3). The column was washed with CH_2Cl_2 and the resulting solution was precipitated in methanol. The pale orange-brown precipitate was filtered, washed with methanol and dried under vacuum to give 0.35 g of polymer, in the case of 40 minutes reaction time (BSP-PMMA-1) and 0.90 g of polymer in the case of 4 h reaction time (BSP-2-PMMA-2). BSP-2-PMMA-1: M_n = 9,800 g/mol, PDI = 1.3. BSP-2-PMMA-2: M_n = 28,000 g/mol, PDI = 1.2.

3.5.2 Work on BSP-OH-1

Materials

1-(2-Hydroxyethyl)-3,3-dimethylindolino-6-nitrobenzopyrylospiran was purchased from TCI chemicals and used as received. Triethylamine, 2-bromo-2-methylpropionyl bromide, copper(I)chloride, copper(II)chloride, HMTETA, and DCM anhydrous were purchased from Sigma–Aldrich and used without further purification. Methyl methacrylate (99% purity, Sigma–Aldrich) was purified by vacuum distillation.

Methods

Molecular weights of polymer were characterized by gel permeation chromatography performed on an Agilent 1200 series equipped with two PL Gel 5 lm Mixed-C 300 x 7.5 mm^2 columns at 40 °C. Tetrahydrofuran (THF) was used as an eluent at a flow rate of 1 mL min^{-1}. Molecular weights were calculated based on PMMA standards. Spectrometric studies were carried out using a Perkin-Elmer

Lambda 900 spectrometer (Foss, Ireland) with a Perkin-Elmer PTP-1 temperature controller. ^{1}H and ^{13}C NMR spectra were recorded at room temperature with a Bruker Avance 400 (400 MHz) and a Bruker Avance Ultrashield 600 (600 MHz). $CDCl_3$ was used as solvent, and signals were referred to the signal of the residual protonated solvent signal. Mass spectra were measured on a Bruker Esquire 3000 LCMS. MALDI-ToF analysis was carried out on a VoyagerDE-STR from Applied Biosystems (laser frequency 20 Hz, 337 nm, and a voltage of 25 kV). The matrix material used was trans-2-[3-(4-tert-butylphenyl)-2-methyl-2-propenylidene] malononitrile (40 mg mL^{-1}). Potassium trifluoroacetic acid was added as cationic ionization agent (5 mg mL^{-1}). The polymer sample was dissolved in hexafluoroisopropanol (HFIP) (1 mg mL^{-1}), in which the matrix material and the ionization agent were added (5:1:5), and the mixture was placed on the target plate.

Kinetic measurements of BMC-PMMA to BSP-PMMA transition

Standard solutions of BSP-PMMA polymers were made up to 1×10^{-4} M in acetonitrile [calculated based on Mn from SEC (PMMA standards)]. Samples were irradiated for 1 min with UV light at 375 nm using an in-house fabricated array based on 375 nm UV LEDs (Roithner Lasertechnik, Vienna, Austria). Note that for all UV–vis studies, the SP samples should be protected from ambient light. Reflectance spectra were recorded using a miniature diode array spectrophotometer (S2000VR®) combined with an FCR-7UV200-2 reflection probe (7×200 μm cores) and a DH-2000-FSH75 deuterium halogen light source (215–1700 nm, Ocean Optics, Eerbeek, The Netherlands). A white reflectance standard WS-1-SL was used to standardize the measurements at 100% reflectance (Ocean Optics, Eerbeek, The Netherlands). The recorded spectra were processed by the Ocean Optics software against a previously recorded reference spectrum of a totally reflective Ocean Optics standard in the dark at the same distance from the reflectance probe.[45]

The kinetic and thermodynamic parameters of the reversion of BMC to BSP were determined at each temperature by monitoring the absorbance decrease at λ_{max} of the BMC isomer after removal of the irradiating source. The first-order rate

constants were estimated by following the decrease of the absorbance at 568 nm in time and subsequently examined using the equation $\ln([A_t]/[A_0]) = -kt$ with A_t and A_0 denote the absorbance at λ_{max} at time *t* and at the beginning of the thermal relaxation process, respectively.[46]

Cation complexation with BSP polymers

First, a stock solution of cobalt nitrate (1×10^{-2} M) in acetonitrile was prepared. The absorbance spectrum of the BSP-PMMA solution (1×10^{-4} M; calculated based on Mn from SEC [PMMA standards]) was measured before illumination with UV light after allowing the solution to stand overnight under dark conditions at room temperature. Then, 2.9 mL of the polymers solution was spiked with 100 μL of the cobalt nitrate stock solution. The mixture was illuminated for 1 min using the UV source, and the absorbance spectrum was taken immediately after illumination. Then, the solution was irradiated with white light for 1 min and the spectrum was taken.

Synthesis of 1'-(2-bromoisobutyryloxyethyl)-3',3'-dimethyl-6-nitrospiro[2H-1-benzopyran-2,2'-indoline] (BSP-Br-1)

A solution of BSP-OH-1 (352 mg, 1 mmol) and triethylamine (0.139 mL, 1 mmol) in 4 mL of dry DCM was stirred at 0 °C under N_2 atmosphere for 1 hour. 2-bromoisobutyryl bromide (0.124 mL, 1 mmol) was added dropwise to the mixture. The resulting solution was stirred at 25 °C overnight. After evaporation of the solvent, the residue was dissolved in diethyl ether. The solution was then extracted with 2 N hydrochloride aqueous solution. The organic phase was dried over $MgSO_4$ and filtered, and the solvent was removed under reduced pressure to leave the product as a red oil. The crude product was purified by flash column chromatography using hexane/DCM (1:1) as the eluent to give BSP-Br-1 (283 mg, 56.3%), as a pale yellow solid; mp 124 °C; Fourier transform infrared spectroscopy (FT-IR): m 1734 cm^{-1}; ^1H NMR (400 MHz, $CDCl_3$, δ, ppm): 1.17 (3H, s, 3'-CH_3), 1.28 (3H, s, 3'-CH_3), 1.90 (6H, s, $(CH_3)_2CBr$), 3.42–3.61 (m, 2H, NCH_2), 4.28–4.36 (m, 2H, OCH_2), 5.99 (1H, d, *J* = 10.4 Hz, 2- CCH=CH), 6.70 (1H, d, *J* = 7.8 Hz, ArH), 6.75 (1H, d, *J* = 8.4 Hz, ArH), 6.89–6.94 (m, 2H, ArH, 2-CCH=CH), 7.10 (1H, d, *J* = 7.2 Hz, ArH),

7.21 (1H, t, *J* = 7.7 Hz, ArH), 8.01–8.03 (m, 2H, ArH). ^{13}C NMR (400 MHz, $CDCl_3$, δ, ppm): 19.79, 25.79, 30.79, 42.09, 52.83, 55.49, 63.90, 106.56, 106.73, 115.52, 118.45, 120.02, 121.84, 122.00, 122.75, 125.94, 127.79, 128.28, 135.72, 141.08, 146.54, 159.34, 171.70; m/z (ESI, %): 501 [molecular peak], 469, 441, 413, 352.

Polymerization procedures BSP-PMMA

The ATRP polymerizations of MMA with the BSP initiator BSP-Br-1 were performed in a moisture and oxygen-free glass tube. BSP-Br-1 (50.3 mg, 0.1 mmol), CuCl (7.9 mg, 0.08mmol), $CuCl_2$ (2.7 mg, 0.02 mmol), and HMTETA (46.1 mg, 0.2 mmol) were mixed at a 1:0.8:0.2:2 molar ratio. MMA was added to the solution, at a molar ratio of 25 or 248, respectively, with respect to BSP-Br-1. THF (10% weight) was used as solvent. The polymerizations were carried out at 60 °C for 3 hours, after which the polymerization mixtures were cooled to room temperature, added to DCM, and filtered through a short column of alumina. The column was washed with DCM, and the resulting solution was precipitated in methanol. The precipitate was filtered, washed with methanol, and dried under vacuum to give 0.049 g of polymer in the case of lower monomer to initiator ratio (BSP-PMMA1; M_n = 3600 g/mol, PDI = 1.3) and 1.04 g in the case of higher monomer to initiator ratio (BSP-PMMA2; M_n = 23,800 g/mol, PDI = 1.1).

3.6 References

1. Roy D., Cambre J.N., Sumerlin B.S. Prog Polym Sci **2010**, *35*, 278.
2. Lee H., Pietrasik J., Sheiko S.S., Matyjaszewski K. *Prog. Polym. Sci.* **2009**, *35*, 24.
3. Ercole F., Davis T.P., Evans R.A. *Polym. Chem.* **2010**, *1*, 37.
4. Schumer J.M., Fustin C.A., Gohy J.F. *Macromol. Rapid Commun.* **2010**, *31*, 1588.
5. Zhao Y., Tremblay L., Zhao Y.J. *J. Polym. Sci. A: Polym. Chem.* **2010**, *48*, 4055.
6. Jin Q., Liu G., Ji J. *J. Polym. Sci. A: Polym. Chem.* **2010**, *48*, 2855.
7. Crano J.C., Flood T., Knowles D., Kumar A., Van Gemert B. *Pure Appl. Chem.* **1996**, *68*, 1395.
8. Byrne R., Ventura C., Lopez F.B., Walther A., Heise A., Diamond D. *Biosens. Bioelectron.* **2010**, *26*, 1392.
9. Minkin V.I. *Chem. Rev.* **2004**, *104*, 2751.
10. Gorner H., Chibisov A.K. *J. Chem. Soc., Faraday Trans.* **1998**, *94*, 2557.
11. Radu A., Byrne R., Alhashimy N., Fussaro M., Scarmagnani S., Diamond D. *J. Photochem. Photobiol., A* **2009**, *206*, 109.
12. Ipe B.I., Mahima S., Thomas K.G. *J. Am. Chem. Soc.* **2003**, *125*, 7174.
13. Andersson J., Li S., Lincoln P., Andreasson J. *J. Am. Chem. Soc.* **2008**, *130*, 11836.
14. Hammarson M., Andersson J., Li S., Lincoln P., Andreasson J. *Chem. Commun.* **2010**, *46*, 7130.
15. Fries K., Samanta S., Orski S., Locklin J. *Chem. Commun.* **2008**, 6288.
16. Fries K.H., Driskell J.D., Samanta S., Locklin J. *Anal. Chem.* **2010**, *82*, 3306.
17. Samanta S., Locklin J. *Langmuir* **2008**, *24*, 9558.
18. Zhao Y. *J. Mater. Chem.* **2009**, *19*, 4887.
19. Lee H., Wu W., Oh J.K., Mueller L., Sherwood G., Peteanu L., Kowalewski T., Matyjaszewski K. *Angew. Chem. Int. Ed.* **2007**, *46*, 2453.
20. Adelmann R., Mela P., Gallyamov M.O., Keul H., Mo¨ ller M. *J. Polym. Sci. A: Polym. Chem.* **2009**, *47*, 1274.
21. Achilleos D.S., Vamvakaki M. *Macromolecules* **2010**, *43*, 7073.
22. Malic N., Campbell J.A., Ali A.S., Francis C.L., Evans R.A. *J. Polym. Sci. A: Polym.*

Chem. **2011**, *49*, 476.

23. Evans R., Hanley T.L., Skidmore M., Davis T.P., Such G.K., Yee L.H., Ball G.E., Lewis D. *Nature Mater.* **2005**, *4*, 249.
24. Such G.K., Evans R.A., P. D.T. *Macromolecules* **2004**, *37*, 9664.
25. Such G.K., Evans R.A., Davis T.P. *Macromolecules* **2006**, *39*, 1391.
26. Such G.K., Evans R.A., Davis T.P. *Macromolecules* **2006**, *39*, 9562.
27. Such G.K., Evans R., Yee L., Davis T. *Polym. Rev.* **2003**, *43*, 547.
28. Ercole F., Davis T.P., Evans R.A. *Macromolecules* **2009**, *42*, 1500.
29. Ercole F., Malic N., Harrisson S., Davis T.P., Evans R.A. *Macromolecules* **2010**, *43*, 249.
30. Byrne R., Stitzel S.E., Diamond D. *J. Mater. Chem.* **2006**, *16*, 1332.
31. Radu A., Scarmagnani S., Byrne R., Slater C., Lau K.T., Diamond D. *J. Phys. D: Appl. Phys.* **2007**, 7238.
32. Zakharova M.I., Coudret C., Pimienta V., Micheau J.C., Delbaere S., Vermeersch G., Metelitsa A.V., Voloshin N., Minkin VI. *Photochem. and Photobiol. Sci.* **2010**, *9*, 199.
33. Zhou J-W., Li Y-T., Song X-Q. *J. Photochem. Photobiol., A* **1995**, *87*, 37.
34. Rosario R., Gust D., Garcia A.A., Hayes M., Taraci J.L., Clement T., Dailey JW., Picraux S.T. *J. Phys. Chem. B* **2004**, *108*, 12640.
35. Rosario R., Gust D., Hayes M., Jahnke F., Springer J., Garcia A.A. *Langmuir* **2002**, *18*, 8062.
36. McCoy C.P., Donnelly L., Jones D.S., Gorman S.P. *Tetrahedron Lett.* **2007**, *48*, 657.
37. Byrne R., Coleman S., Gallagher S., Diamond D. *Phys. Chem. Chem. Phys.* **2010**, *12*, 1895.
38. Byrne R., Fraser K.J., Izgorodina E., MacFarlane D.R., Forsyth M., Diamond D. *Phys. Chem. Chem. Phys.* **2008**, *10*, 5919.
39. Coleman S., Byrne R., Minkovska S., Diamond D. *J. Phys. Chem. B* **2009**, *113*, 15589.

40. Byrne R., Diamond D. *Nature Mater.* **2006**, *5*, 421.

41. Gorner H. *Phys. Chem. Chem. Phys.* **2001**, *3*, 416.

42. Stitzel S., Byrne R., Diamond D. *J. Mater. Sci.* **2006**, *41*, 5841.

43. Coleman S., Byrne R., Alhashimy N., Fraser K.J., MacFarlane D.R., Diamond D. *Phys. Chem. Chem. Phys.* **2010**, *12*, 7009.

44. Chibisov A.K., Gorner H. *Chem. Phys.* **1998**, *237*, 425.

45. Scarmagnani S., Walsh Z., Slater C., Alhashimy N., Paull B., Macka M., Diamond D. *J. Mater. Chem.* **2008**, *18*, 5063.

46. Flannery J.B. *J. Am. Chem. Soc.* **1968**, *90*, 5660.

Chapter 4

Spiropyran-Terminated Polymers *Via* Click Chemistry

Dr Silvia Giordani (Trinity College Dublin) is greatfully acknowledged for access to the Perkin Elmer LS 55 Fluorimeter and the helpful discussions.

4.1 Introduction

Previously we have demonstrated the effect of incorporating a single benzospiropyran (BSP) unit into a hydrophobic polymer matrix, such as PMMA. The remarkable changes in the polymer chemo and light-responsive properties of the BSP-PMMA have led us to modify hydrophilic polymers, by introducing the BSP feature. A number of attempts to incorporate spiropyran molecules into polymer systems have been reported.[1-3] When the spiropyran groups are covalently bonded to the polymer, their photodegradation, a limitation to practical application, can be reduced.[4,5] An opportunity for covalently binding BSP units onto polymeric matrices is offered by the click chemistry reactions devised by Sharpless, and in particular the CuAAC with the formation of 1,2,3-triazoles from azides and terminal acetylenes.[6] This type of reaction is particularly appealing due to the simple reaction conditions, tolerance to oxygen and water, high yields, simple product isolation and almost perfect fidelity in the presence of a wide variety of other functional groups.[6-9] Despite the great potential of spiropyrans and the versatility of CuAAC, only a few examples of functionalized polymers with BSP units, produced by click chemistry have been reported in the literature. In 2008 Zhang *et al.* exploited click chemistry to prepare four photochromic dendrimers from a BSP bearing azido functionality. All the BSP dendrimers show typical photochromic properties with superior performance over the corresponding single photochromic unit (**Figure 4.1**).[7]

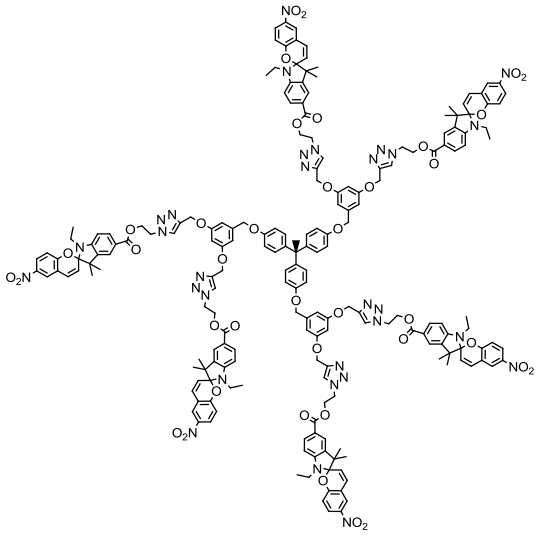

Figure 4.1 Example of BSP dendrimer obtained by CuAAC coupling of azide functional BSP to acetylenic functionalized dendritic structures.[7]

The Fujiwara group exploited click chemistry to prepare a novel BSP dimer that was subsequently used for the synthesis of BSP-based poly(L-lactide) and poly(ethylene glycol). These polymeric systems could be employed as controlled molecular machines in sensing and delivery systems (**Figure 4.2**).[2]

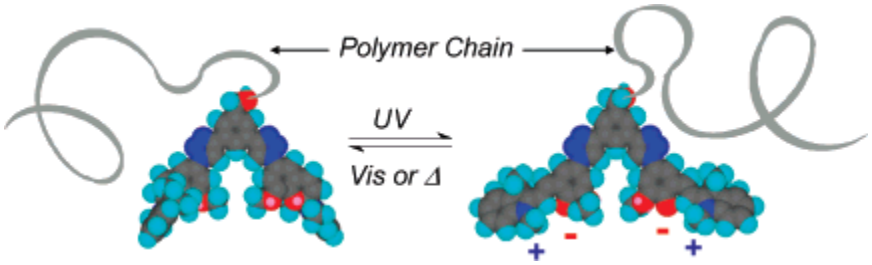

Figure 4.2 Representation of the BSP polymer conjugate prepared from a BSP dimer obtained by CuAAC coupling of azide functional BSP and 3,5-Diethynylbenzylalcohol.[2]

In 2011 Bertoldo *et al.* synthetized a light-responsive polysaccharide by derivatizing, through CuAAC, a N_3-functionalyzed chitosan with a propyne BSP compound (**Figure 4.3**).[4]

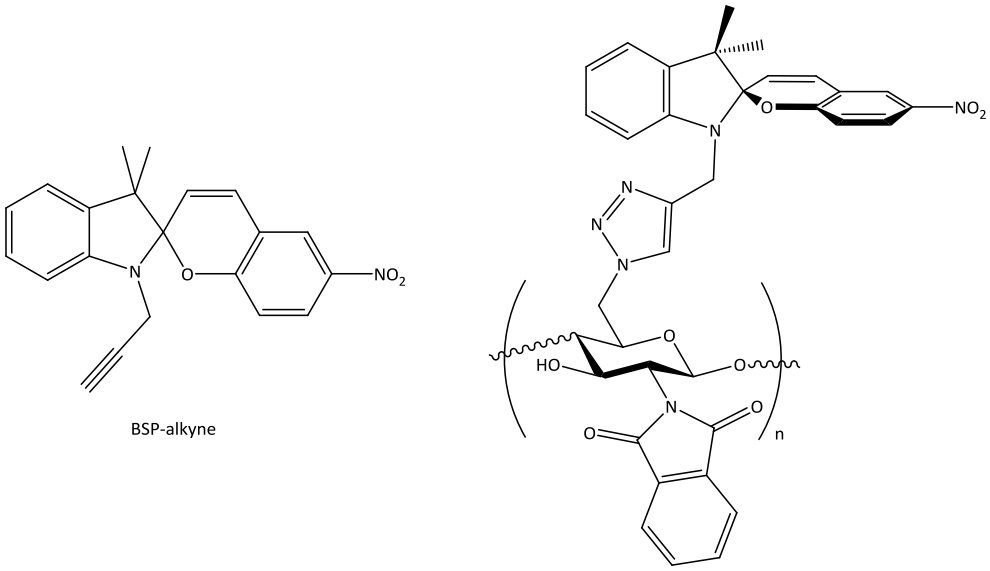

Figure 4.3 Structures of propyne BSP derivative (left) and BSP polysaccharide (right) obtained by click chemistry of and 6-azido-6-deoxy N-phthaloyl chitosan and the spiropyran derivative containing an alkynyl group.[4]

In this work, we have synthetized and characterized the BSP derivative with a propyne pedant group and studied its photochromism, solvatochromism and

acidochromism. Furthermore, we have exploited the alkyne functional group of the BSP compound to demonstrate a BSP-based polymeric system starting from commercially available polymers, through CuAAC.

4.2 Results and Discussion

CuAAC was chosen for the synthesis of hydrophilic BSP polymers due to its high efficiency, fidelity and tolerance to a variety of functional groups. BSP bearing an alkyne moiety (BSP-alkyne) was synthesized, according to the standard path for preparing BSP as reported in the literature.[4] The commercial 2,3,3-trimethyl indolenine was alkylated on the nitrogen atom with 1-tosyl-2-propyne to give a tosylate indoleninium salt. The genarated salt was converted into the corresponding methylene base under basic conditions. Condensation of the latter product with 2-hydroxy-5-nitro benzaldehyde led to the formation of the desired BSP derivative bearing an alkyne function (**Scheme 4.1**). After purification by column chromatography, the product was obtained in 40% yield as a bright yellow solid.

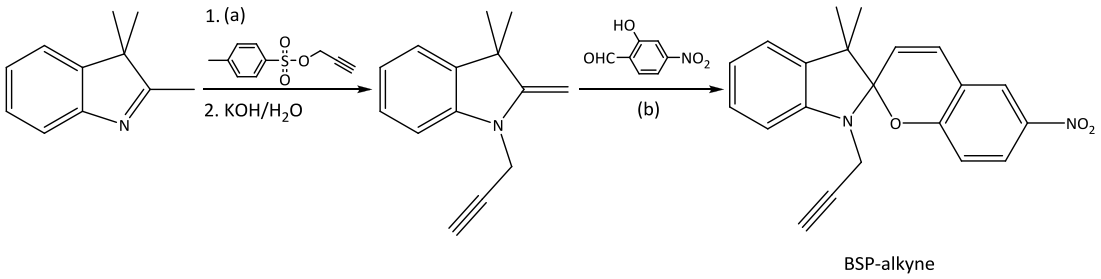

Scheme 4.1 Synthesis of BSP-alkyne. Reaction conditions: (a) N_2, 80 °C, 3 h; (b) EtOH, 82°C, 4 h.

The ^{1}HNMR shows characteristic peaks for BSP derivatives: two singlets of the methyl groups on the indoline part at 1.20 and 1.30 ppm (i) and a series of peaks ranging from 5.90 to 8.04 ppm (a-c, g, h, and j). Characteristic peaks can be assigned to the terminal alkyne group at 2.09 ppm (e) and the methylene group adjacent to the nitrogen atom at 3.88 and 4.03 ppm (d), as shown in **Figure 4.4.** FT-IR and ^{13}CNMR spectroscopies confirmed the structure of BSP-alkyne. All the data collected are in agreement with the literature.[4]

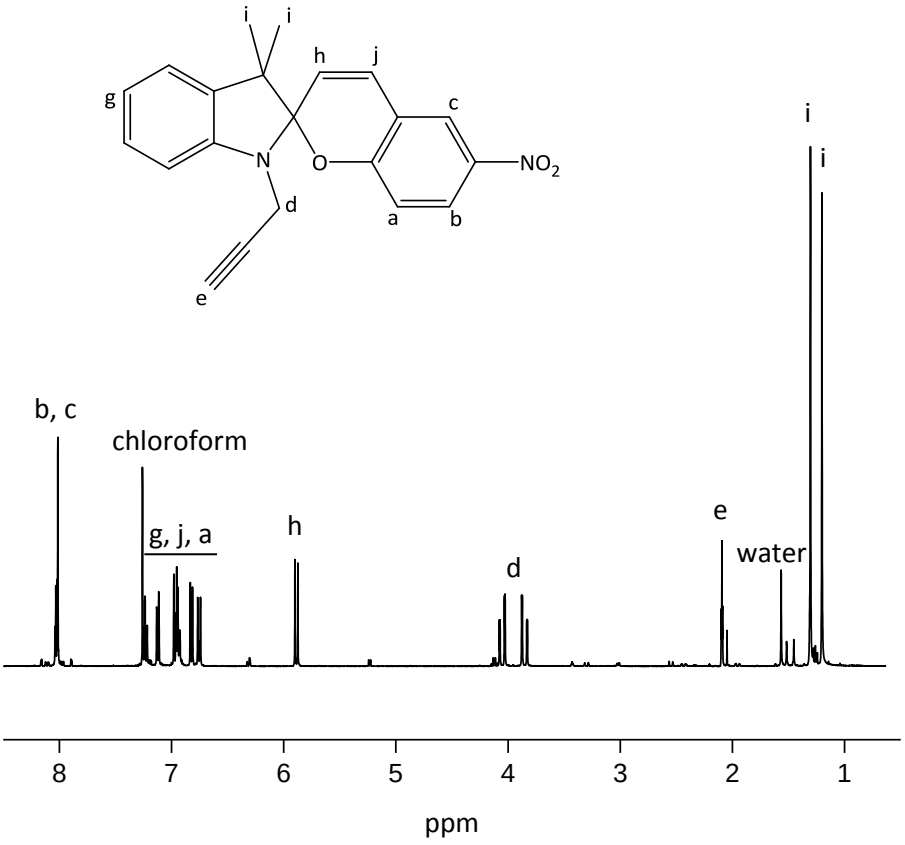

Figure 4.4 ^{1}HNMR spectrum of BSP-alkyne in chloroform.

The click chemistry reaction between the generated BSP-alkyne and a set of azide-functionalized polymers was studied. In particular, we performed the CuAAC on single or double end-functionalized poly(ethylene glycol) (PEG) derivatives, in order to obtain hydrophilic polymers bearing one or two BSP terminal units after the click chemistry reactions. Furthermore, we selected an azide double end-functionalized poly(propylene oxide) (PPO), a hydrophobic PEG analogue, and synthesized the corresponding BSP polymer through CuAAC to investigate the influence of a hydrophobic environment on the reaction and on the photochromic properties of the BSP-modified polymer produced. All the azide-functionalized polymers employed are commercially available (**Figure 4.5**).

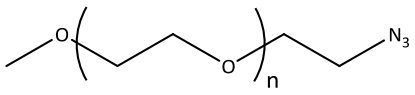

N_3-PEG-1000 (*M*n=1000 g/mol)
N_3-PEG-2000 (*M*n=2000 g/mol)

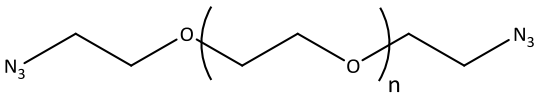

bis-N_3-PEG-2000 (*M*n=2000 g/mol)

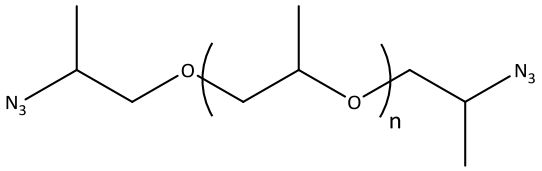

bis-N_3-PPO-2000 (*M*n=2000 g/mol)

Figure 4.5 Structures of the azide end-functionalized polymers, used as starting material for the synthesis of BSP end-functionalized polymers.

The click chemistry reactions were carried out using the BSP-alkyne and the particular polymer in THF in the presence of the catalytic system Cu(I)/PMDETA and a small amount of sodium ascorbate, according to a method reported in the literature.[4] The reactions were allowed to proceed for 60 hours at 40 °C (**Scheme 4.2**). The success of the reaction was confirmed by FT-IR. Comparing the FT-IR spectra of the polymers before and after the click chemistry reaction, the disappearance of the peak at 2103 cm^{-1}, corresponding to the azide moiety is evident (**Figure 4.6**). The absence of the azide functions in the polymer after the, reaction, is evidence of the BSP-alkyne bonding through 1,3-dipolar cycloaddition.

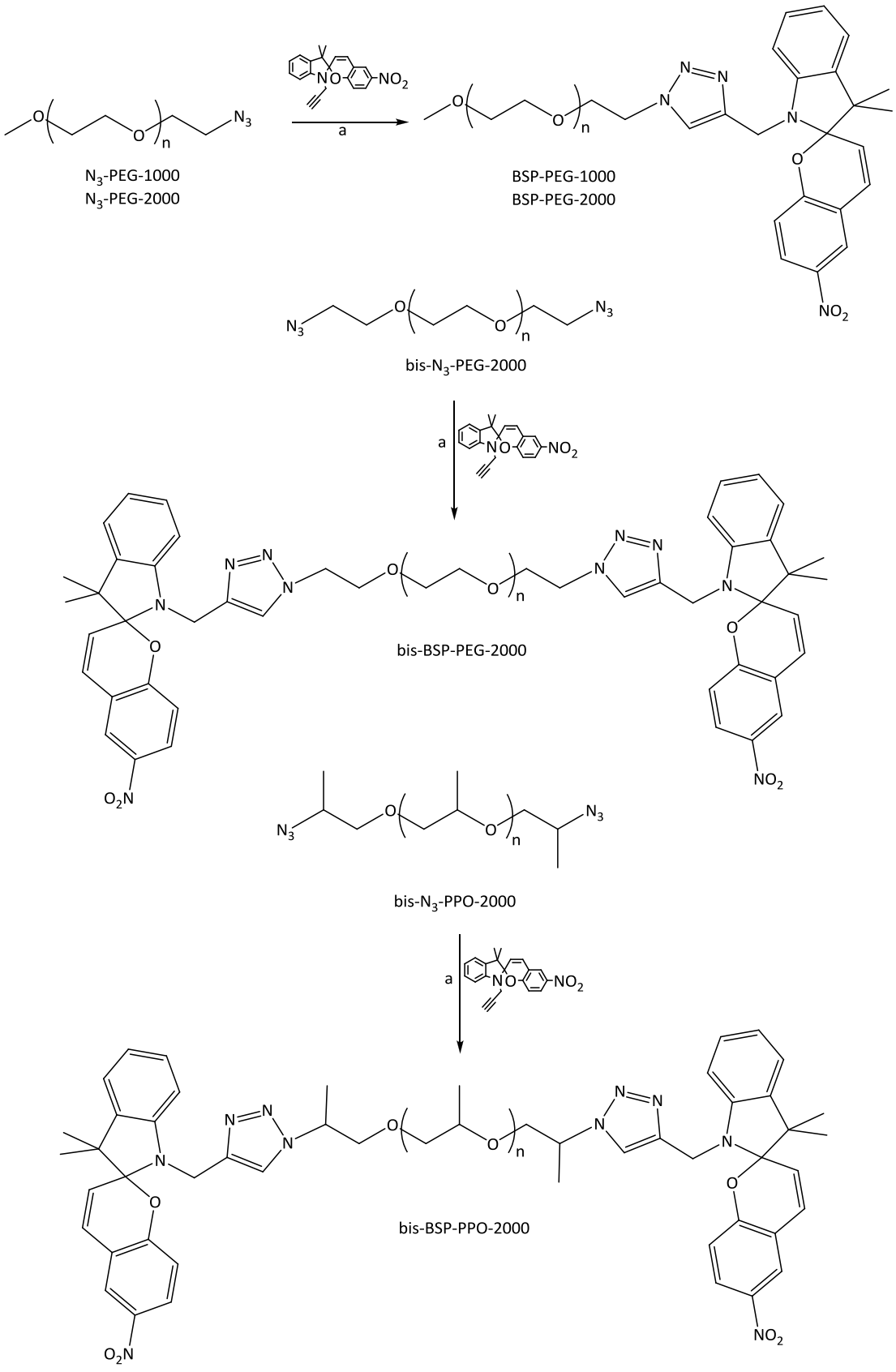

Scheme 4.2 Synthesis of BSP functionalized PEG and PPO. Reaction conditions: (a) BSP-alkyne (1 eq), sodium ascorbate (0.25 eq), CuBr (0.5 eq), PMDETA (0.5 eq), THF, 40°C, 60 h.

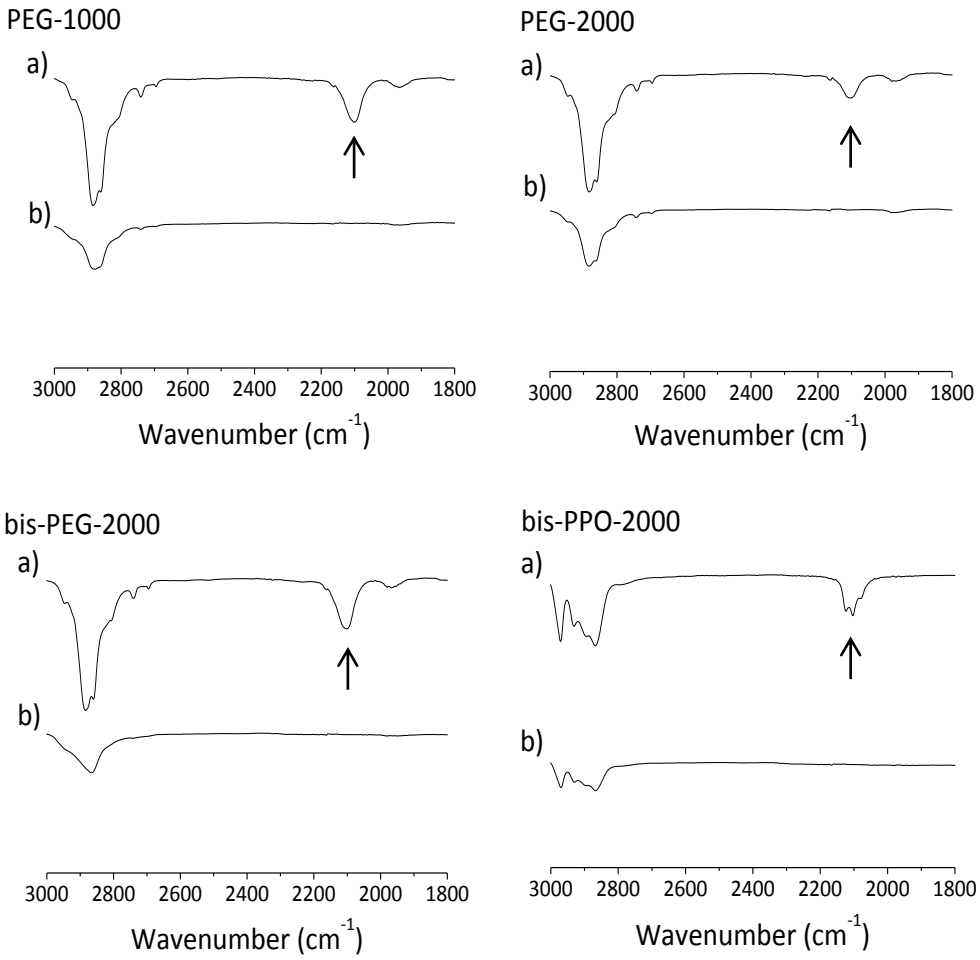

Figure 4.6 FT-IR spectra of the polymers before (a) and after (b) the click chemistry reaction. Arrow marks PEG/PPO azide peak.

4.2.1 Solvatochromism of BSP-alkyne

Solvatochromism is the ability of a chemical substance to change color on variations in the polarity of the solvent medium, which typically involves a change in the position and intensity of the UV-Vis absorption band of the molecule when measured in different solvents. As previously described, the family of benzospiropyrans undergoes solvatochromism.[10-12]

Spectroscopic studies were carried out on the BMC form of BSP-alkyne (BMC-alkyne) in different solvents (**Figure 4.7**). Stock solutions of BSP-alkyne were prepared and stored in the dark to equilibrate overnight in acetonitrile (ACN), dichloromethane (DCM), diethyl ether (Et_2O), ethanol (EtOH) and tetrahydrofuran (THF) with a concentration of $1x10^{-4}$ M. They were irradiated with a UV light source at a wavelength of 365 nm and the absorbance spectra for each of them were collected. As shown in **Table 1**, λ_{max} of BMC-alkyne undergoes red and blue shifts depending on the solvent type. Among the solvents analyzed, the lowest λ_{max} value is found with EtOH (558 nm). This value increases to 574 nm in ACN, 594 nm in DCM and 598 nm in THF. The highest value is observed for Et_2O (606 nm) (**Figure 4.8**).

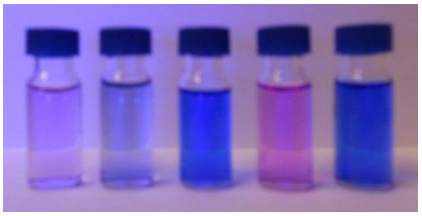

Figure 4.7 Image showing the color change of BMC-alkyne in five different solvent (1×10^{-4} M). From left to right: acetonitrile, dichloromethane, diethyl ether, ethanol, tetrahydrofuran.

According to the solvent dipolarity scale (SdP scale),[13,14] based on two ideal molecular probes: ttbP9 and DMANF (respectively 3,20-di-*tert*-butyl-2,2,21,21-tetramethyl-5,7,9,11,13,15,17,19-docosanonaene and 2-*N*,*N*-dimethylamino-7-nitrofluorene, **Figure 4.9**), among the analyzed solvents ACN is the most polar (0.974), followed by EtOH (0.783), DCM (0.769), THF (0.634) with Et_2O being the least polar (0.385). The absorbance shifts of BMC-alkyne in different solvents are in agreement with the SdP scale, except for ACN and EtOH. According to the SdP, ACN is the most polar among the five solvents, with a dipolarity value of 0.974, while ethanol has a lower dipolarity value of 0.783. Contrary to the expectations, the

lowest λ_{max} for BMC-alkyne is not shown in ACN but in EtOH. This is probably due to the protic solvent nature of EtOH. In the literature, it has been reported that protic solvents form H-bonds with the open BMC. Therefore the BMC ground state is stabilized and the energy difference between the ground and excited states becomes higher, resulting in a lower λ_{max} (**Figure 1.2**).[15,16]

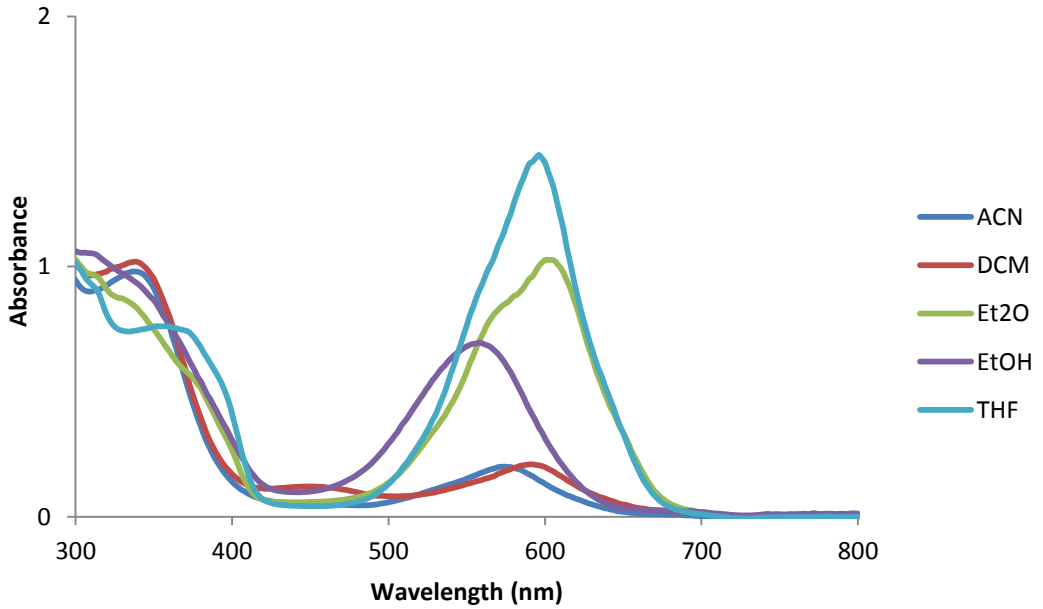

Figure 4.8 Absorbance spectra of BMC-alkyne in five different solvents (concentration 1 x 10^{-4} M). BMC-alkyne λ_{max} undergoes blue shift as the solvent polarity increases (the lowest λ_{max} is 558 nm in ethanol) and red shift as the solvent become less polar (the highest λ_{max} is 606 nm in diethyl ether).

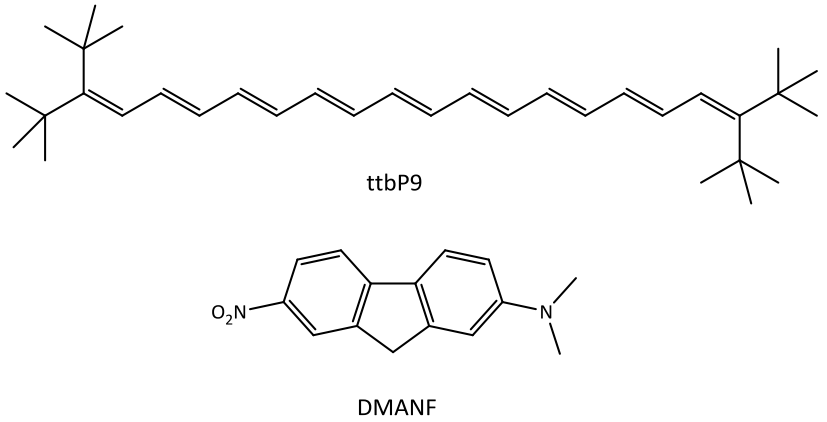

Figure 4.9 Structures of ttbP9 and DMANF molecular probes, used to determine the SdP solvent dipolarity scale.[14]

Kinetic studies were performed to investigate the solvent influence on the ring closing process of the BMC-alkyne, which is known to follow first-order kinetics.[17] The BMC-alkyne form was induced by exposure to UV light for 1 minute and the absorbance value of the BMC-alkyne at its λ_{max} was recorded in each solvent at fixed time intervals (every 0.05 s) as the equilibrium between the SP and MC form was re-established (**Figure 4.10**). These experiments were repeated three times, using fresh sample every time. During these measurements the samples were kept in the dark to avoid the influence of ambient light. From these measurements, the first-order rate constants *k* for the transition BMC-alkyne to BSP-alkyne were determined by plotting ln(*A*0/*A*t) versus time. A linear correlation between BMC-alkyne (λ_{max}) and its thermal relaxation rate constant (*k*) was found in each solvent, as shown in **Figure 4.10**. The values of these kinetic constants *k* are gathered in **Table 1.**

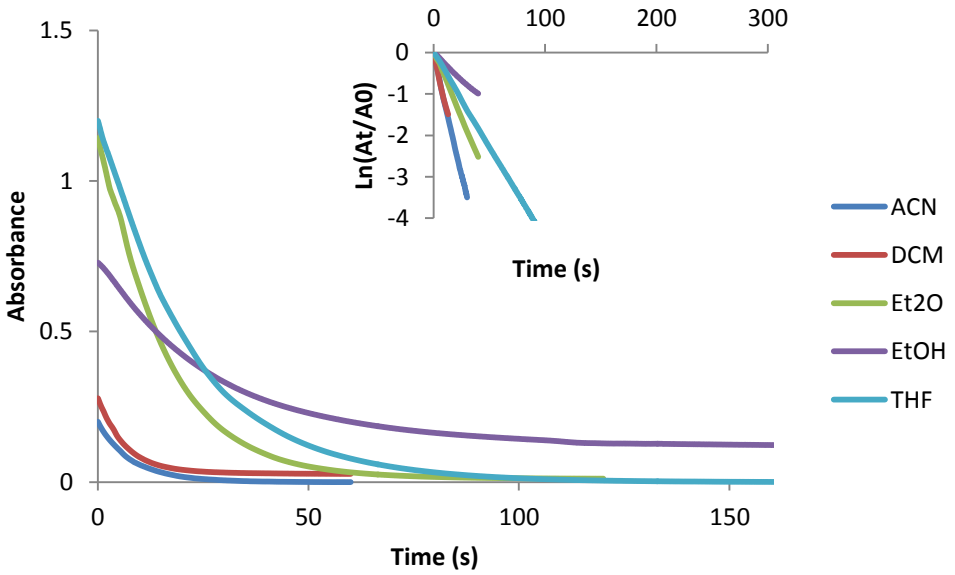

Figure 4.10 Absorbance decrease of the BMC-alkyne λ_{max} in different solvents (1 x 10^{-4}M) as function of time for the transition of BMC-alkyne to BSP-alkyne after removing the UV light source. Top right: corresponding plots of ln(*A*t/*A*0) versus time, showing a linear correlation between BMC-alkyne (λ_{max}) and its rate constant in each solvent.

Table 1 BMC-alkyne λ_{max} values in different solvents reported with the SdP values of each solvent. These values are followed by the values of the relaxation rate constants *k* for the transition of BMC-alkyne to BSP-alkyne at their λ_{max} values. The rate constants are compared in terms of ratio to ring closure kinetics in ethanol.

Solvent	BMC-alkyne λ_{max} (nm)	SdP	*k* (s^{-1})	Ratio to Ethanol
DCM	594	0.769	11.7×10^{-2}	4.6
ACN	574	0.974	11.6×10^{-2}	4.5
Et_2O	606	0.385	6.5×10^{-2}	2.5
THF	598	0.634	4.5×10^{-2}	1.8
EtOH	558	0.783	2.6×10^{-2}	1.0

The ring closure kinetics of the transition of BMC-alkyne to BSP-alkyne is fast in all the analyzed solvents but its rate constant depends on the solvent type. In ACN and DCM the ring closure is extremely fast and within 30 seconds the BMC-alkyne is completely reconverted back to BSP-alkyne with *k* values of 1.16×10^{-1} s^{-1} and 1.17×10^{-1} s^{-1} respectively. In Et_2O and THF the *k* value decreases to 6.48×10^{-2} s^{-1} and 4.53×10^{-2} s^{-1} respectively and the complete conversion to the SP form is not achieved within 60 seconds. The relaxation time determined in ethanol is much slower than that found in ACN and DCM; their *k* values for the transition of BMC-alkyne to BSP-alkyne are respectively 4.5 and 4.6 times faster than in ethanol. As previously mentioned EtOH stabilizes the BMC form through the formation of H-bonds, leading to a slower conversion back to the closed BSP form when compared to the other analyzed solvents.

As shown in **Figure 4.8**, the absorbance spectrum in DCM has two absorption bands: the λ_{max} band (594 nm) due to BMC-alkyne species and a band at a value of 450 nm, which is probably due to a photochemical reaction of BMC-alkyne with the solvent.[18] In the absorbance spectra of the BMC-alkyne both in Et_2O and THF a shoulder is found at around 582 nm and 570 nm respectively (**Figure 4.8**). This could be attributed to the presence of aggregates. It is well known that in non-polar environments the open BMC form tends to associate into stack-like arrangements.

In the literature two types of aggregates that vary depending on the arrangement of the molecular dipoles of the BMC form have been reported. The so-called J-aggregates with molecular dipoles arranged in parallel (head-to-head) have absorption spectra shifted to longer wavelengths, as compared with the isolated BMC molecules, while for the H-aggregates, with an antiparallel (head-to-tail) structure, produce spectra that are shifted to shorter wavelengths (**Figure 4.11**).[11,19] Furthermore, in the absorbance spectrum of BMC-alkyne in THF an extra band at 368 nm is clearly visible (**Figure 4.8**). This is an uncommon band and it could be attributed either to the aggregation of the BMC molecules or to the presence of other isomers of the BMC form. As previously discussed, the presence of more than one BMC isomer in solution has been widely reported in the literature and has been shown in several studies, using various techniques including transient spectroscopy and low temperature NMR experiments.[11,20-22] Our specific case is peculiar because the absorption band is visible at room temperature and it is stable in time. The results of further experiments undertaken to determine the nature of this absorption band will be revealed in the following paragraphs.

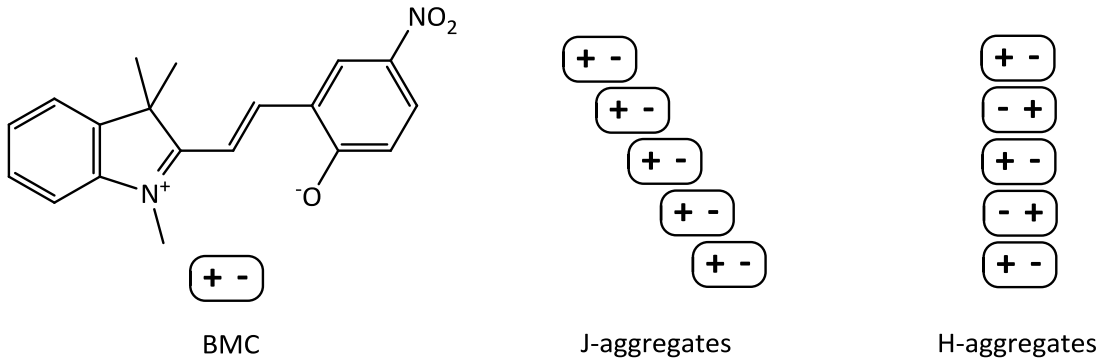

Figure 4.11 Representation of J- and H-aggregates of BMC.[11]

4.2.2 Study of BSP-alkyne UV-Vis spectra at various concentrations

To investigate the nature of the band at 368 nm in the absorption spectrum of BMC-alkyne in THF, several studies at different concentrations were performed. Stock solutions of BSP-alkyne in THF ($1x10^{-4}$ M, $0.5x10^{-4}$ M, $1x10^{-5}$ M) were prepared and stored in the dark to equilibrate overnight. The visible spectra of BMC-alkyne at these concentrations in THF were collected at different time points (every 6 seconds), after exposure to 1 minute of UV light (365 nm). As shown in **Figure 4.12** the visible spectra variations of BMC-alkyne at these concentrations in THF were collected at different time points are similar, with an isosbestic point at 348 nm that implies the decoloration process to be a simple reaction.[10,22] In other words, the absorbing components are linked by a single reaction.[23,24] The absorbance values at λ_{max} (598 nm) were extrapolated and plotted against time from the collected spectra, in order to determine the kinetic constant value for each concentration (**Table 2**). The transition of BMC-alkyne to BSP-alkyne follows first-order kinetics very well and a linear correlation between ln(*A*0/*A*t) and time was found. The variation in concentration of BSP-alkyne left the ring closure rate and the spectra shape practically unvaried.

Similar kinetic studies were performed on the absorption band at 368 nm, based on the absorbance values extrapolated from the spectra collected over time. In this case the study was inaccurate because the variations in absorbance are significantly smaller and so it is more difficult to draw any meaningful conclusions.

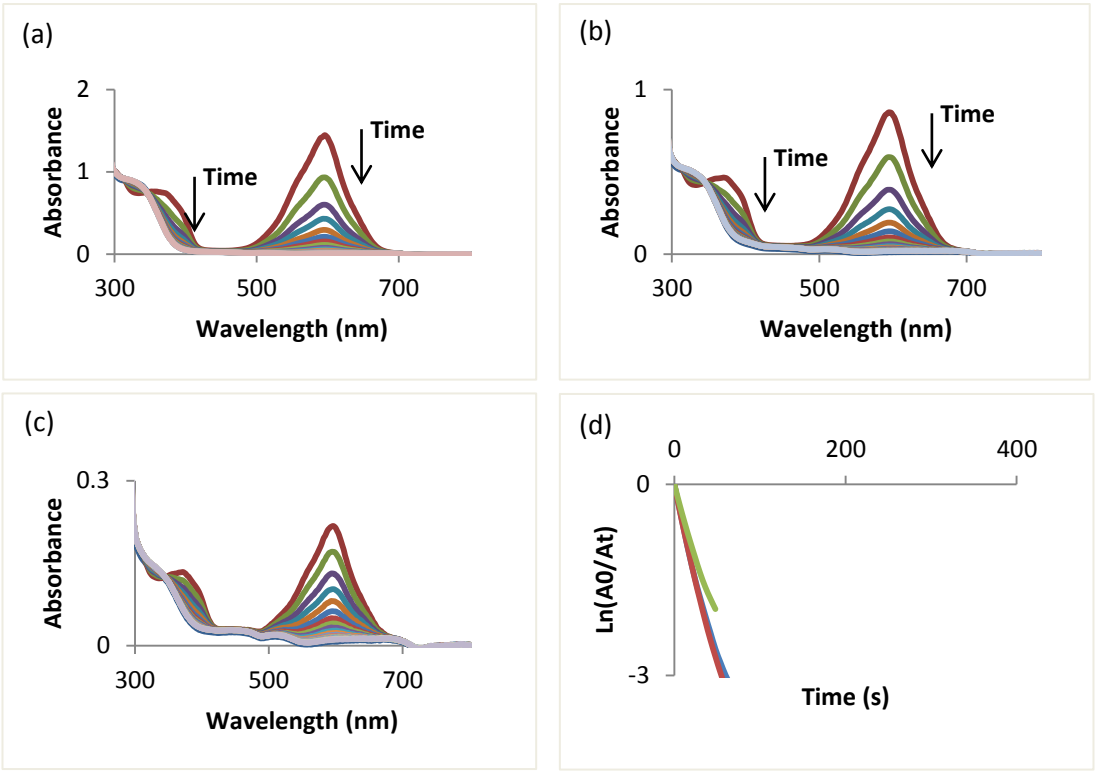

Figure 4.12 (a) Absorbance spectra variations of $1x10^{-4}$ M BMC-alkyne in THF after exposure to UV light for 1 minute. Time intervals: 6 s; (b) Absorbance spectra variations of $0.5x10^{-4}$ M BMC-alkyne in THF after exposure to UV light for 1 minute. Time intervals: 6 s; (c) Absorbance spectra variations of $1x10^{-5}$ M BMC-alkyne in THF after exposure to UV light for 1 minute. Time intervals: 6 s; (d) Plots of ln(*A*t/*A*0) versus time corresponding to the ring closing process of BMC-alkyne, showing a linear correlation between BMC-alkyne (λ_{max}) and its rate constant for each concentration: $1x10^{-4}$ M (blue line), $0.5x10^{-4}$ M (red line) and $1x10^{-5}$ M (green line).

Table 2 Values of the relaxation rate constants *k* for the transition of BMC-alkyne to BSP-alkyne in tetrahydrofuran for the following concentrations: $1x10^{-4}$ M, $0.5x10^{-4}$ M, $1x10^{-5}$ M at room temperature (λ_{max} 598 nm).

Sample	**$1x10^{-4}$ M BMC-alkyne**	**$0.5x10^{-4}$ M BMC-alkyne**	**$1x10^{-5}$ M BMC-alkyne**
k_{598} (s^{-1})	$4.8x10^{-2}$	$5.2x10^{-2}$	4.1×10^{-2}

To investigate the nature of the band at 368 nm, an absorbance diagram (E-diagram) of the system for each concentration was plotted (**Figure 4.13**). The E-diagrams are constructed from the spectra of the transition BMC-alkyne to BSP-alkyne, taking the absorbance values for different measured wavelengths at the same time intervals and plotting the absorbance at one wavelength versus the

absorbance at the others. The resulting curves provide information on the reaction; if there is a linear correlation between the values the reaction is uniform. In other words, the reaction involves only one linear independent step and then the absorption bands shown by UV-Vis spectra correspond to species which are simultaneously present in solution.[10,25] Therefore, the spectra features are in agreement with the hypothesis previously formulated: the presence of other isomers of the BMC form in solution.[22]

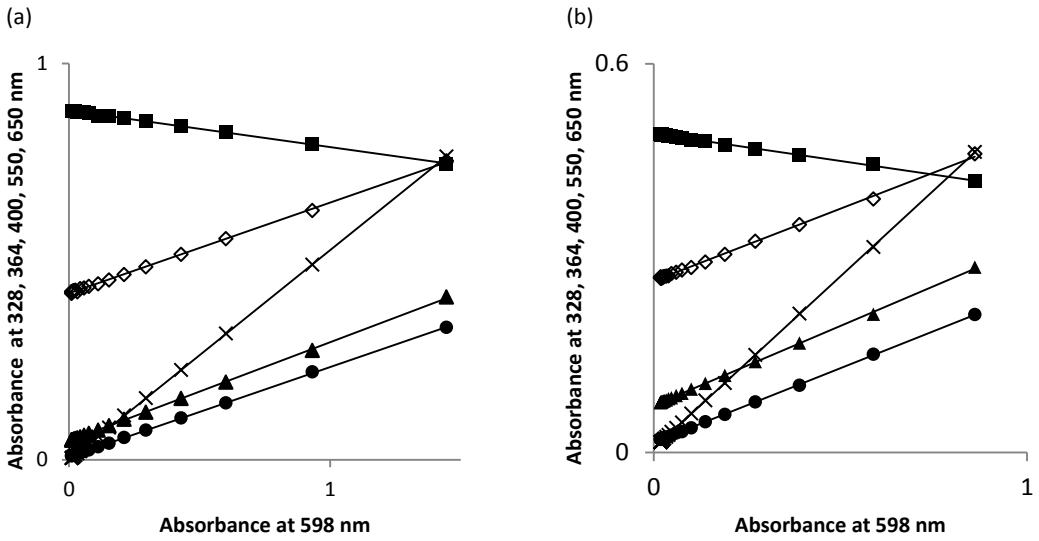

Figure 4.13 E-diagrams for the transition of BMC-alkyne to BSP-alkyne for **(a)** $1x10^{-4}$ M solution and **(b)** $0.5x10^{-4}$ M solution, obtained using the corresponding collected spectra. The absorbance value at 598 nm is plotted against the absorbance values at 328 nm (■), 368 (◊), 400 nm (▲), 550 nm (x) and 650 nm (●).

4.2.3 Fluorescence spectroscopy of BSP-alkyne

As widely discussed in this thesis, irradiation of BSP with UV light generates the open BMC isomer, which is an emitting species since its planar structure allows conjugation through the whole molecule backbone.[26] The emission of BSP-alkyne and the corresponding BMC form in THF ($1x10^{-4}$M) was investigated and the collected emission spectra are reported in **Figure 4.14**. A stock solution of BSP-alkyne was prepared and stored in the dark overnight. A sample of this solution was exposed to UV light for 1 minute to induce the formation of BMC-alkyne, and the emission spectra after excitation at 440 nm and 594 nm of BSP-alkyne and BMC-alkyne were collected. The emission spectrum of the sample after excitation at 594 nm (**Figure 4.14**, right) shows an emission band ($\lambda_{max,em}$= 663 nm) with a shoulder at 710 nm which is approximately specular to the absorption band (**Figure 4.12** a, red line), as expected.

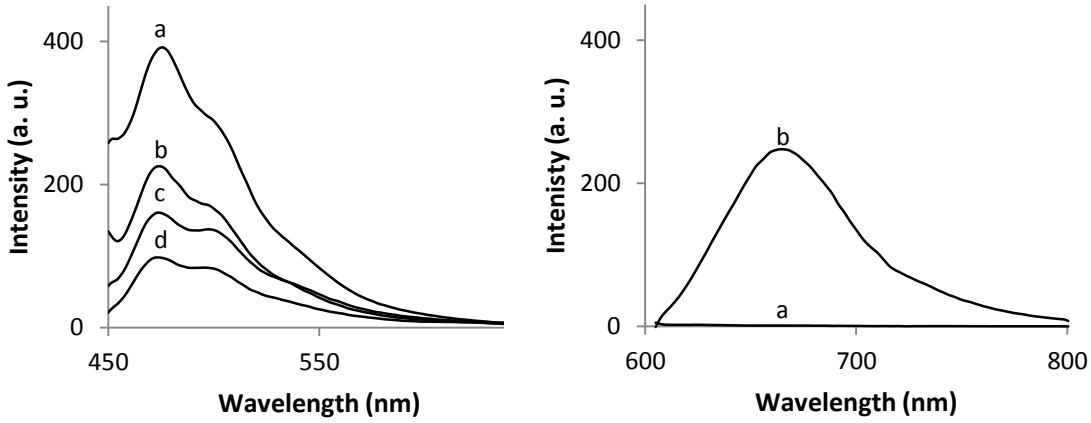

Figure 4.14 Emission spectra of BSP-alkyne and BMC-alkyne in THF ($1x10^{-4}$M) after excitation at 440 nm (Left) and 594 nm (right). Emission spectrum before (a) and after (b) exposure to UV light for 1 minute. Emission spectrum after maintaining the same sample for 4 (c) and 10 (d) minutes in dark.

The emission spectra of the sample after excitation at 440 nm is more complicated; the sample before exposure to UV light showed an emission band with a maximum at 474 nm and a shoulder at 492 nm (**Figure 4.14**, left, spectrum a). This band changed shape after exposing the sample to UV light (365 nm) for 1 minute, the intensity of the band decreased (**Figure 4.14**, left, spectra b and c) and after 10 minutes in the dark the shoulder at 492 nm appeared to be as comparatively

intense as the peak at 474 nm. This behavior indicates the presence of a rather complex system which needs further studies to be fully explained.

4.2.4 Acidochromism of BSP-alkyne

As already mentioned, the phenolate anion in the BMC isomer can bind protons (**Scheme 4.3**). The protonation of BMC can be detected by a change in the absorption spectrum (protonated BMC typically absorbs at around 450 nm) and a consequent variation in color (when the BMC binds protons, the solution turns yellow).[27-30]

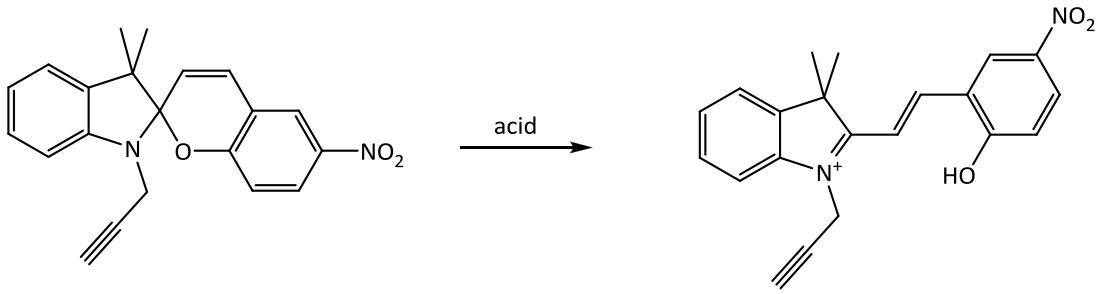

Scheme 4.3 The acid-induced conversion of BSP-alkyne to form the protonated BMC-alkyne (BMCH-alkyne).

Acidochromism of BSP-alkyne was investigated in order to exclude the possibility that the band at 368 nm was due to an accidental acid contamination. 10 equivalents of trifluoroacetic acid (TFA) were added to a solution of BSP-alkyne in THF ($1x10^{-4}$ M) and the resulting mixture was stirred and exposed to UV light (365 nm) for 1 minute. As shown in **Figure 4.15**, the appearance of a band at 455 nm is clear and it is due to the formation of the protonated BMC-alkyne (BMCH-alkyne). Furthermore the intensity of the absorption band at λ_{max} (598 nm) decreases after acid addition because part of the BMC is protonated. 27 These results exclude the possibility that the band at 368 nm in the absorption spectrum of BMC-alkyne in THF is due to an acid contamination.

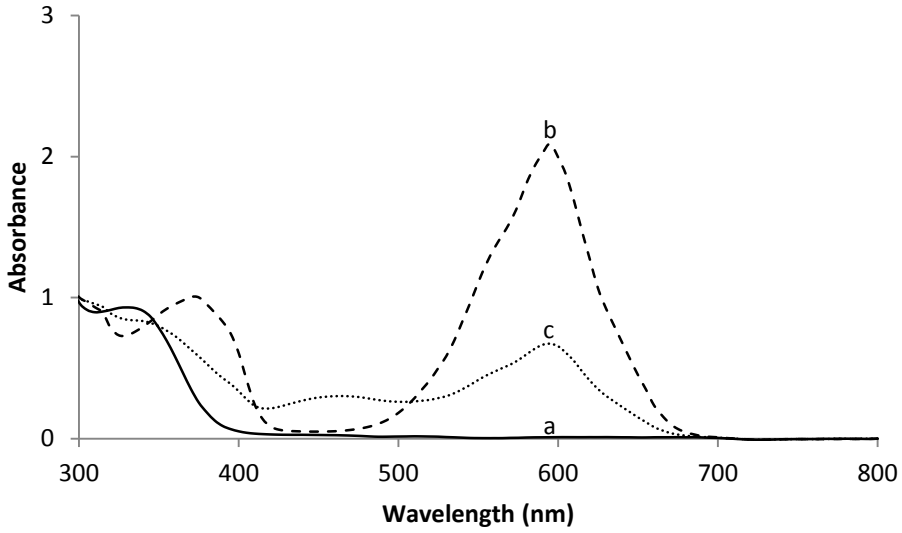

Figure 4.15 Absorbance spectra of BMC-alkyne in THF ($1x10^{-4}$ M) (a) before, (b) after exposure to UV light for 1 minute and (c) after addition of 10 equivalents of TFA and exposure to UV light for 1 minute.

Since protonation of BMC retards its ring-closure,[31] NMR studies on BMCH-alkyne were performed. The ^{1}HMNR spectra of BSP-alkyne in $CDCl_3$ before and immediately after adding 10 equivalents of TFA were collected (**Figure 4.16**). The addition of acid to BSP-alkyne led to the protonation of BMC-alkyne. The loss of the chiral spirocentre simplified the spectrum; the two singlets of the methyl groups (i) on the indoline part at 1.20 and 1.30 ppm in BSP-alkyne merged into one singlet at 1.66 ppm, while the two doublets due to the protons of the methylene group (d) adjacent to the nitrogen atom at 3.88 and 4.03 ppm in BSP-alkyne became a singlet shifted to 4.69 ppm. The signal due to the terminal alkyne group (e) were shifted from 2.09 ppm in BSP-alkyne to 2.43 ppm and the series of peaks ranging from 5.90 to 8.01 ppm (a-c, g, h, and j) were shifted to a range from 6.55 to 8.18 ppm.

The ^{1}HMNR of the same sample maintained in the dark for 17 hours showed the presence of another species in addition to the protonated MC isomer found previously. As shown in **Figure 4.16**, two signals at 1.66 and 1.87 ppm can be assigned to the methyl groups (i), two singlets at 4.69 and 5.31 ppm can be attributed to the methylene group (d) and two signals at 2.43 and 2.71 ppm are due to the terminal alkyne group (e). Indeed, two signals can be assigned to every proton of the BMCH-alkyne form, indicating the presence of two isomers of the protonated BMC-alkyne with a ratio of 2:1. After maintaining the sample in the dark

for six days, all the signals due to the first BMCH-alkyne isomer disappeared and only the signals attributed to the second BMCH-alkyne isomer were visible. Comparing these results with previous NMR studies on another BSP derivative[32] and supported by numerous studies on the BSP ring-opening mechanism[11,19] and SP acidochromism,[28] it is reasonable to assume that the acid addition to the BSP-alkyne solution in $CDCl_3$ induces the ring-opening, leading to the formation of one of the protonated BMC-alkyne isomers, which subsequently converts to a more stable isomer. As already stated, BMC isomers differ dependent on the geometrical arrangements along the central chain of the three partial C-C double bonds and they are labeled by a sequence of three C or T letters, indicating their cis or trans configuration, respectively. The protonated BMC-alkyne isomers shown in the ^{1}HNMR spectra could be the CCC, which is the first isomer formed after the C-O bond cleavage and the TTC isomer because it is the most stable structure, according to theoretical modeling calculations.[11,21] The structure of BMCH-alkyne was confirmed by ^{13}CNMR. Further experiments are needed to attribute for certain the signals of the ^{1}HNMR spectra recorded to particular BMCH-alkyne isomers.

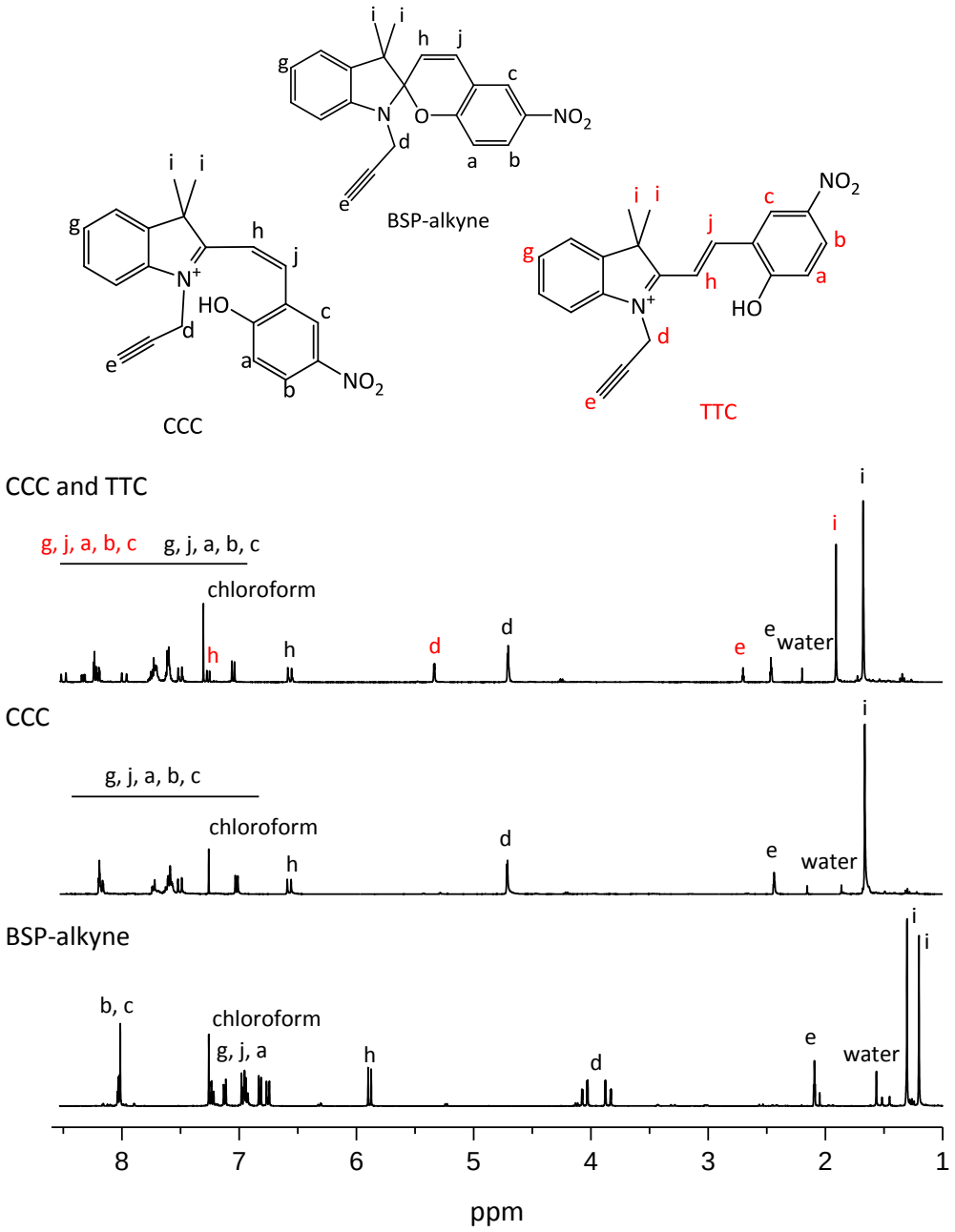

Figure 4.16 Structures of BSP-alkyne and BMCH-alkyne isomers and the corresponding ^{1}HNMR spectra. Bottom spectrum: BSP-alkyne, middle spectrum: BMCH-alkyne isomer (probably CCC isomer) recorded immediately after the addition of 10 eq of TFA, top spectrum: BMCH-alkyne isomers (probably a mixture of CCC and TTC isomers) recorded after keeping the sample for 6 days in the dark.

4.2.5 Photochromism of BSP-PEG and BSP-PPO derivatives

Preliminary studies were carried out to determine the photochromic properties of the BSP-functionalized polymers previously synthetized and depicted in **Figure 4.17**. The absorbance spectra of these compounds were measured in THF as it is a common solvent to dissolve polymers. [*Note*: all polymer concentrations for the measurements were calculated based on the polymer *M*n provided by polymer supplier Specific Polymers, and assume that this *M*n value remains unvaried after the binding of BSP units]. Photochromism was observed for all the polymers, upon exposure to UV light for one minute, a strong long-wavelength absorption band was observed at 584 nm for all the derivatives, this being associated with a change from colorless (BSP) to an indigo solution (BMC; **Figure 4.18**). All the spectra showed another absorption band at 368 nm that resembled the band observed in the spectrum of the simple BSP-alkyne.

The measured absorption maximum represents a significant blue-shift compared with BSP-alkyne previously studied; this may be due either to a more polar environment caused by the polar bonded polymers surrounding the BSP group and/or to a modification of the electronic effect of the different substituent linked to the indoline section of BSP.

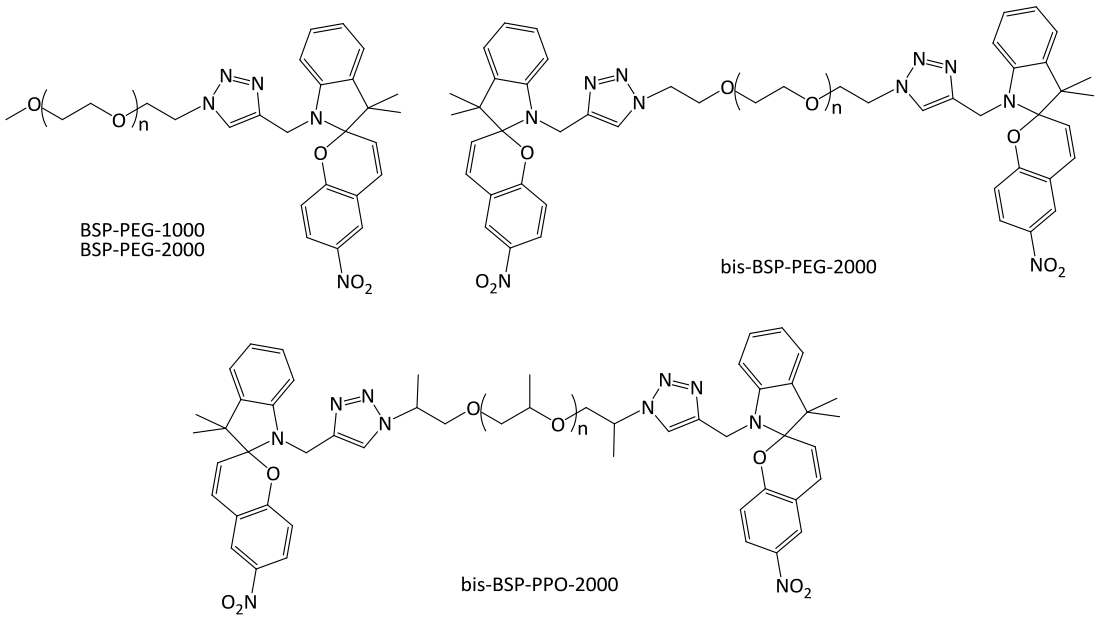

Figure 4.17 Structures of PEG and PPO functionalized with BSP-alkyne.

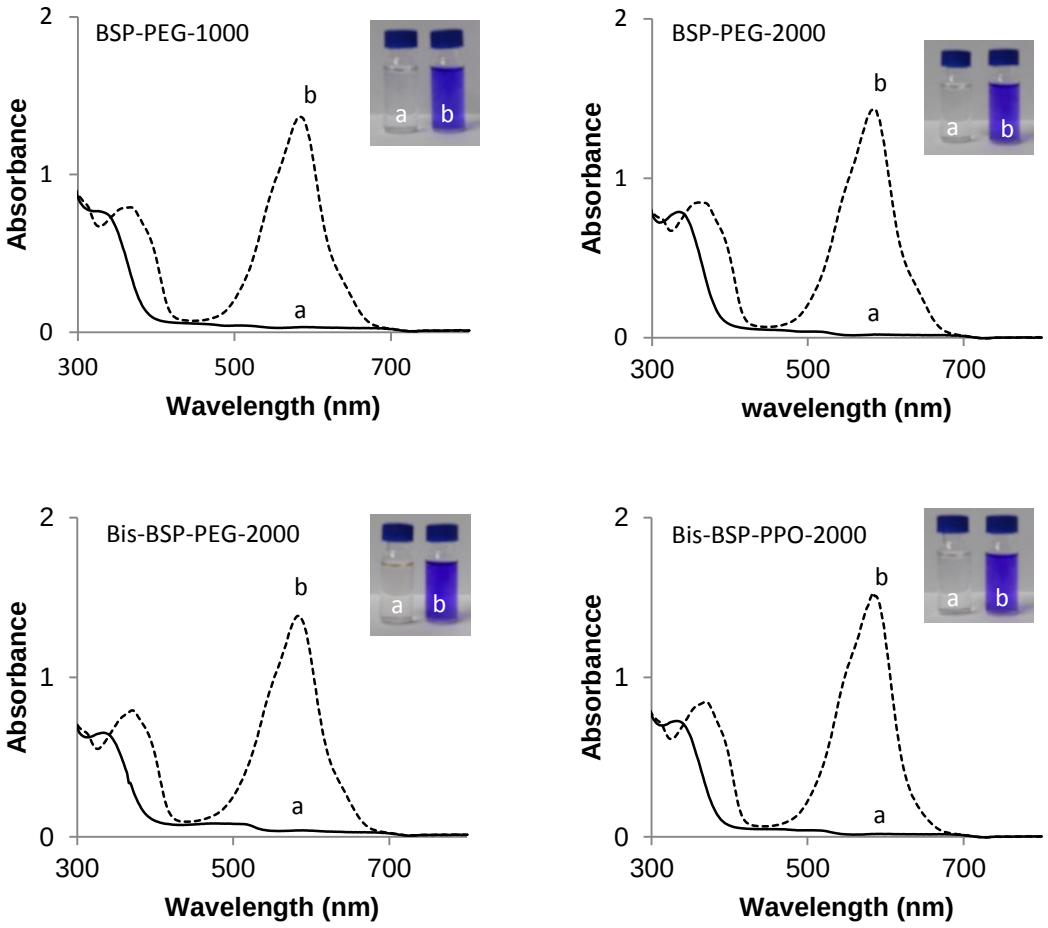

Figure 4.18 UV-Vis spectra of the BSP functionalized polymers ($1x10^{-4}$ M in THF) before (a) and after (b) 1 minute of UV (365 nm) irradiation.

The ring-closure of the BMC to the BSP form is induced upon removal of the UV light source or by irradiation with visible light. Preliminary kinetic studies were performed at room temperature to investigate how the length of the polymer and the presence of another BSP group influence the ring-closure kinetics of the BMC, which is known to follow first-order kinetics.[17] This involves inducing the formation of the BMC isomer in the polymers by exposure to the UV light for 1 minute and recording the absorbance value at the λ_{max} upon removal of the UV light. Samples were kept in the dark during the measurements to avoid the influence of ambient light.[33] **Figure 4.19** shows the reduction of the absorbance at the λ_{max} for the transition from BMC to BSP for all the polymers at room temperature.

From these measurements, the first-order rate constants *k* for the transition of BMC to BSP were determined by plotting ln(At/A0) versus time. A linear correlation between BMC (λ_{max}) and its rate constant was found for each polymer (**Table 3**).

The ring closure kinetics of the transition of BMC to BSP are comparable for all the polymers: their rate constants have similar values. Therefore, at room temperature the nature of the polymer backbone linked to the BSP units or its molecular weight have a small influence on the ring closure kinetics, which is slightly faster in the case of Bis-BSP-PEG-2000 with a *k* value of 1.62×10^{-2} s^{-1} while it is slightly slower for Bis-BSP-PPO-2000, with a *k* value of 1.09×10^{-2} s^{-1}. In all the analyzed polymers the complete conversion from BMC to their BSP form is not achieved within four minutes. Comparing these measurements on BSP functionalized polymers with the single BSP-alkyne molecule, the effect of the polymer matrix is undeniable. Indeed, the transition from BMC to BSP form of all the polymers is much slower in comparison with the simple BSP-alkyne molecule. In particular the transition from BMC-alkyne to BSP-alkyne is 4.2 times faster compared to Bis-BSP-PPO-2000.

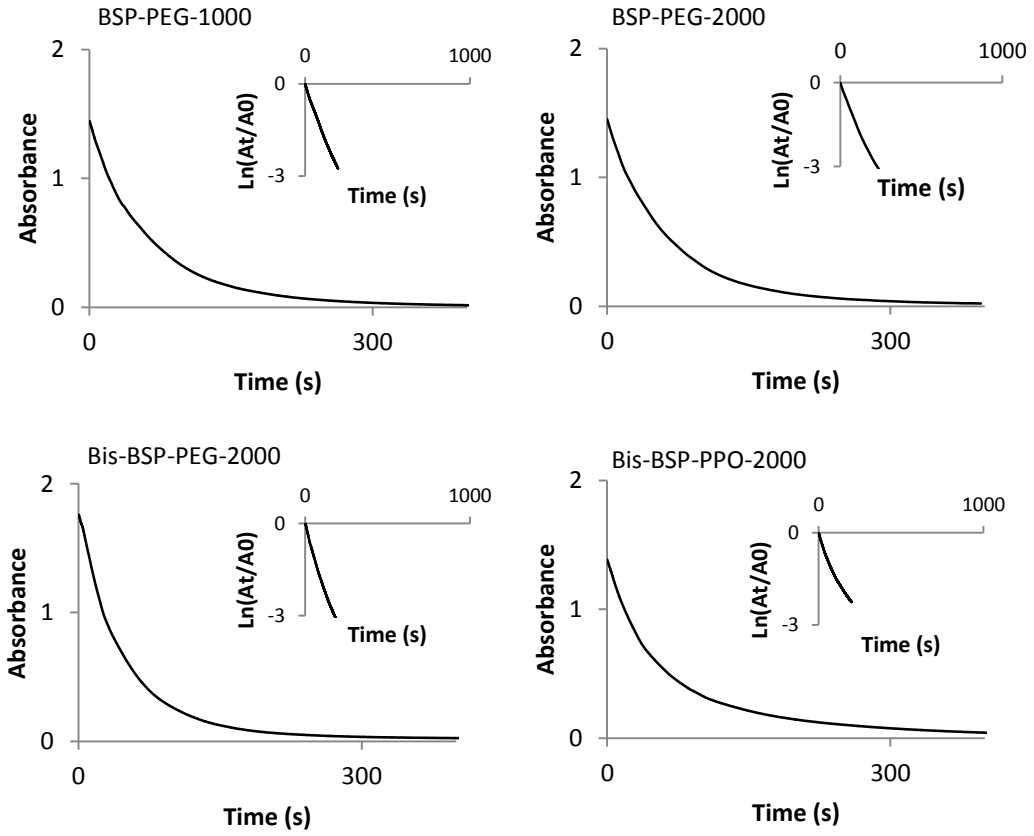

Figure 4.19 Absorbance decrease at λ_{max} (584 nm) in THF as a function of time for the transition of BMC to BSP after removing the UV light source at room temperature for all the polymers and their corresponding plots of ln(*A*t/*A*0) versus time. A linear correlation between BMC (λ_{max}) and its rate constant is revealed for each polymer.

Table 3 Values of the relaxation rate constant *k* for the transition of BMC to BSP for all the polymers measured in THF ($1x10^{-4}$ M) at room temperature (λ_{max} 584 nm). The rate constants are compared in terms of ratio to ring closure kinetic of the single molecule BSP-alkyne.

	BSP-PEG-1000	**BSP-PEG-2000**	**Bis-BSP-PEG-2000**	**Bis-BSP-PPO-2000**
K_{584} (s^{-1})	$1.37x10^{-2}$	$1.29x10^{-2}$	$1.62x10^{-2}$	$1.09x10^{-2}$
Ratio to BSP-alkyne	3.3	3.5	2.8	4.2

In order to determine the uniformity of the process an E-diagram of the system for each polymer was plotted, taking the absorbance values for 336, 370, 400, 550, 650 and 584 nm at time intervals and combining the first listed wavelengths with the last one. A diagram with the absorbance values at 336, 370, 400, 550, and 650 nm plotted versus the absorbance value at 584 nm is obtained for each polymer (**Figure 4.20**). A linear correlation between wavelengths was found for all the polymers, indicating that the reaction involves only one linear independent step.[10,22,25] These results are analogous to the spectrum features previously found for the single BSP-alkyne molecule.

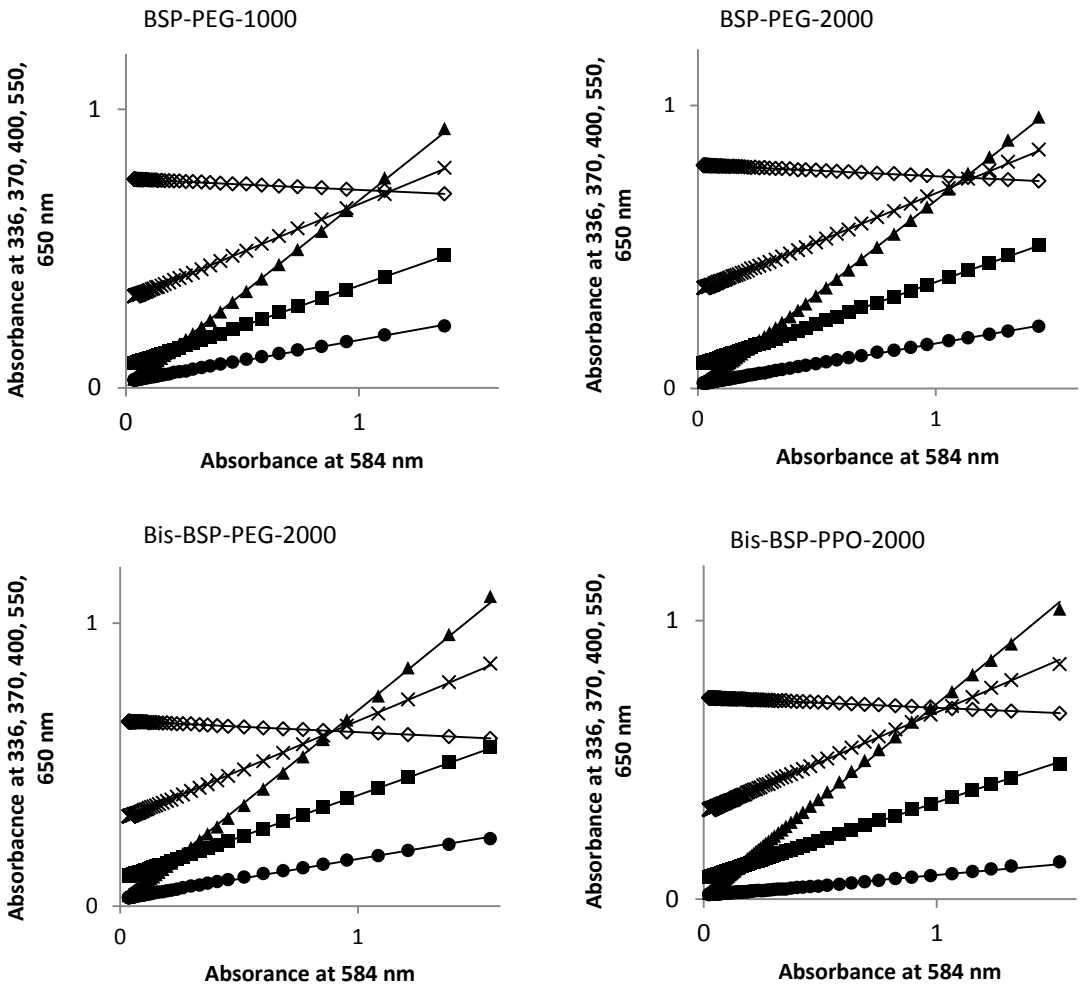

Figure 4.20 E-diagrams for the transition from BMC to BSP form of BSP-PEG and BSP-PPO derivatives in THF ($1x10^{-4}$ M), obtained using the corresponding collected spectra. The absorbance values at 336 nm (◊), 370 nm (x), 400 nm (■), 550 nm (▲) and 650 nm (●) are plotted against the absorbance value at 584 nm.

4.2.6 Fluorescence spectroscopy of BSP-PEG and BSP-PPO derivatives

Emission spectroscopy of BSP-PEG and BSP-PPO derivatives in THF was carried out. Stock solutions of BSP-PEG-1000 ($1x10^{-5}$M), BSP-PEG-2000 ($0.5x10^{-5}$M), bis-BSP-PEG-2000 ($1x10^{-5}$M), bis-BSP-PPO-2000 ($1x10^{-5}$M) were prepared *in situ* by dilution of the corresponding $1x10^{-4}$ M solution in THF, previously prepared and stored in the dark. Samples of these solutions were exposed to UV light (365 nm) for one minute to generate the BMC form and the emission spectra after excitation at 580 nm of BSP and BMC form of the polymers were collected. As shown in **Figure 4.21** all the polymers emitted and their emission bands showed a maximum at shorter wavelengths in comparison with the single molecule BSP-alkyne, as expected from the corresponding absorption spectra. BSP-PEG-1000 shows an emission band ($\lambda_{max,em}$=623 nm) with a shoulder at 676 nm, while BSP-PEG-2000 shows an emission band ($\lambda_{max,em}$=632 nm) with two shoulders at 662 nm and 684 nm. The emission bands of Bis-BSP-PEG-2000 and Bis-BSP-PPO-2000 ($\lambda_{max,em}$=630 nm and $\lambda_{max,em}$=620 nm, respectively) are broad and no shoulders are visible. The presence of two BSP units bonded to the polymer might influence its fluorescence producing a broader spectrum. Since the quantum yields of the compounds were not measured, it is difficult to draw any conclusions from the relative intensities of their emission bands.

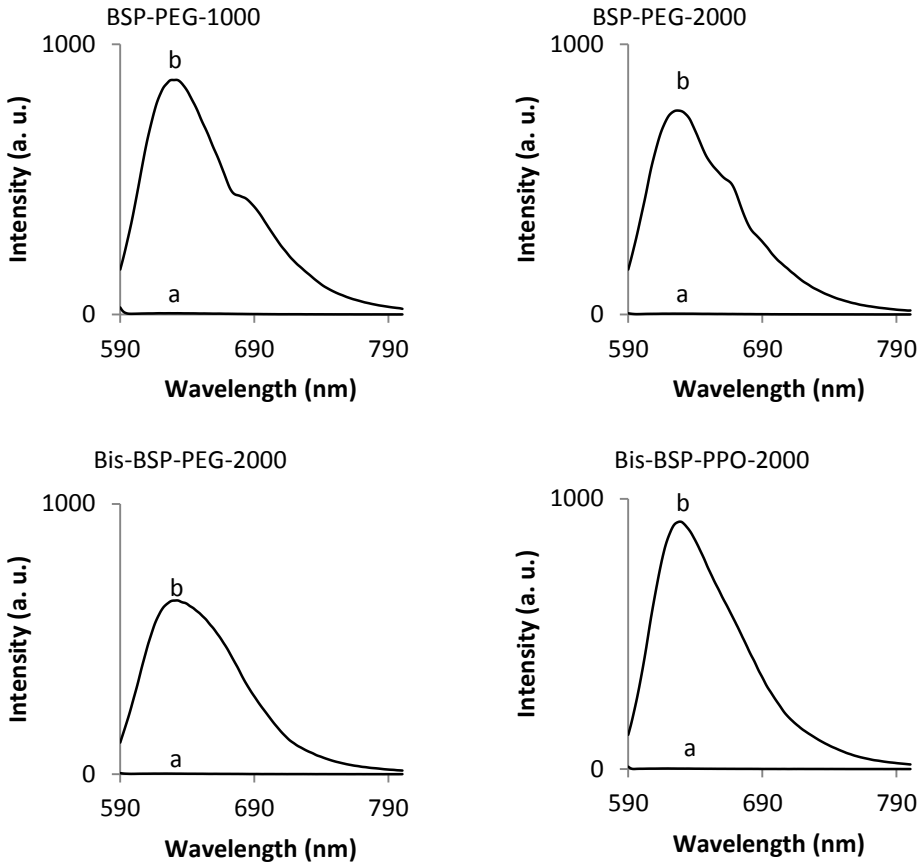

Figure 4.21 Emission spectra (λ_{exc}=580 nm) of BSP-PEG and BSP-PPO in THF ($0.5x10^{-5}$M for BSP-PEG-2000 and $1x10^{-5}$M for the other polymers) before (a) and after (b) exposure to UV light (365 nm) for 1 minute.

The switching efficiency of these compounds was studied by measuring the fluorescence response behavior (λ_{exc}=580 nm) of their BMC form after irradiating the sample with UV light (365 nm) for 1 minute several times. After every measurement the BMC form was allowed to completely reverse back to the BSP form and the sample was kept in the dark during the experiment to avoid the interference of ambient light. **Figure 4.22** shows that BSP-PEG and BSP-PPO derivatives are capable of undergoing a number of cycles between high and low fluorescence intensity values by repetitive sequence of irradiation with UV light and dark. Even if the loss of signal is quite significant for all the polymers, after the 4^{th} cycle the fluorescence intensity is about the 50% of the initial value, the fluorescence response is still considerable since the intensity is above 320 in all the cases.

As already mentioned, photodegradation of BMC is well-known and occurs when a photochromic compound is switched repeatedly between two forms over a certain number of times, mainly due to prolonged exposure to UV light.[34,35] In the literature it has been reported that reducing the degree of motion of BMC increases its photostability.[5,36] Since covalently bonding the BSP to the polymer limits the photochromic units' freedom,[5,30] it is reasonable to argue that the loss in signal recorded during the fluorescence measurements of the BSP-PEG and BSP-PPO derivatives could be due to the physical state of the sample. Investigating the behavior of these polymers in the solid state will help to validate this point.

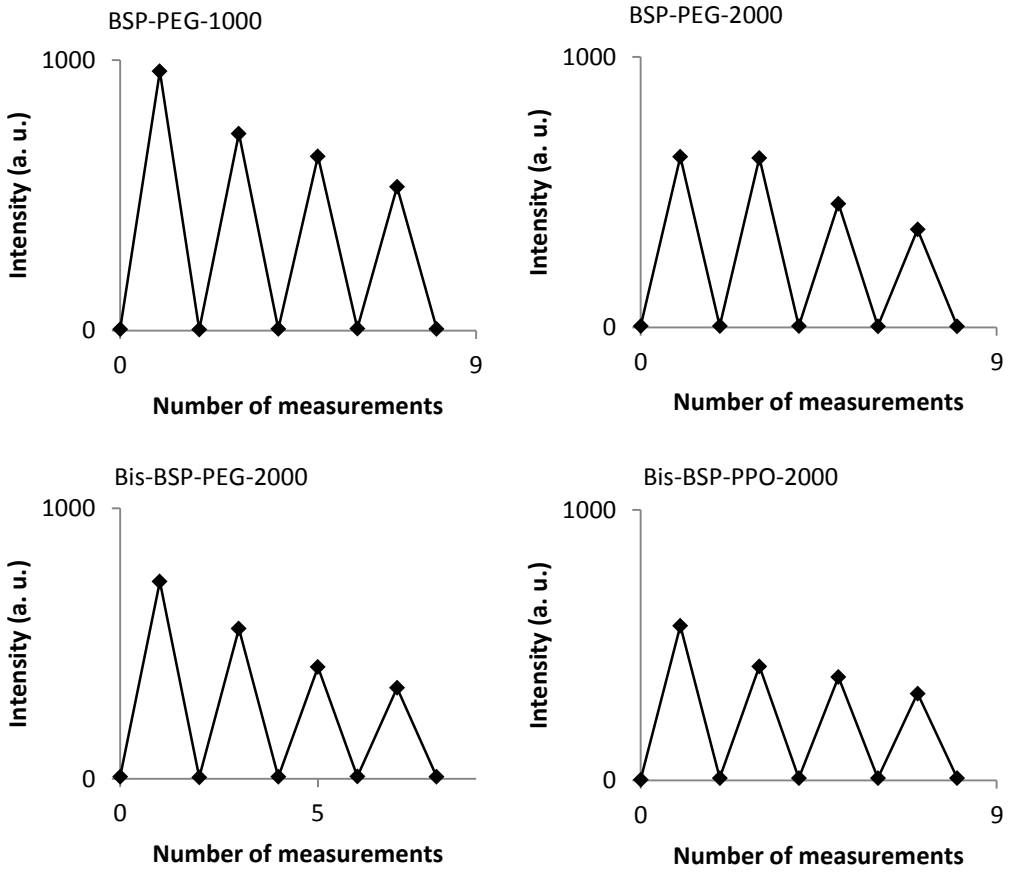

Figure 4.22 Fluorescence intensity change of BSP-PEG and BSP-PPO at their corresponding $\lambda_{max,\ em}$ after UV light exposure for 1 minute and thermal relaxation cycles.

4.3 Conclusions

BSP-alkyne was synthetized and its photochromic, solvatochromic and acidochromic properties were studied by UV-Vis, ^{1}H NMR and fluorescence spectroscopy. The features of the collected spectra suggest the presence of more than one BMC-alkyne isomer in solution at room temperature. This finding could open up new investigation opporunities to further understand this photochromic unit. BSP-alkyne was then used for the synthesis of BSP functionalized PEG and PPO derivatives and their photochromic properties were investigated at room temperature using UV-Vis spectroscopy and fluorescence spectroscopy. All the polymers analysed showed considerable photochromism. The ring-closure kinetics of all the synthetized compounds were studied at room temperature and the free BSP-alkyne molecule revealed a significantly higher rate constant in comparison with the BSP unit incorporated in the polymer. The nature of the polymer backbone linked to the BSP units and the molecular weight of the polymer have a small influence on the ring-closure rate constant at room temperature. Studies concerned with the photodegradation of the synthesized polymers were performed and revealed low photostability in solution. Further studies of these materials in their solid state need to be performed in order to determine the feasibility of their applicability within nanotechonology.

4.4 Experimental part

Materials

2,3,3-Trimethylindolenine, 1-tosyl-2-propyne, 2-hydroxy-5-nitro benzaldehyde, N_3-PEG-1000 (poly(ethylene glycol) *M*n=1000 g/mol), sodium ascorbate, copper(I)bromide and PMDETA were purchased from Sigma-Aldrich and used without further purification.1'-(propargyl)-3',3'-dimethyl-6-nitrospiro[2H-1-benzopyran-2,2'-indoline] was synthesized modifying a procedure reported in literature. 4 N_3-PEG-2000 (poly(ethylene glycol) *M*n=2000 g/mol), bis-N_3-PEG-2000 (poly(ethylene glycol) *M*n=2000 g/mol) and bis- N_3-PPO-2000 (poly (propylene oxide) *M*n=2000 g/mol) were purchased from Specific Polymers and used as received.

Methods

Proton Nuclear Magnetic Resonance spectra were recorded at room temperature with a Bruker Avance 400 (400 MHz) and a Bruker Avance Ultrashield 600 (600 MHz). Deuterated Chloroform ($CDCl_3$) was used as solvent, and signals were referred to the signal of the residual protonated solvent signal. Chemical shifts are reported in ppm and coupling constants in Hertz. Carbon NMR spectra were recorded on Bruker Avance Ultrashield 600 (600 MHz) with total proton decoupling. ATR-FTIR spectra were collected on a Perkin Elmer Spectrum 100 in the spectral region of 650-4000 cm^{-1} and were obtained from 4 scans with a resolution of 2 cm^{-1}. A background measurement was taken before the sample was loaded onto the ATR unit for measurements. Absorption spectra were recorded using a Cary 50 UV–vis spectrophotometer. Emission measurements were carried out with a Perkin Elmer LS 55 Fluorimeter. Quartz cuvettes of 1 cm path length were used. The solutions were irradiated by means of a standard 20W 365 nm UV lamp.

Synthesis of 1'-(propargyl)-3',3'-dimethyl-6-nitrospiro[2H-1-benzopyran-2,2'-indoline] (BSP-alkyne)[4]

1st step - Synthesis of 1-propargyl-2,3,3-trimethylindoleninium tosylate

2,3,3-Trimethylindolenine (1.2 mL, 7 mmol) and 1-tosyl-2-propyne (1.5 mL, 8.7 mmol) were mixed and heated at 78 °C for 3 hours. The reaction mixture was

allowed to cool to room temperature. The resulting dark violet crude material was used without further purification.

2nd step - Synthesis of 1-propargyl-2,3,3-trimethylindolenine

20 mL of a 0.5 M solution of KOH (11 mmol) in water were added to 1-propargyl-2,3,3-trimethylindoleninium tosylate (2.6 g, assuming 7 mmol). The resulting mixture was stirred for 45 minutes at room temperature and then extracted with Et_2O. The organic phase was dried over $MgSO_4$ and filtered. The solvent was removed by rotary evaporation, leading to the desired product as a dark orange oil. The product was immediately used in the following step without further purification.

3rd step – Synthesis of 1'-(propargyl)-3',3'-dimethyl-6-nitrospiro[2H-1-benzopyran-2,2'-indoline] (BSP-alkyne)

To a solution of 1-propargyl-2,3,3-trimethylindolenine (2.6 g, assuming 7 mmol) in EtOH (11 mL) 2-hydroxy-5-nitro benzaldehyde (1.64 g, 9.8 mmol) was added. The reaction mixture was heated under reflux for 4 hours. The reaction mixture was allowed to cool to room temperature of its own accord, the solvent was removed under reduced pressure to give the crude product as a dark purple oil. After purification through silica gel column chromatography (7/3 *n*-hexane/ethyl acetate as eluent) the propargyl spirobenzopyran (0.97 g, 2.8 mmol, 40%) was obtained as a bright yellow solid.^{1}H NMR (600 MHz, $CDCl_3$, δ, ppm): 1.20 (3H, s, 3'-CH_3), 1.30 (3H, s, 3'-CH_3), 2.08-2.10 (1H, m, HC≡C), 3.88 (1H, dd, *J* =18.2 Hz, *J* =2.4 Hz, NCH_2), 4.03 (1H, dd, *J* =18.2 Hz, *J* = 2.7 Hz, NCH_2), 5.09 (1H, d, *J* = 10.2 Hz, 2-CC*H*=CH), 6.75 (1H, d, *J* = 9.9, ArH), 6.82 (1H, d, *J* = 7.8 Hz, ArH), 6.91-6.99 (2H, m, ArH, 2-CCH=C*H*), 7.10-7.14 (1H, m, ArH), 7.21-7.26 (1H, m, ArH), 8.00-8.04 (2H, m, ArH); ^{13}C NMR (600 MHz, $CDCl_3$, δ, ppm): 160.2, 146.1, 141.5, 136.8, 129.4, 128.2, 126.5, 123.0, 122.0, 121.4, 121, 119, 116.5, 108.8, 106.4, 80.2, 80.0, 53.2, 33.0, 26.6, 20.5.

Synthesis of BSP-PEG and BSP-PPO derivatives

N_3-PEG-2000 (200 mg, 0.1 mmol) was dissolved in 4 mL of tetrahydrofuran and BSP-alkyne (38 mg, 0.11 mmol), 6.25 µL of an aqueous freshly prepared 4M solution

of sodium ascorbate (0.025 mmol) were added. CuBr (7.2 mg, 0.05 mmol) and PMDETA (10.44 µL, 0.05 mmol) were used as catalyst. The reaction mixture was stirred at 40 ^{o}C for 60 h under nitrogen, then precipitated twice in diethyl ether and further purified through dialysis against THF (cut off 1000 g/mol) to give 90 mg of BSP-PEG-2000. The identical synthetic and purification procedure was used for the synthesis of BSP-PEG-1000, bis-BSP-PEG-2000 and bis-BSP-PPO-2000. In all the cases the absence of the azide groups was confirmed by FT-IR.

UV-Vis spectroscopic studies on BSP-alkyne solvatochromism

$1x10^{-4}$ M stock solution of BSP-alkyne in acetonitrile, dichloromethane, diethyl ether, ethanol and tetrahydrofuran were prepared dissolving 1.7 mg of BSP-alkyne in 50 mL of the corresponding solvent and stored in the dark at room temperature. Then 3 ml of each solution were exposed to UV light irradiation for 1 minute and the absorbance spectra were recorded. The absorbance decrease at λ_{max} of BMC-alkyne was monitored, after removal of the irradiating source, in each solvent every 0.05 second for not more than 160 seconds, in order to evaluate the ring closing kinetic over time. The first-order rate constants were estimated by following the decrease of the absorbance at λ_{max} in time and subsequently examined using the equation $\ln([A\mathrm{t}]/[A0]) = -kt$ with At and A0 denote the absorbance at λ_{max} at time *t* and at the beginning of the thermal relaxation process, respectively.[37]

UV-Vis spectroscopic studies on BSP-alkyne at various concentrations

$1x10^{-4}$ M stock solution of BSP-alkyne in tetrahydrofuran was prepared dissolving 1.7 mg of BSP-alkyne 50 mL of solvent. $0.5x10^{-4}$M, $1x10^{-5}$M solutions of BSP-alkyne in tetrahydrofuran were prepared by dilution of the $1x10^{-4}$ M stock solution. All these solutions were kept kept in the dark at room temperature. Then 3 ml of each solutions were irradiated with UV light for 1 minute and absorption spectra were recorded every 6 seconds. The absorbance values at λ_{max} (598 nm) were extrapolated and plotted against time from the collected spectra, in order to evaluate the ring closing kinetic constant value for each concentration. The first-order rate constants were examined using the equation $\ln([A\mathrm{t}]/[A0]) = -kt$ with At

and A0 denote the absorbance at λ_{max} at time *t* and at the beginning of the thermal relaxation process, respectively.[37]

E-diagrams for each concentration were generated by extrapolating the absorbance values at determined wavelengths from each collected spectrum and plotting these values against the absorbance values of a defined wavelength.[10]

Fluorescence spectroscopic studies on BSP-alkyne

$1x10^{-4}$ M stock solution of BSP-alkyne in tetrahydrofuran was prepared dissolving 1.7 mg of BSP-alkyne 50 mL of solvent and stored in the dark at room temperature. Excitation wavelengths were set at 440 and 594 nm. Fluorescence emission spectra of BMC-alkyne were recorded before and after photoisomerisation of BSP-alkyne by exposure to UV light for 1 minute.

UV-Vis spectroscopic studies on acidochromism of BSP-alkyne

$1x10^{-4}$ M stock solution of BSP-alkyne in tetrahydrofuran was prepared dissolving 1.7 mg of BSP-alkyne 50 mL of solvent and stored in the dark at room temperature.

3 ml of solution were exposed to 1 minute of UV light irradiation and the absorbance spectrum was recorded. The same sample was kept in the dark until complete thermal relaxation and then 300 µL of a solution of TFA in THF ($1x10^{-2}$ M) were added and the spectrum after irradiating with UV light for 1 minute was recorded.

^{1}H NMR studies on acidochromism of BSP-alkyne

10 mg of BSP-alkyne were dissolved in 0.75 mL of $CDCl_3$, the sample was kept in the dark and stored at room temperature overnight. After recording ^{1}HNMR spectrum, 10 equivalents of TFA were added to the sample and another ^{1}HNMR spectrum were collected immediately. The addition of acid produced a change in colour the solution turned yellow. The same sample was maintained in the dark and two ^{1}HNMR spectra were collected after 17 hours and 6 days.

UV-Vis spectroscopic studies on photochromism of BSP-PEG and BSP-PPO derivatives

Approximately, $1x10^{-4}$ M stock solutions of BSP-PEG-1000, BSP-PEG-2000, bis-BSP-PEG-2000 and bis-BSP-PPO-2000 in tetrahydrofuran were prepared [Note: all polymer concentrations for the measurements were calculated based on the polymer *M*n given by provider company Specific Polymers, assuming that their *M*n is unvaried after binding BSP units] and stored in the dark at room temperature.

Then 3 ml of each solution were exposed to UV light irradiation for 1 minute and the absorbance spectra were recorded. The absorbance decrease at λ_{max} (584 nm) was monitored, after removal of the irradiating source, for each polymer every 0.05 second for 400 seconds, in order to evaluate the ring closing kinetic over time. The first-order rate constants were estimated by following the decrease of the absorbance at λ_{max} in time and subsequently examined using the equation $\ln([A_t]/[A_0]) = -kt$ with A_t and A_0 denote the absorbance at λ_{max} at time *t* and at the beginning of the thermal relaxation process, respectively.[37]

E-diagrams were generated by extrapolating the absorbance values at determined wavelengths from each collected spectrum and plotting these values against the absorbance values of a defined wavelength.[10]

Fluorescence spectroscopic studies on BSP-PEG and BSP-PPO derivatives

Stock solutions of BSP-PEG-1000, BSP-PEG-2000, bis-BSP-PEG-2000 and bis-BSP-PPO-2000 in tetrahydrofuran were prepared [*Note*: all polymer concentrations for the measurements were calculated based on the polymer *M*n given by provider company Specific Polymers, assuming that their *M*n is unvaried after binding BSP units] and stored in the dark at room temperature. $1x10^{-5}$M solution of BSP-PEG-1000, bis-BSP-PEG-2000, bis-BSP-PPO-2000 and $0.5x10^{-5}$M BSP-PEG-2000 were prepared by dilution from the corresponding stock solution. Excitation wavelength was set at 580 nm. Fluorescence emission spectra of BSP-PEG-1000, BSP-PEG-2000, bis-BSP-PEG-2000 and bis-BSP-PPO-2000 were recorded before and after photoisomerisation by exposure to UV light for 1 minute.

4.5 References

1. Such G., Evans R., Yee L., Davis T. *Polym. Rev.* **2003**, *43*, 547.
2. Fukushima K. V.AJ,FT. *Chem. Mat.* **2007**, 644.
3. Tomasulo M. G.S,RFM. *Adv. Funct. Mat.* **2005**, 787.
4. Bertoldo M., Nazzia S., Zampano G., Ciardelli F. *Carbohydr. Polym.* **2011**, *85*, 401.
5. Klajn R. *Chem. Soc. Rev.* **2013**, DOI:10.1039/c3cs60181a.
6. Kolb H.C., Finn M.G., Sharpless K.B. *Angew. Chem. Int. Ed.* **2001**, *40*, 2004.
7. Zhang Q. N.Z,YY,QS,TH. *Macromol. Rapid Commun.* **2008**, 193.
8. Golas P.L., Matyjaszewski K. *QSAR Comb. Sci.* **2007**, *26*, 1116.
9. Hawker C.J., Wooley K.L. *Science* **2005**, *309*, 1200.
10. Dürr H., Bouas L.H. *Photochromism: molecules and systems*. Boston: Elsevier; **2003**.
11. Minkin V.I. *Chem. Rev.* **2004**, *104*, 2751.
12. Reichardt C., Welton T. *Solvents and solvent effects in organic chemistry.* Weinheim, Germany: Wiley-VCH; **2010**.
13. Catalán J., López V., Pérez P., Martin-Villami l.R., Rodriguez J.G. *Liebigs Ann.* **1995**, 241.
14. Catalán J. *J. Phys. Chem. B* **2009**, 5951.
15. Suzuki T., Lin F.T., Priyadashy S., Weber S.G. *Chem. Commun.* **1998**, 2685.
16. Castro P.J., Gómez I., Cossi M., Reguero M. *J. Phys. Chem. A* **2012**, *116*, 8148.
17. Gorner H. *Phys. Chem. Chem. Phys.* **2001**, *3*, 416.
18. Negri R.M. *J. Chem. Educ.* **2001**, *78*, 645.
19. Berkovic G., Krongauz V., Weiss V. *Chem. Rev.* **2000**, *100*, 1741.
20. Chibisov A.K., Gorner H. *Chem. Phys.* **1998**, *237*, 425.
21. Emsting N.P., Arthen-Engeland T. *J. Phys. Chem.* **1991**, *95*, 5502.
22. Li Y., Zhou J., Wang Y., Zhang F., Song X. *J. Photochem. Photobiol. A* **1998**, *113*, 65.
23. Tratnyek P.G., Reilkoff T.E., Lemon A.W., Scherer M.M., Balko B.A., Feik L.M., Henegar, D. B. *Chem. Educator* **2001**, *6*, 172.

24. Chylewski C. *Angew. Chem. Inter. Ed.* **1971**, *10*, 195.

25. Mauser H., Gaugliz G. *Photokinetics: theoretical fondamentals and applications*. New York: Elsevier; **1998**.

26. Natali M., Aakeröy C., Desper J., Giordani S. *Dalton Trans.* **2010**, *39*, 8269.

27. Raymo F.M., Giordani S. *J. Am. Chem. Soc.* **2001**, *123*, 4651.

28. Wojtyk J.TC., Wasey A., Xiao N.N., Kazmaier P.M., Hoz S., Yu C., Lemieux R.P., Buncel E. *J. Phys. Chem. A* **2007**, *111*, 2511.

29. Raymo F.M. *Adv. Mater.* **2002**, *14*, 401.

30. Radu A., Byrne R., Alhashimy N., Fussaro M., Scarmagnani S., Diamond D. *J. Photochem. Photobiol. A* **2009**, *206*, 109.

31. Kang H., Lee Y.S., Kim E., Kang Y., Kim D.W., Lee C. *Mol. Cryst. Liq. Cryst.* **2003**, *406*, 363.

32. Raymo F.M., Giordani S. *J. Org. Chem.* **2003**, *68*, 4158.

33. Stitzel S., Byrne R., Diamond D. *J. Mater. Sci.* **2006**, *41*, 5841.

34. Li X., Li J., Wang Y., Matsuura T., Meng J. *J. Photochem. Photobiol. A* **2004**, *161*, 201.

35. Bilski P., McDevitt T., Chignell C.F. *Photochem. and Photobiol.* **1999**, *69*, 671.

36. Tork A., Boudreault F., Roberge M., Ritcey A.M., Lessard R.A., Galstian T.V. *Appl. Optics* **2001**, *40*, 1180.

37. Flannery J.B. *J. Am. Chem. Soc.* **1968**, *90*, 5660.

Chapter 5

Spiropyran-Based Polymers: ATRP *vs* Click Chemistry

5.1 Introduction

Previously we have demonstrated that one or two benzospiropyran (BSP) end-groups of a polymer chain influence the polymer properties, such as photochromism, metal binding and fluorescence. The light responsive behaviour of the BSP-PMMA, BSP-PEG and BSP-PPO derivatives synthetized have been widely discussed in the previous chapters. The considerable results obtained in modulating polymer properties by placing one or two chromophores into a polymer chain have inspired us to design polymers incorporating multiple chromophoric units in defined positions. In the literature there are several examples of well-defined polymers incorporating BSP forming fascinating microstructures.[1] As previously mentioned, in 2007 Matyajaszewski *et al.* synthesized a diblock copolymer of poly(ethylene glycol) and poly(spiropyran-containing methacrylate) by ATRP.[2] This amphiphilic block copolymer, bearing 8 BSP units, formed micelles for efficient encapsulation and release of hydrophobic dye. (**Figure 1.13**).[2] In 2008 Chen et al. obtained an amphiphilic triblock copolymer by ATRP, containing 3 BSP units able to form micelles in aqueous media exploitable as a novel scaffold for fluorescence resonance energy transfer. (**Figure 5.1**).[1]

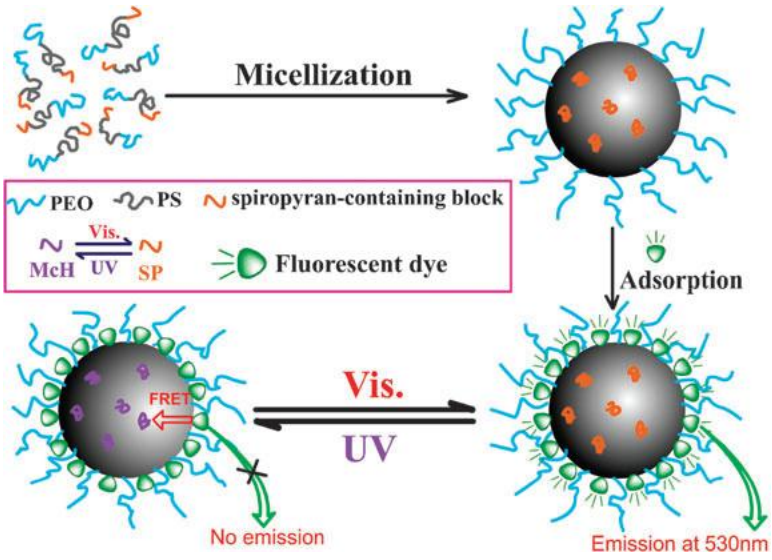

Figure 5.1 Formation of a Fluorescence resonance energy transfer system by a triblock copolymer micelle and reversible fluorescence modulation for a hydrophobic fluorescent dye with the micelle as the scaffold.[1]

In 2010 Jin et al. disclosed a photo and thermo double-responsive block copolymer forming micelles and reverse micelles in aqueous solution. The copolymer was synthesized by ATRP of a spiropyran-containing methacrylate with di(ethylene glycol)methyl ether methacrylate, contained 9 units of BSP. (**Figure 5.2**).[3] Vamvakaki presented the copolymerization of 2-(dimethylamino)ethyl methacrylate (DMAEMA) and BSP-methacrylate to synthesize free copolymers and spherical polymer brushes from silica nanoparticles.[4,5] Locklin reported the ATRP synthesis of a series of higher molecular weight spiropyran-containing methacrylate copolymers with compositions of BSP between 10-100%.[6]

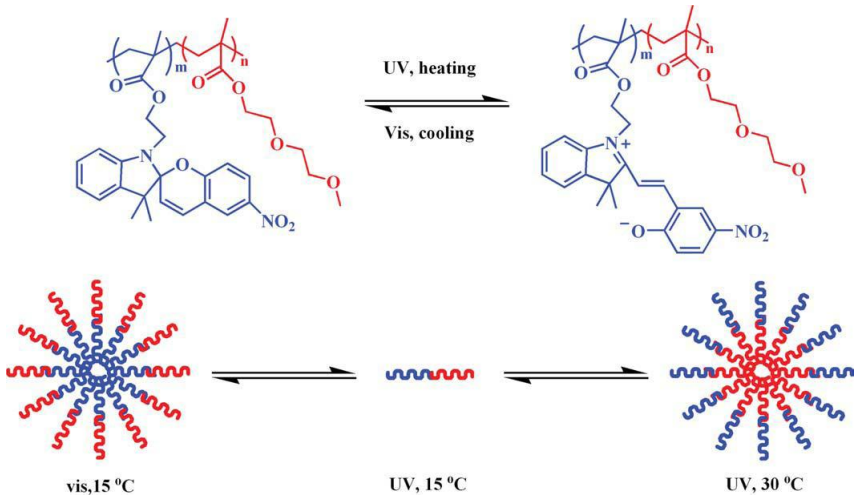

Figure 5.2 Schematic representation of double-responsive micellarization of PSPMA-b-PDEGMMA in aqueous solution.[3]

The use of controlled radical polymerization (CRP) techniques enables the generation of polymers with photochromic units in defined positions either pendant to the polymer backbone or as the polymer end-group.[7] The advancements CRP permits to design, develop and synthetize polymers with distinctive architectures leading to multiple morphologies, including micellar structures and vesicles. We are interested in synthesizing well-defined polymeric systems with complex architectures such as star and graft copolymers bearing a high density of BSP units in the side chain to produce highly responsive light-mediated smart materials (**Figure 5.3**). Molecular brushes are a special type of graft copolymer in which multiple polymer chains are grafted to a linear polymer backbone.[8] The main chain is generally referred to as the backbone, while the branches are referred as the side

chains. The shape of the molecular brushes depends on the ratio between the length of the the backbone and the side chains. When the backbone is much longer than the side chains, the polymer adopts a cylindrical shape, while if the backbone is shorter than the side chains, the polymer adopt a spherical shape that resembles star polymers.[8]

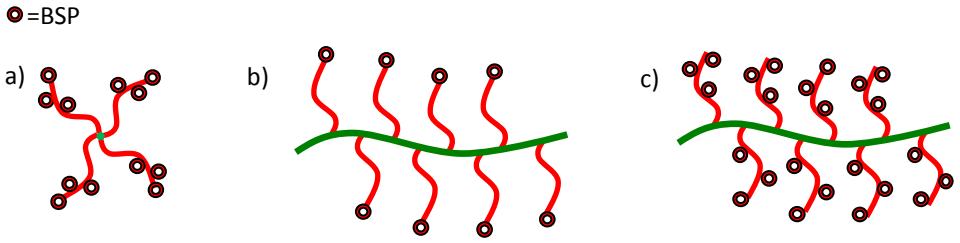

Figure 5.3 Representation of targeted BSP containing polymer architectures. a) Star-like architecture; b) molecular brushes with a BSP pendant to the polymer backbone and c) molecular brushes with multiple BSP pendant to the polymer backbone.

When carrying out ATRP of BSP functional acrylate we observed that the reaction was inhibited in the presence of BSP. As this appeared in contrast to previous reports[1-7] we verified this observation in a series of experiments and explored alternative routes to polymers with high BSP content by employing 'click' chemistry.

5.2 Results and Discussion

5.2.1 Synthesis of BSP-polymers ATRP versus click chemistry

ATRP is one of the most successful techniques for the synthesis of well-defined polymers with designed molecular weights and narrow molecular weight distributions. In the literature most of the reports on BSP polymers synthesized by controlled radical polymerization involve polymers with no more than 10 BSP units. Locklin's work in 2010 represents the only exception: in his paper he described the synthesis and the characterization of a series of spiropyran-containing methacrylate copolymers with a composition of BSP between 10-100%.[6] Encouraged by the results of our literature research, we decided to synthesize well-defined spiropyran-containing acrylate polymers with complex architectures that bear a high density of BSP, using ATRP.

We first synthesized a BSP functional acrylate monomer (BSPA), using a modified literature procedure[9] starting from BSP-OH-1, as shown in **Scheme 5.1**. The monomer was obtained in 72% yield as a yellow solid. The structure of the monomer was confirmed by ^{13}C and ^{1}H NMR, as shown in **Figure 5.4**.

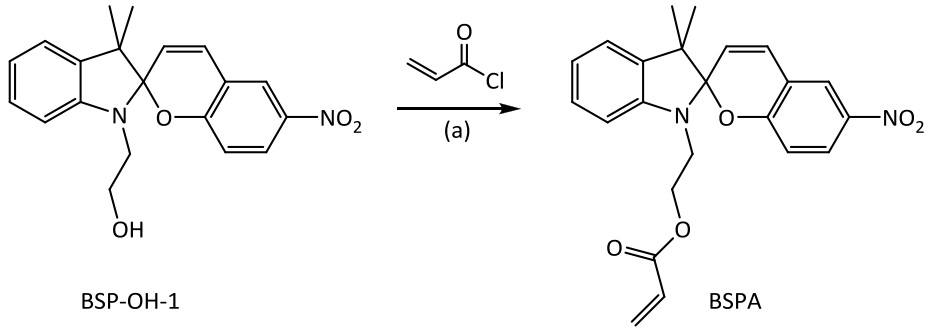

Scheme 5.1 Synthesis of BSPA. Reaction conditions: (a) Et_3N (2 eq), N_2, THF, 0 °C, 15 h.

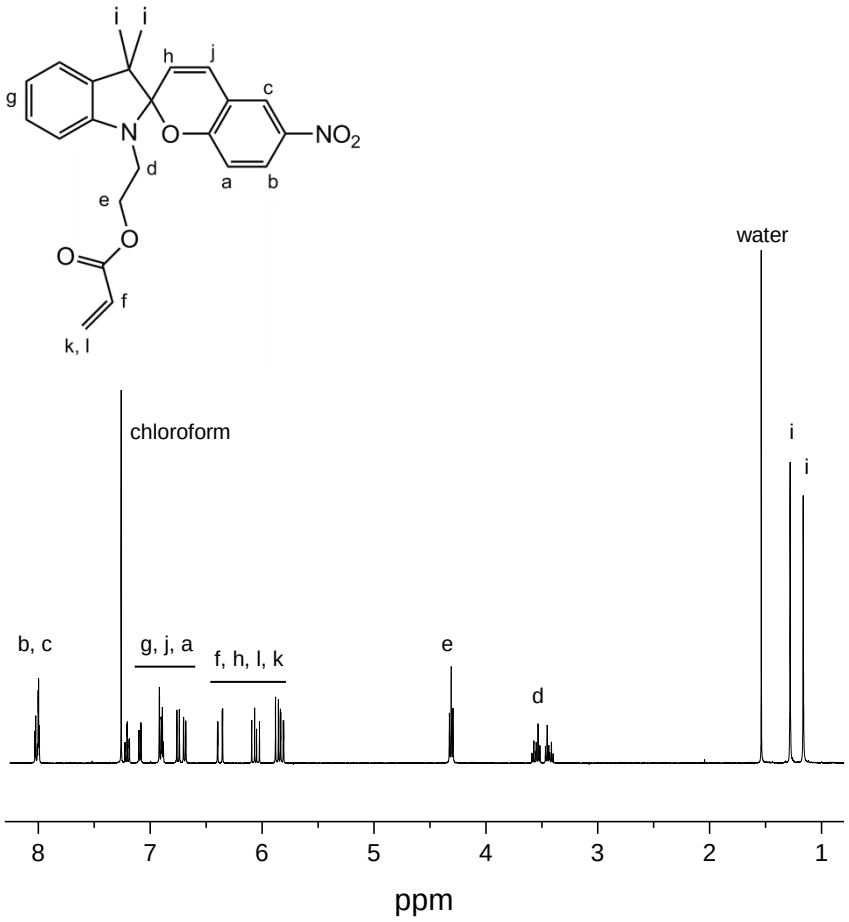

Figure 5.4 ^{1}H NMR spectrum of BSP functionalized monomer (BSPA) in chloroform.

The ^{1}H NMR shows characteristic peaks for BSP derivatives: two singlets of the methyl groups on the indoline part at 1.16 and 1.28 ppm (i) and the series of peaks ranging from 5.87 to 8.26 ppm (a–c, g, h, and j). Characteristic peaks can be assigned to the methylene and methine groups of the acrylate monomer at 5.82, 6.06 and 6.38 ppm (k, f, l), the multiplets of the methylene groups adjacent to the nitrogen and oxygen atom centered at 3.5 (d), and 4.3 ppm (e), respectively. The latter experienced a shift from 3.77 upon esterification with acryloyl chloride.

In order to synthesize complex polymers with star-shaped and hyperbranched architecture, we have prepared, following the procedures reported in literature,[10,11] appropriate initiators from which polymer chains can be grown. For the preparation of star-like polymers a tetrafunctional initiator for ATRP was synthetized, as shown in **Scheme 5.2**, by esterification with an α-bromo acid halide, starting from the commercially available pentaerythritol.[10] After recrystallization, the pure product

was obtained in 40% yield as white crystals. The structure of the four-arm initiator was confirmed by ^{1}H NMR.

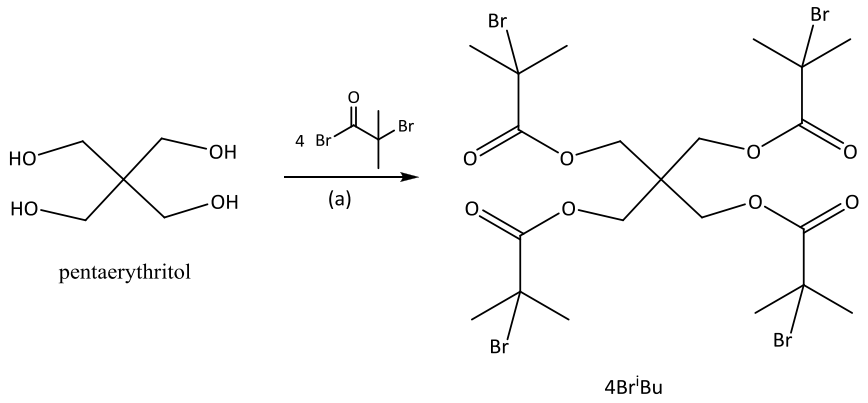

Scheme 5.2 Synthesis of the tetrafunctional initiator pentaerythritol tetrakis(2-bromoisobutyrate) (4Br^{i}Bu) from Pentaerythritol. Reaction conditions: (a) Et_3N (4 equiv), N_2, THF, 0 °C, 15 h.

For the synthesis of molecular brushes a set of macroinitiators with different molecular weights were prepared using ATRP, following a modified literature procedure.[11] Poly(2-bromoisobutyryloxyethyl methacrylate) (PBiBEMA) macroinitiators were synthetized in two steps (**Scheme 5.3**), starting from the commercial 2-(trimethylsilyloxy) ethyl methacrylate (HEMATMS). In the first step HEMATMS was polymerized by ATRP using ethyl 2-bromoisobutyrate (EBiB) as the initiator, CuCl/$CuCl_2$ and HMTETA as the catalytic system and anisole as the solvent. In order to vary the molecular weights of the resulting polymers, different initial monomer-to-initiator ratios or different reaction times were used and the reactions were stopped once the monomer conversion reached around 75% (monitored by ^{1}H NMR). The structure of the poly(trimethylsilyloxyethyl methacrylate) (PHEMATMS) was confirmed by ^{1}H NMR. In the second step, PHEMATMS was esterified with 2-bromoisobutyryl bromide in conjunction with the *in situ* deprotection of the silyl ester, in the presence of KF, tetrabutylammonium fluoride (TBAF) and 2,6-ditert-butylphenol. The latter was used as an inhibitor to prevent cross-linking (**Scheme 5.3**).[12]

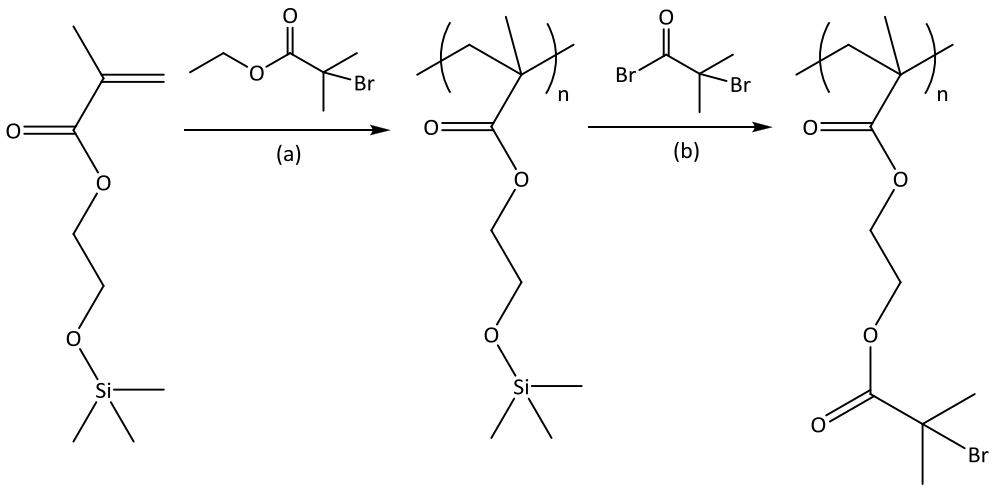

Scheme 5.3 General synthesis of the multibromo macroinitiator PBiBEMA. Reaction conditions: (a) CuCl/$CuCl_2$/HMTETA (0.8/0.2/1), N_2, anisole, 60 °C; (b) KF/TBAF, 2,6-di tert butyl phenol, THF, room temperature**.**

The PBiBEMA ATRP macroinitiators were characterized by GPC (**Table 1**) and ^{1}H NMR (**Figure 5.5**). In the ^{1}H NMR spectrum the signal at 0.15 ppm corresponding to the TMS group disappeared while a signal at 1.97 ppm (e) is clearly visible, indicating the presence of the methyl groups of 2-bromoisobutyryl units. The molecular brushes will be generated by grafting polymer chains from the macroinitiators.

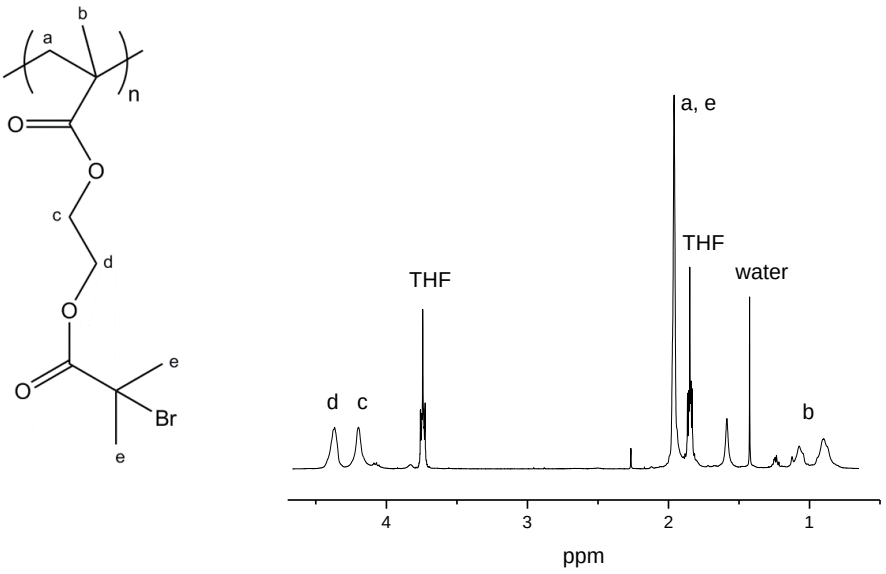

Figure 5.5 ^{1}H NMR spectrum of PBiBEMA macroinitiator in chloroform.

Table 1 Characterization of the PBiBEMA macroinitiator prepared by ATRP.

Entry	Conv[(a)] (%)	M_n[(b)](g/mol)	PDI[(b)]
PBiBEMA1	77	3,600	1.1
PBiBEMA2	72	4,900	1.1
PBiBEMA3	70	5,800	1.2
PBiBEMA4	79	7,300	1.1

(a) Determined by ^{1}HNMR spectroscopy from integration of peaks at the relative peaks at 6.20 ppm and 6.47 ppm, indicative of the presence of HEMATMS. (b) from GPC analysis.

Our initial intention was to use ATRP to grow BSP acrylate monomer from the four-arm initiator and the multibromo macroinitiators. Numerous polymerizations were performed to obtain BSP based graft copolymers, including both the homo and copolymerization of BSPA with methylmethacrylate (MMA) and n-butyl acrylate (n-BA) varying the reaction conditions (i.e. temperature, reaction time, catalytic system and stoichiometry) but a well-defined graft copolymer was not obtained. Employing a mathacrylate functional BSP did not result in any improvement.

Intrigued by these negative results and the limited literature concerning the controlled radical polymerization of BSP acrylate monomers, we investigated the influence of BSP on ATRP. In a series of control experiments, ATRP of MMA was conducted under standard reaction conditions (EBiB as the initiator, CuCl/$CuCl_2$ and 1,1,4,7,10,10-hexamethyltriethylenetetraamine (HMTETA) as the catalytic system in anisole, 60°C, 35 minutes) in the presence of various ratios of a non-polymerizable BSP-OH-1 to initiator (**Scheme 5.4**). When the ratio of BSP-OH-1 to the ATRP initiator was below 1, the BSP derivative did not significantly affect the control of the ATRP process (entry 2, **Table 2**) and a polymer with similar molecular weight and dispersity compared to the product generated from the reaction without BSP-OH-1 was obtained (entry 1, **Table 2**). In both cases the monomer conversion was around 80% as determined by ^{1}H NMR spectroscopy using the integrals of MMA double bond peaks at 5.56 ppm and 6.10 ppm (**Figure 5.6**). When the BSP-OH-1 to initiator ratio was > 1 (entry 3 and 4, **Table 2**), the ^{1}H NMR spectra showed the

disappearance of the MMA double bond peaks but no polymer was formed as illustrated in **Figure 5.6** for the reaction with a molar ratio of BSP-OH-1 to EBiB of 4:1 (entry 3 **Table 2**). To exclude any misinterpretation of data, the monomer consumption was also monitored gravimetrically, confirming that the reduction of the double bond signals in the ^{1}H NMR spectra was indeed due to a reaction rather than evaporation. These results suggest that if ATRP is carried out in the presence of an excess of a BSP derivative, the latter interferes with the radical process, consuming the monomer and impeding the polymer formation. To further verify this finding, a set of reactions under the same experimental conditions was carried out in the presence of BSP-OH-1 omitting either monomer or initiator. The ^{1}H NMR spectrum of the product obtained after the reaction without monomer (ratio BSP-OH-1 to initiator = 0.8; entry 5, **Table 2**) machtes the ^{1}H NMR of BSP-OH-1, suggesting no reaction occurred under these conditions. In contrast, the results of the reaction carried out without inititiator but in the presence of MMA (entry 6, **Table 2**) resembled the results obtained in the presence of an excess of BSP derivative. Indeed, in the ^{1}H NMR spectrum of the final product the peaks 5.56 ppm and 6.10 ppm, indicative of the presence of the MMA double bonds, were considerably reduced with respect to the ^{1}H NMR of the initial reaction mixture (**Figure 5.6**). According to the peak integration, around 75% of the double bonds were consumed without any detectable polymer formation.

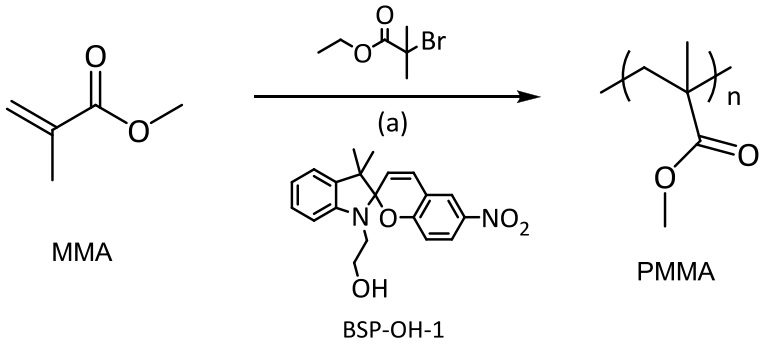

Scheme 5.4 MMA polymerization used as standard reaction to study the effect of BSP-OH-1 on ATRP. Reaction conditions: (a) CuCl/$CuCl_2$/HMTETA (0.8/0.2/1), N_2, anisole, 60 °C, 35 min. The same reaction was performed adding different amounts of BSP-OH-1.

Table 2 Experimental conditions for MMA ATRP polymerization in the presence of BSP-OH-1 and data collected after the reaction.

Entry	BSP-OH-1 (mmol)	MMA (mmol)	EBiB (mmol)	Monomer Consum[(a)] (%)	M_n [(c)] (g/mol)	PDI[(c)]
Test 1	–	20	1	78.5	2,700	1.3
Test 2	0.8	20	1	80.2	2,600	1.2
Test 3	4.0	20	1	100	–	–
Test 4	8.0	20	1	83.6[(b)]	–	–
Test 5	0.8	–	1	–	–	–
Test 6	0.8	20	–	74.3	–	–

(a) Determined by ^{1}H NMR spectroscopy from integration of peaks at 5.56 ppm and 6.10 ppm, indicative of the presence of MMA double bonds. (b) At this concentration BSP-OH-1 was only partially soluble in THF. (c) from GPC analysis.

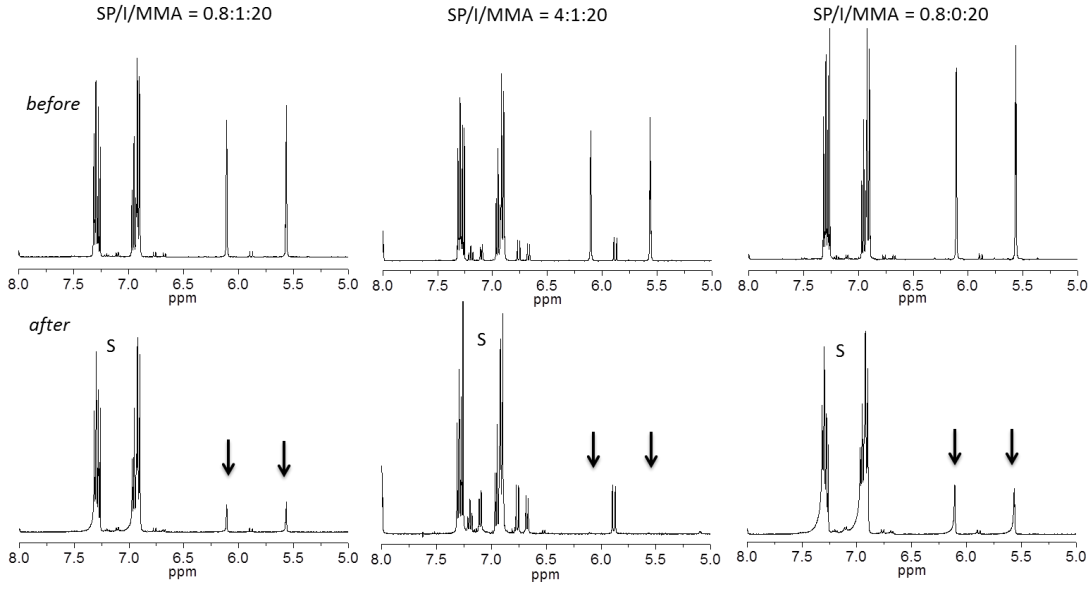

Figure 5.6 Representative sections of ^{1}H NMR spectra of MMA ATRP in the presence of BSP-OH-1 at different ratios in chloroform. Top row: spectra of sample taken before the start of the ATRP; bottom row: spectra of samples taken after 35 minutes of reaction. The peaks of the reaction solvent anisole (S) were used as internal standard. Reactant ratios refer to entries in **Table 2** (from left to right: entries 2, 3 and 6). Arrows mark the reduced MMA double bond peaks.

In the literature the ability of BSP to form biradicals by the homolytical cleavage of the BSP C-O bond is widely reported (**Figure 5.7**).[13,14] The involvement of the BSP biradicals in the consumption of double bonds cannot be confirmed without extensive additional experiments and sophisticated analysis. However, it can be speculated that they might cause interference with the radical polymerization, leading to an inhibition of the ATRP. In the presence of an excess of BSP with respect to the radical species this process would be more pronounced, while at a low ratio, as is the case for BSP functional ATRP initiators, it does not significantly influence the polymerization. These obsevations suggest that the formation of high molecular weight polymers and polymer architectures with a high BSP density by ATRP, and possibly CRP techniques in general, would suffer from this side-reaction. Indeed, most literature examples of CRP of BSP-functional monomers involve polymers with no more than 10 BSP units or/and employ copolymerization approaches.[1-4,15] To the best of our knowledge only Locklin described the synthesis of a series of spiropyran-containing methacrylate copolymers with a composition of BSP between 10-100% and with more than 10 BSP units by ATRP. However, no reaction yields were disclosed in this publication.[6]

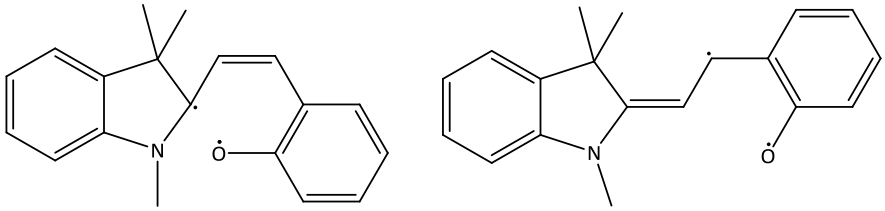

Figure 5.7 Diradicals formed by homolytical cleavege of the C_{spiro}-O bond in BSP derivatives.

To overcome the difficulties observed in the ATRP process we devised an alternative route to analogous polymers via the attachment of BSP to a preformed polymer. This concept was previously explored by Möller on copolymers obtained by reversible addition fragmentation chain transfer (RAFT).[16] In this example, carboxylic acid functional BSP units were conjugated to hydroxyl groups of the comonomer hydroxyethyl methacrylate by esterification. Here, we investigated the scope of copper-catalyzed azide-alkyne 1,3-dipolar cycloaddition (CuAAC) click chemistry due to its high efficiency in polymer functionalization and compatibility

with ATRP.[17-21] This strategy involved using ATRP to synthetize a well-defined polymer backbone bearing side chain azide or alkyne functional groups for CuAAC of a BSP with the appropriate clickable functionality (**Scheme 5.5**). According to Matyjaszewski, the ATRP of propargyl methacrylate (route a, **Scheme 5.5**) leads to polymers with high polydispersities and multimodal molecular weight distributions, presumably due to radical addition to the alkyne groups and possible coordination of copper catalyst to the monomer.[17] The route selected involved the synthesis of well-defined azide-functional polymers and their orthogonal conjugation by reaction with an alkyne functional BSP (route b, **Scheme 5.5**).[22]

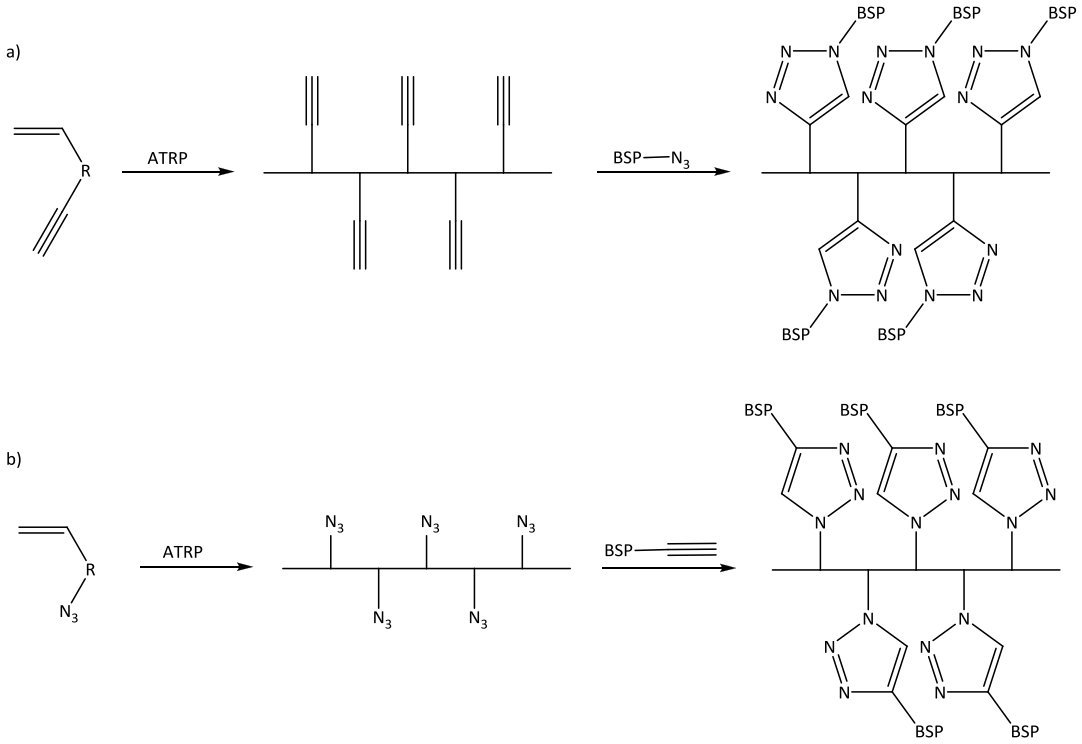

Scheme 5.5 The incorporation of BSP units pendant to an ATRP-generated polymer backbone by click chemistry.

A BSP bearing an alkyne moiety (BSP-alkyne) was synthesized, according to the standard path for preparing BSP and varying a procedure reported in literature, as previously discussed (**Scheme 5.6**).[22]

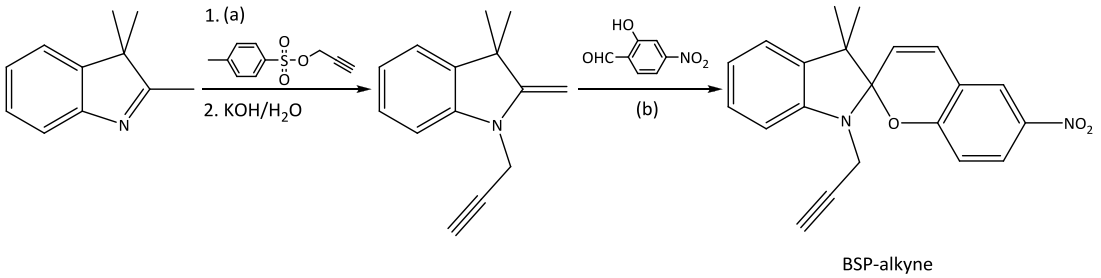

Scheme 5.6 Synthesis of BSP-alkyne. Reaction conditions: (a) N_2, 80 °C, 3 h; (b) EtOH, 82°C, 4 h.

The bromide groups of the multibromo macroinitiator PBiBEMA3 (M_n = 5,800 g/mol) were substituted by azide groups through nucleophilic substuitution with sodium azide **Scheme 5.7**. The ratio of azide to bromide was varied to obtain polymers with different densities of azide groups. The degree of substitution can be estimated by ^{1}H NMR spectroscopy (**Figure 5.8**) from the ratio of the methyl group signals (e) at 1.97 ppm (bromide substituted) and 1.46 ppm (azide substituted). Three polymers with a theoretical N_3/Br ratios of 1, 0.7 and 0.4 were synthesized (**Table 3**). GPC analysis confirmed the retained monomodality and low dispersity of the polymers after azidation with an unchanged M_n as the azide content increases (**Table 3**). The presence of the azide groups was further evident from the peak at 2111 cm^{-1} in the FT-IR spectra showing different relative intensities in accordance with the azide feed ratio and the ^{1}H NMR results (**Figure 5.9**).

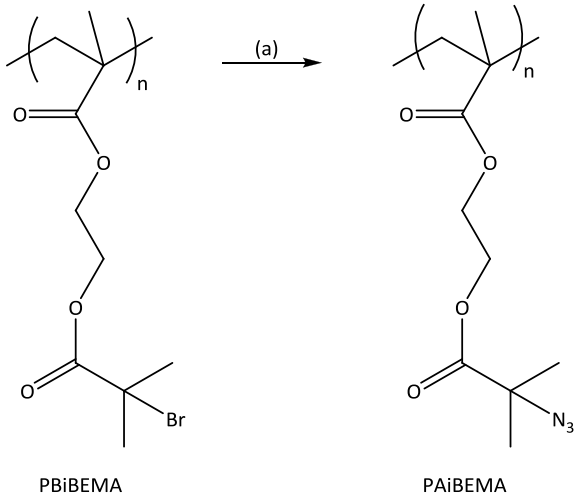

Scheme 5.7 Azidation of the PBiBEMA multibromo macroinitiator, leading to poly(2-azidoisobutyryloxyethyl methacrylate) (PAiBEMA). Reaction conditions: (a) NaN_3, DMF, room temperature, 20 h.

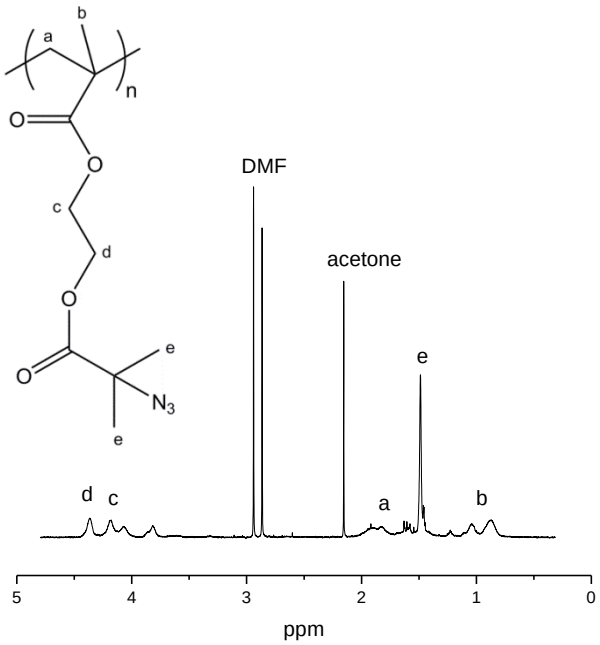

Figure 5.8 ^{1}H NMR spectrum of the the azide functional polymer entry 1, **Table 3**

Table 3 Characterization of the polymers bearing an azide functionality in the side chain by bromide substitution on PBiBEMA3 (M_n of 5,800 g/mol, PDI = 1.2) using various ratios of NaN_3 to PBiBEMA3.

Entry	N_3/Br ratio[(a)]	M_n[(b)] (g/mol)	PDI[(b)]
1	1	6,100	1.2
2	0.7	6,000	1.2
3	0.4	6,000	1.3

(a) Estimated from ^{1}H NMR spectra using the relative peak intensities of (e) at 1.97 ppm (bromide substituted) and 1.46 ppm (azide substituted). Due to a peak overlapping a slight error in the quantification may occur. (b) from GPC analysis.

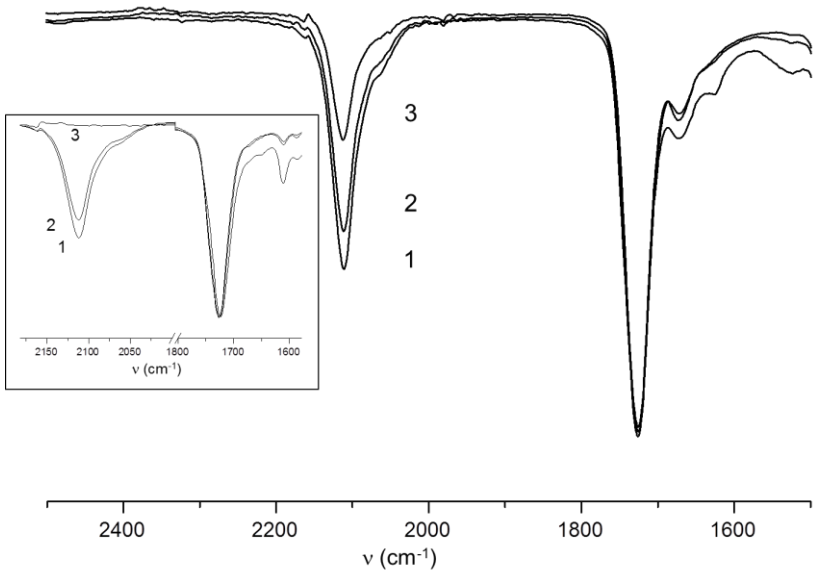

Figure 5.9 FT-IR spectra of polyazides (entry 1, 2, 3, Table 2). Inset: FT-IR spectra after click reaction of BSP-alkyne onto the polyazides. The carbonyl peak of the polymer was used to normalize the spectra.

The CuAAC reaction was performed with BSP-alkyne on completely azide functionalized polymers at 40 °C for 60 hours using CuBr and N,N,N',N'',N''-pentamethyldiethylenetriamine (PMDETA) as the catalytic system (**Scheme 5.8**). ^{1}H NMR spectra of the obtained polymers showed characteristic peaks at 7.98 ppm (m, l) and between 6.48 ppm and 7.18 ppm (h, j, k) of the aromatic BSP protons, the BSP peak at 7.49 ppm (f) and the typical signals of the backbone polymer, confirming that the reaction occurred (**Figure 5.10**).

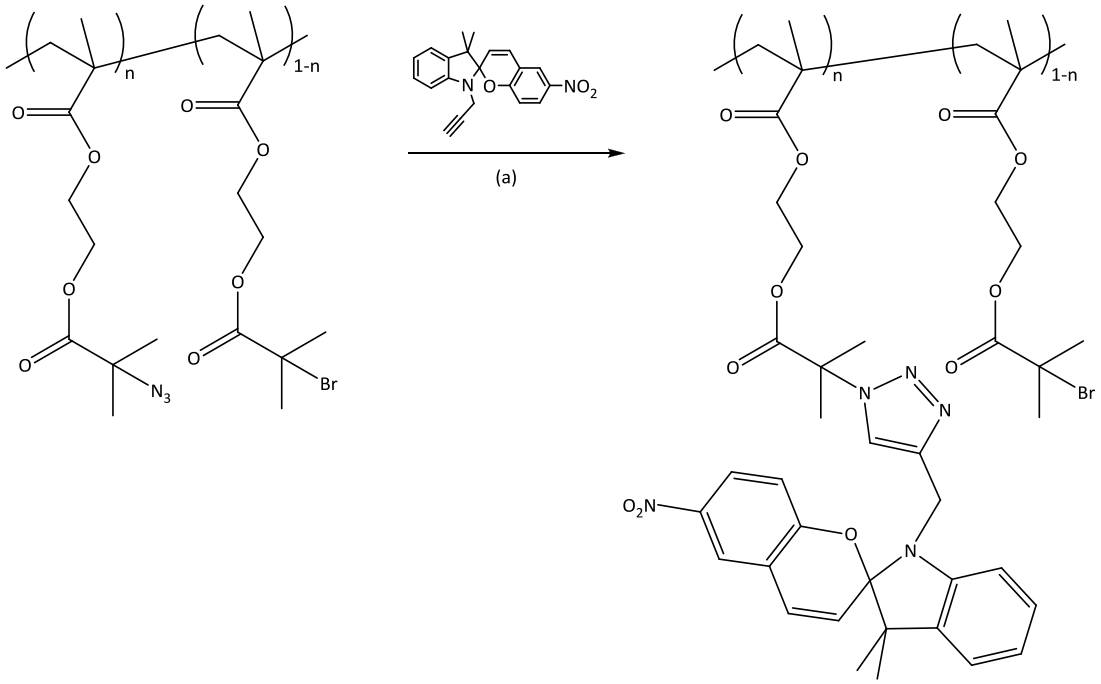

Scheme 5.8 Click chemistry reaction between a BSP derivative containg an alkyne function (BSP-alkyne) and a polymer bearing azide moieties on the side chains (PAiBEMA). Reaction conditions: (a) CuBr/PMDETA (1/1), sodium ascorbate, THF, 40 °C, 60 h.

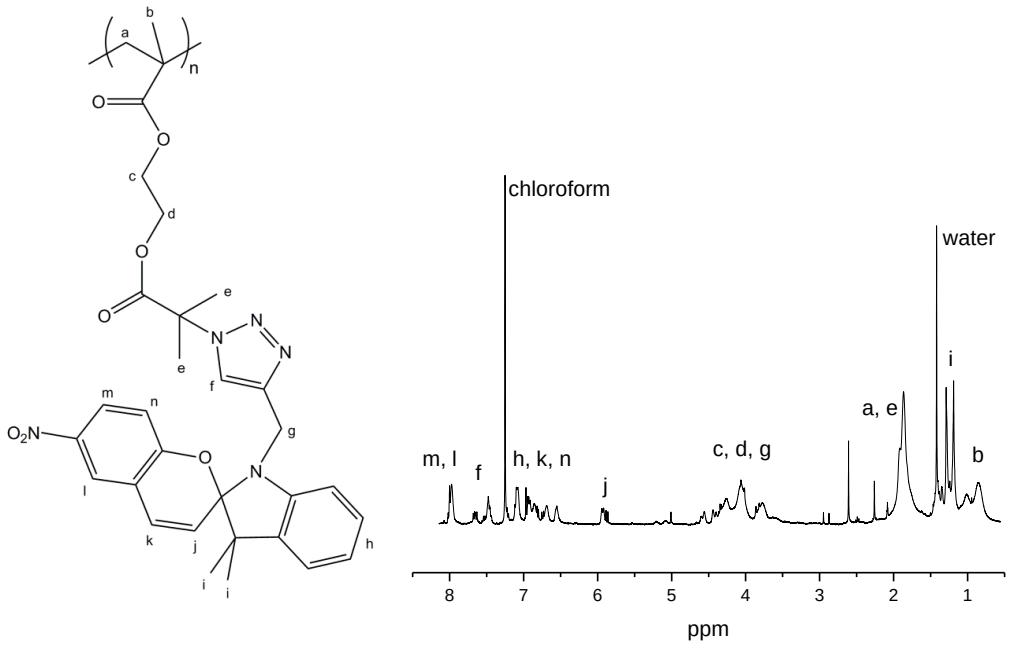

Figure 5.10 ^{1}H NMR spectra of the BSP-based polymer obtained after the click chemistry reaction.

Quantification of the reaction yield proved difficult due to overlapping signals. FT-IR spectra revealed a significant amount of remaining azide groups (2111 cm^{-1}) for polymers with higher azide density of 100 and 70% (entries 1 and 2, **Table 3**) probably due to steric hindrance (note that the spectra in the inset of **Figure 5.9** are

normalized to the carbonyl peaks of the polymer precursor). On the other hand, quantitative conversion of the azide groups was observed for the polymer with about 40% azide substitution (entry 3, **Table 3**) as evident from the complete disappearence of the azide band at 2111 cm^{-1}. While higher densities of BSP side groups would require further optimization of the polymer structure (e.g. introduction of spacers), the results confirm that post-polymerization BSP conjugation is clearly superior to the direct controlled radical polymerization of BSP monomers.

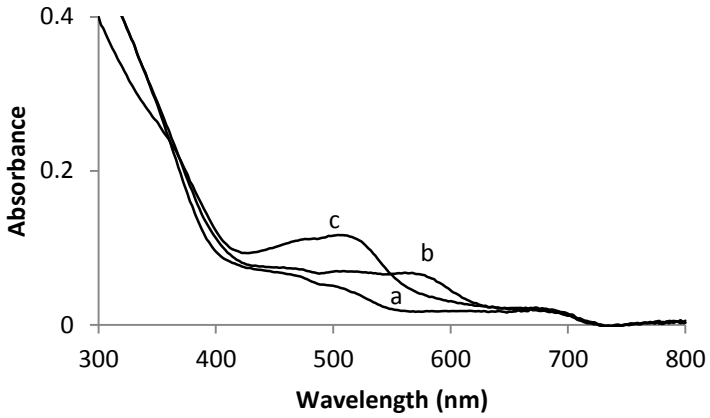

Figure 5.11 UV-Vis spectra BSP functional polymer (40 % SP) before (a), after (b) 60 s of UV (365 nm) irradiation and (c) after addition of equal molar equivalents of $Co(NO_3)_2$ and 60 s of UV (365 nm) irradiation (1 x 10^{-4} M in DCM).

The photoisomerism of the BSP functional polymer (40 % BSP) upon exposure to UV light was studied in dichloromethane (DCM). The polymer exhibits conventional BSP-BMC photochromism with a long-wavelength absorption band located at 580 nm (**Figure 5.11**, spectrum b). The negatively charged phenolate group in the BMC form has ion-binding characteristics.[23,24] The binding results in a shift in absorbance, which corresponds to a color change of the solution. In order to confirm that this property is maintained, the optical properties and complexation behavior of PAiBEMA (40 % SP) were investigated with Co^{2+}. For these experiments, 1x10^{-4} M solutions of the polymer was kept in the dark before equal molar equivalents of solution of the metal nitrate in DCM were added. The colorless solutions were exposed to UV light for 1 minute to promote the complexation after which a pink colour was observed. The absorption spectrum shows a new peak 510 nm that corresponds to the complex formation (**Figure 5.11**, spectrum c).[25]

5.2.2 Synthesis of BSP-conjugated polymers through ATRP and click chemistry

We have demonstrated that combining ATRP and click chemistry for the synthesis of BSP based polymers is clearly superior to the direct controlled radical polymerization (CRP) of BSP monomers. Following this path, we have successfully synthetized BSP based polymers but we could not reach 100% BSP conjugation, probably due to sterical hindrance. Therefore, it was decided to introduce a spacer on the side chain of the polymer backbone in order to ease the BSP-alkyne click reaction and to use an azido-containing monomer to facilitate direct functionalization via azide-alkyne. In the literature it has been reported that azide moieties are compatible with CRP techniques, including RAFT[26] and ATRP.[21,27] We opted for 6-azidohexyl methacrylate as a monomer assuming this to be an appropriately-sized spacer to facilitate a high yielding click reaction on the polymer. Moreover, it is well-known that organic azide can explosively decompose with little input of external energy,[28] but the carbon to nitrogen ratio of this azide molecule can be considered safe to work with under controlled reaction conditions.[29] The azido-containing monomer was synthesized by two-step reaction, modifying and combining two procedures reported in literature.[21,30] 6-azido-1-hexanol was prepared through nucleophilic substitution of 6-chloro-1-hexanol with sodium azide and then it was reacted with methacryloyl chloride under mild conditions to give the 6-azidohexyl methacrylate (AHMA) in good yield, after purification through silica chromatography (**Scheme 5.9**). The success of the synthesis was showed by ^{1}H NMR. After the first step reaction the signal at 3.56 ppm due the methylene group bonded to the chloride moiety (a) shifted to 3.27 ppm, indicating that the full conversion into the azide functionality was achieved. The ^{1}H NMR of the product obtained after the second step showed signal shift due to the OH functionalized methylene group from 3.64 ppm to 4.14 (f), indicating the ester formation. Another evidence of the product formation is the typical peaks of the methacrylate portion, i. e. two signals at 5.55 ppm (g') and 6.09 ppm (g) of the methylene group and the singlet at 1.94 ppm (h) due to the methyl group. As expected, the chemical shift of the peak corresponding to the azide-substituted methylene group (a) is unvaried, and the signals of the remaining methylene groups slightly changed their shapes and chemicals shifts (**Figure 5.12**). The structure of the products was further

confirmed by FT-IR spectroscopy. The spectrum of 6-azido-1-hexanol shows a sharp peak at 2094 cm^{-1} corresponding to the azide functionality. The spectrum of AHMA reveals the azide peak at 2094 cm^{-1} in addition to another sharp peak at 1714 cm^{-1} due to the carbonyl group (**Figure 5.13**).

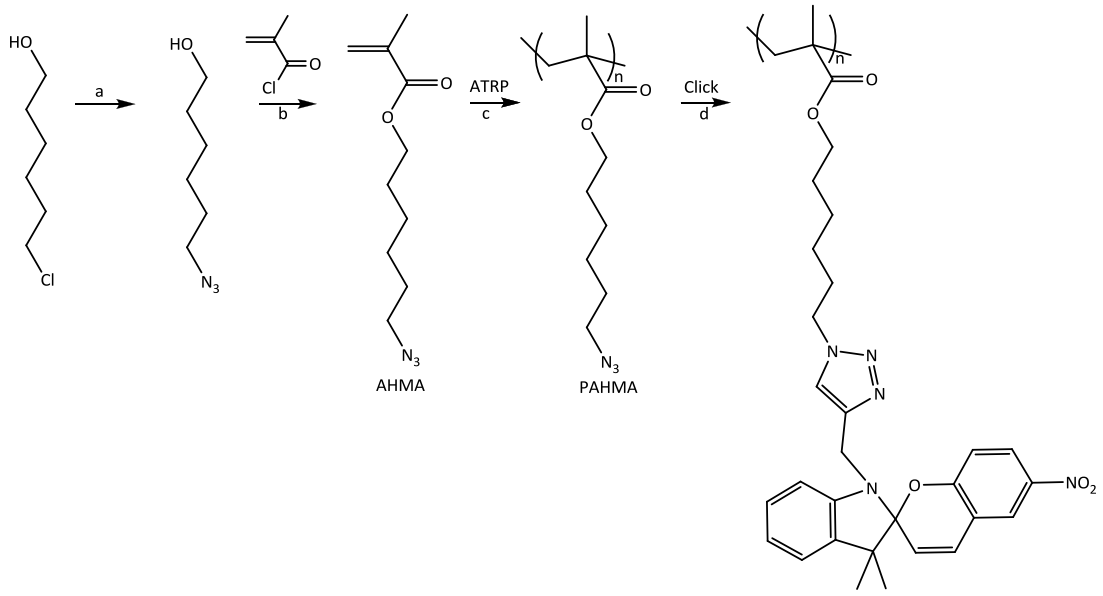

Scheme 5.9 Synthesis of 6-azidohexyl methacrylate (AHMA), its polymerization and click reaction of poly(6-azidohexyl methacrylate) (PAHMA) with BSP-alkyne. Reaction conditions: (a) NaN_3, DMF/H_2O, 75 °C, 22 h; (b) Et_3N, DCM, N_2, 0 °C, 24 h; (c) EBiB, CuCl/PMDETA (1/1), IPA, 30°C, 195 min and (d) BSP-alkyne, CuBr/PMDETA (1/1), sodium ascorbate, THF, 40°C, 60 h.

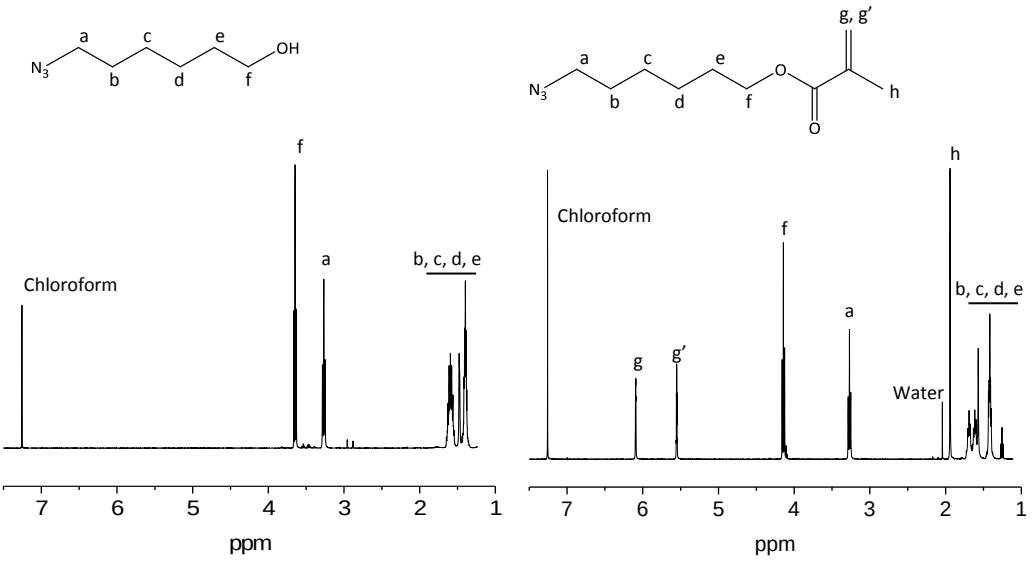

Figure 5.12 ^1H NMR of 6-azido-1-hexanol (left) and 6-azidohexyl methacrylate (right) in chloroform.

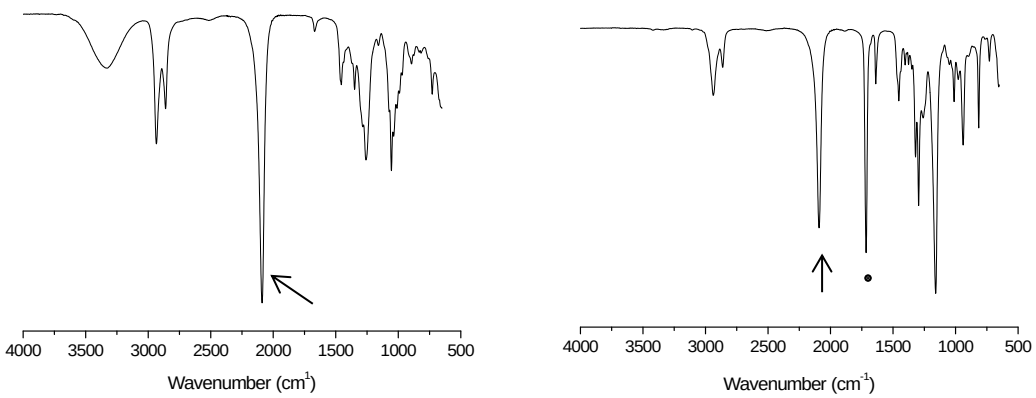

Figure 5.13 FT-IR of 6-azido-1-hexanol (left) and 6-azidohexyl methacrylate (right). Arrows mark the azide peaks and the dot marks the carbonyl peak.

A linear polymer was synthesized through ATRP, using the 6-azidohexyl methacrylate as monomer, EBiB as the initiator and CuCl and PMDETA as catalytic system. The polymerization was performed at 30 °C for 195 minutes in isopropyl alcohol (IPA) (**Scheme 5.9**) resulting in linear poly(6-azidohexyl methacrylate) (PAHMA) with an M_n of 9,200 g/mol and a PDI of 1.2 (**Figure 5.14**). In the ^{1}H NMR spectrum the signals of the methylene groups bonded to the azide functionality and the ester group are clearly visibly at 3.34 ppm (a) and 3.96 ppm (f), respectively. In addition typical signals of the polymeric methylene groups (b-g) at 1.32 ppm to 1.83 ppm and the methyl groups between 0.80 ppm and 1.03 ppm (h) can be observed (**Figure 5.16**, top spectrum). Moreover, FT-IR analysis is in agreement with the structure of the polymer showing a sharp peak at 2095 cm^{-1} indicating the presence of the azide functionality and a sharp peak at 1728 cm^{-1} corresponding to the carbonyl moiety (**Figure 5.15**).

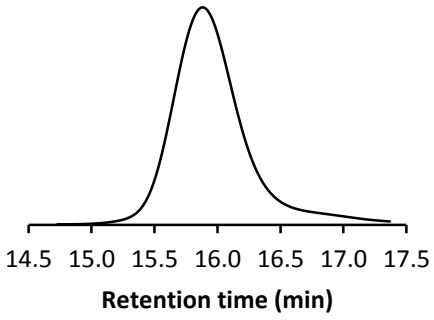

Figure 5.14 SEC Chromatogram of linear PAHMA (9,200 g/mol, PDI: 1.2).

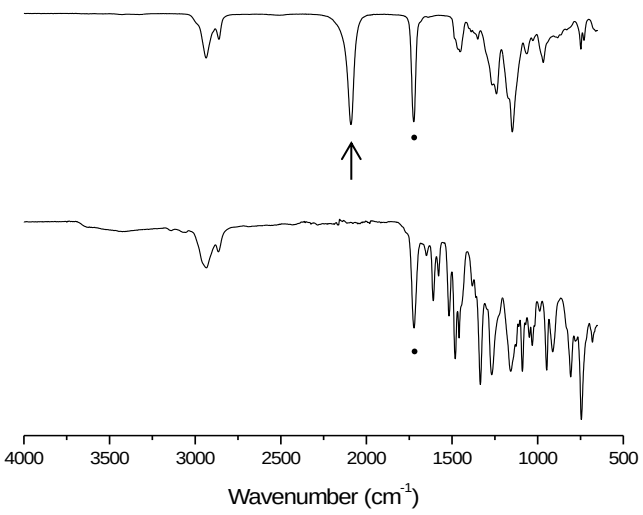

Figure 5.15 FT-IR spectra of poly(6-azidohexyl methacrylate) before (top) and after (bottom) click reaction with BSP-alkyne. The arrow marks the azide peak and the dots mark the carbonyl peaks.

A click reaction was carried out between BSP-alkyne and the synthesized linear polyazide at 40 °C for 60 hours in the presence a small amount of sodium ascorbate, using the heterogeneous catalytic system CuBr/PMDETA and THF as solvent (**Scheme 5.9**), slightly modifying a literature procedure.[22] The polymer obtained was firstly purified through precipitation in methanol and then through dialysis against THF for two days to ensure that all the BSP-alkyne was removed. The success of the rection was evident from the total disappearence of the azide peak at 2095 cm^{-1} in the FT-IR spectrum, while the carbonyl peak at 1728 cm^{-1} remains unchanged. This result confirmed that the reaction occurred with 100% efficiency. The quantitative conversion of the azide to the corresponding triazole was further confirmed by ^{1}H NMR spectroscopy with the emergence of the triazole proton at 7.45 ppm (**Figure 5.16**, bottom spectrum, peak E) and the shift of the azidomethylene signal from 3.34 ppm to 4.41 ppm (**Figure 5.16**, middle and bottom spectra, peak a). Furthermore, typical signals of the BSP moiety (A-C, G, H and J) can clearly be observed in the ^{1}H NMR spectrum of the polymer (**Figure 5.16**, bottom spectrum). We were unable to collect a meaningful GPC chromatogram of the linear poly(BSP hexyl methacrylate) (PBSPHMA), probably due to some interactions between the photochromic BSP moiety on the polymer and the stationary phase of the GPC column. This is supported by the fact that even low molecular weight BSP

compounds resulted in bimodal GPC traces. While relative molar mass and PDI can thus not be reported, it is reasonable to assume that except for the increase in mass due to the addition of BSP units no change to the polymer structure occurred.

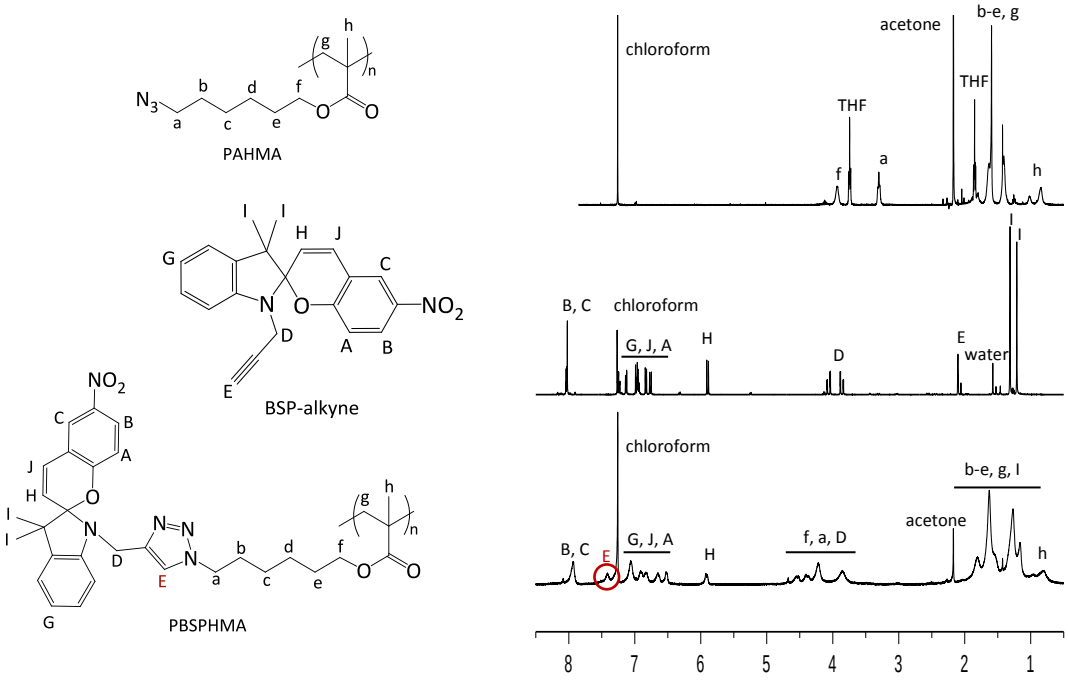

Figure 5.16 ^{1}H NMR spectra of PAHMA (top spectrum), BSP-alkyne (middle spectrum) and PBSPHMA (bottom spectrum) generated through click chemistry reaction of BSP-alkyne onto PAHMA. The red circle in the bottom spectrum highlights the presence of the triazole proton E.

The same synthetic route was exploited for the synthesis of BSP containing star-like and molecular brush architectures. As shown in **Scheme 5.10** the four-arm initiator (**Scheme 5.2**) was used to obtain a well-defined four-arm star-like PAHMA, and the multibromo macroinitiator PBiBEMA (**Table 1**, M_n = 3,600) (**Scheme 5.3**) was employed to synthesize a molecular brush PAHMA. The corresponding GPC graphs are monomodal and narrow as shown in **Figure 5.17**. An M_n of 10,200 g/mol was obtained for the star-like polymer, while 22,100 g/mol was obtained for the polymer brush (**Table 4**). The ^{1}H NMR (**Figure 5.18**) and FT-IR (**Figure 5.19**) spectra of the star-like and molecular brush PAHMA match the spectra of the related linear polymer (**Figure 5.16** and **Figure 5.15**) with all the characteristic peaks present.

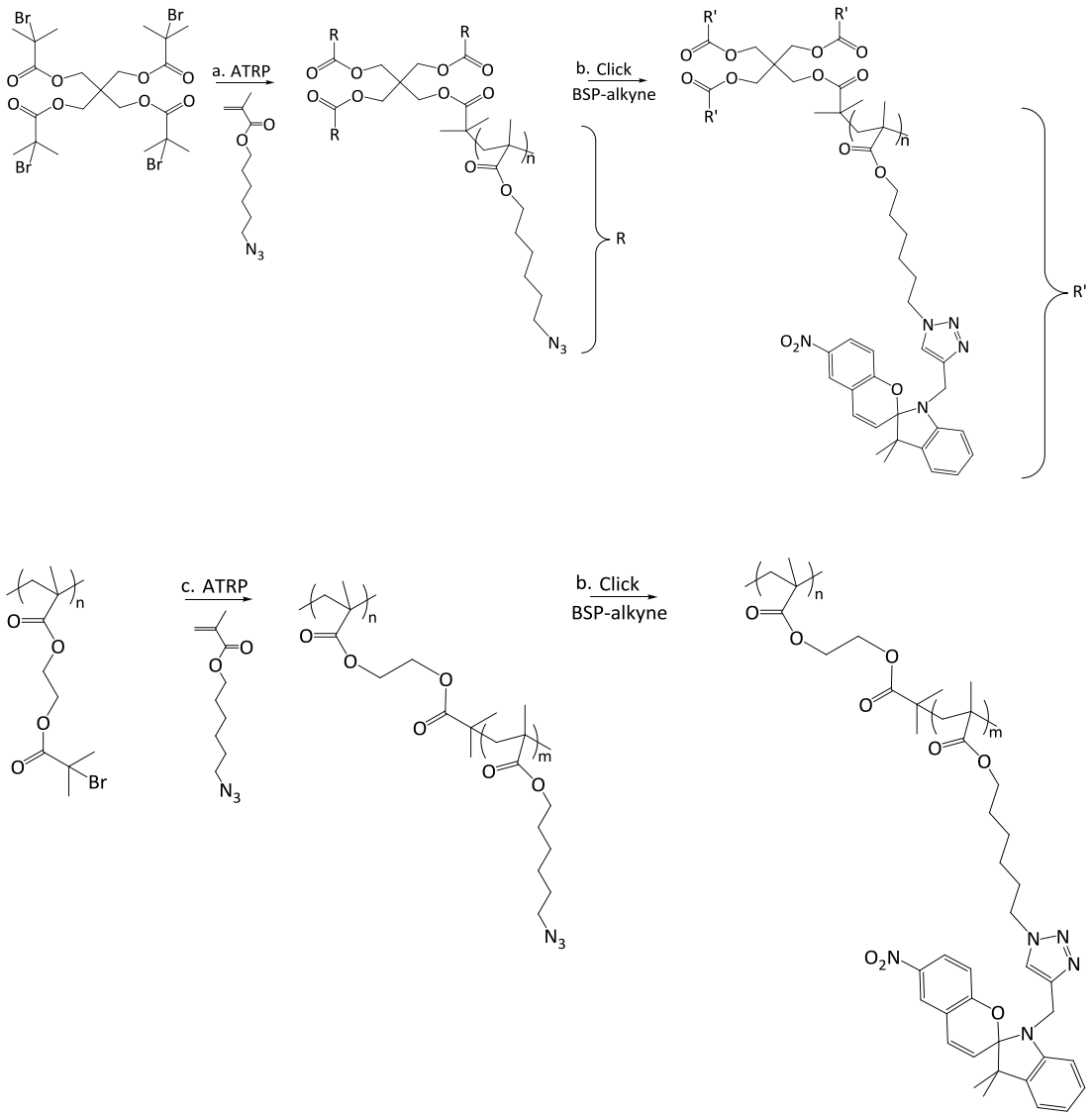

Scheme 5.10 Synthesis of BSP based PAHMA with star-like (top) and molecular brush architecture (bottom). Reaction conditions: (a) EBiB, CuCl/PMDETA (1/1), IPA, 30 °C, 50 min; (b) BSP-alkyne, CuBr/PMDETA (1/1), sodium ascorbate, THF, 40 °C, 60 h and (c) EBiB, CuCl/PMDETA (1/1), IPA, 30 °C, 40 min.

Table 4 Characterization of the PAHMA macroinitiator prepared by ATRP.

PAHMA	Conv[(a)] (%)	M_n[(b)] (g/mol)	PDI[(b)]
Linear	60	9,200	1.2
Star-like	48	10,200	1.2
Molecular brush	70	22,100	1.2

(a) Determined by ^{1}HNMR spectroscopy from integration of peaks at the relative peaks at 5.55 ppm and 6.09 ppm, indicative of the presence of AHMA. (b) from GPC analysis.

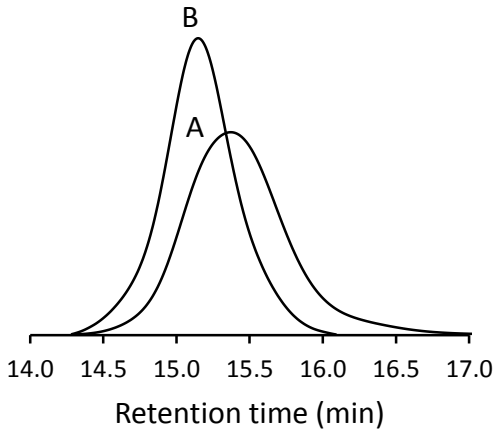

Figure 5.17 SEC of (A) star-like PAHMA (10,200 g/mol, PDI: 1.2) and (B) molecular brush PAHMA (22,100 g/mol, PDI: 1.2).

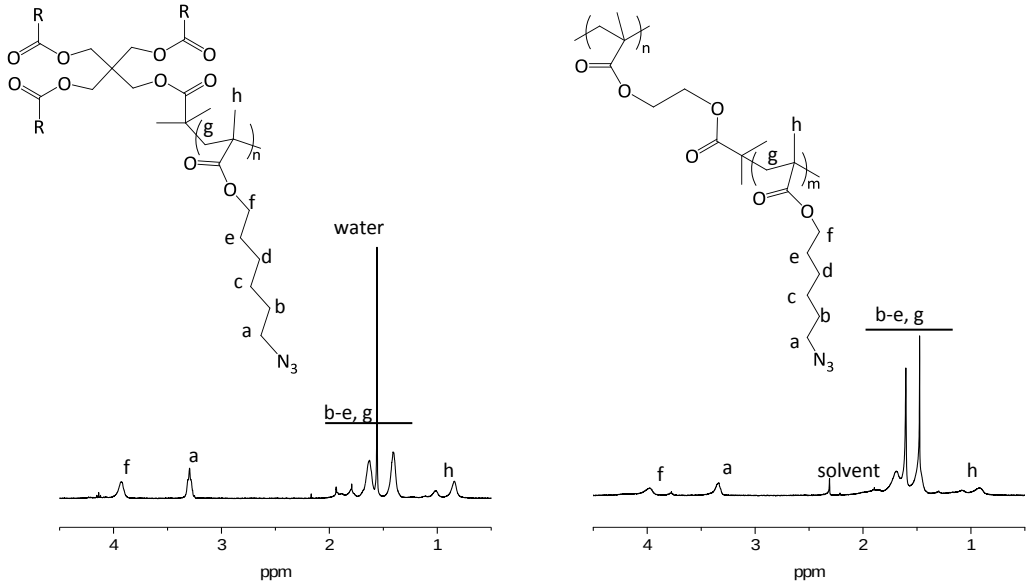

Figure 5.18 ^{1}H NMR spectra of star-like PAHMA (left) and molecular brush PAHMA (right).

The click reaction between BSP-alkyne and the synthesized polymers was performed and led to the corresponding BSP-functionalized polymers with star-like and molecular brush architectures. The success of the reaction is evident from the complete disappearence of the azide peak at 2094 cm^{-1} in the FT-IR spectra (**Figure 5.19**) suggesting quantitative conversion into the triazole for both polymers. This approach thus leads to polymers with a BSP moiety on every repeating unit which was not possible to achieve by direct ATRP of BSP monomers or click reaction without spacer. ^{1}H NMR spectroscopy confirmed the presence of the BSP units on

the polymers, even though the collected spectra were not well-resolved, probably due to the arrangements of the polymers in solution (**Figure 5.20**).

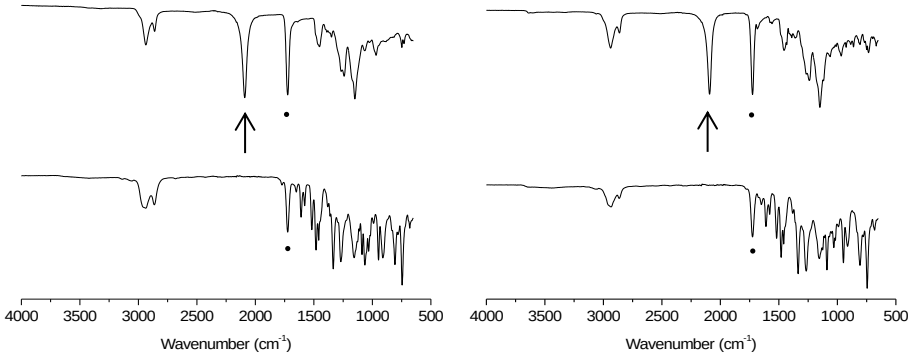

Figure 5.19 FT-IR spectra of star-like PAHMA (left spectrum) and molecular brush PAHMA (right spectrum) before (top) and after (bottom) click reaction with BSP-alkyne. The arrows mark the azide peaks and the dots mark the carbonyl peaks.

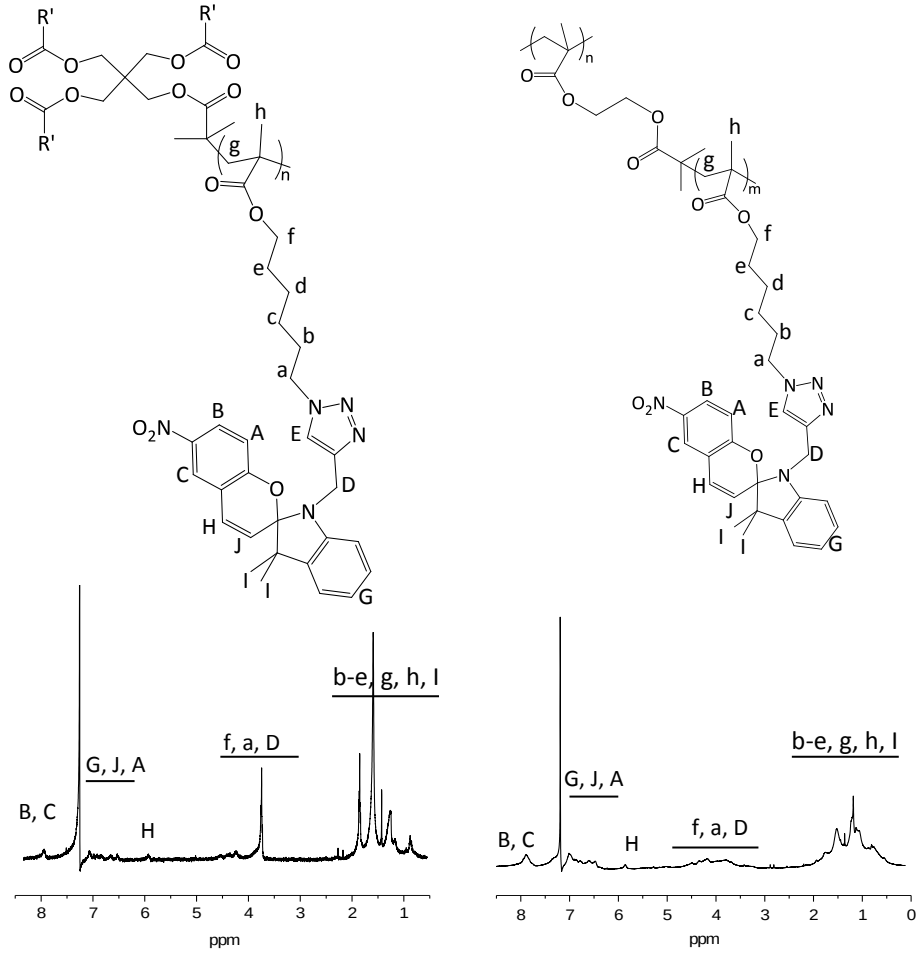

Figure 5.20 ^{1}H NMR spectra of poly (BSP hexyl methacrylate) with star-like (left) and molecular brush (right) architectures.

5.2.3 Photochromic properties of linear, star-like and molecular brush PBSPHMA

As widely discussed in this work, BSP has the ability to switch from an uncharged and colorless form to the zwitterionic, planar and highly colored benzomerocyanine form upon irradiation with UV light (**Scheme 1.2**). The photoisomerism of PBSPHMA with different molecular architectures was studied to investigate the influence of the polymer architecture on the photochromic behaviour of the multiple BSP units covalently bonded to the polymers. The absorbance spectra of linear, star-like and molecular brush PBSPHMA were measured in THF as the polymers possess good solubility in this solvent. Stock solutions of the polymers were prepared and stored in the dark to equilibrate overnight with a concentration of $0.5x10^{-4}$ M for the linear and the molecular brush polymers and $0.5x10^{-5}$ M for the star-like polymer [*Note*: all PBSPHMA polymer concentrations for the measurements were calculated based on the polymer M_n from SEC (PMMA standards) of the corresponding PAHMA precursor polymer]. All polymers exhibited typical BSP photochromism, i. e. a strong long-wavelength absorption band at 580 nm, resulting in a change in solution color from colorless to deep violet (**Figure 5.21**). The measured absorption maximum is remarkably blue-shifted compared with BSP-alkyne previously studied. This may be either due to the electronic effect of the triazole group linked to the indoline section of BSP and/or to interaction effects of the BMC units in close proximity, generating a polar environment.

Other spectral features of all polymers are similar to the spectrum of BSP-alkyne in THF (**Figure 4.8**), for example another absorption band at 370 nm and an isosbestic point at 340 nm were observed. E-diagrams of the polymers were plotted, taking the absorbance values for 328, 370, 400, 550 and 650 nm at time intervals and plotting them against the absorbance values for 580 at the same time intervals (**Figure 5.22**). As in the case of BSP-alkyne and the BSP-PEG and BSP-PPO derivatives previously studied, a linear correlation between wavelengths was found for all the polymers. This suggests that, also in this case, the reaction involves only one linear independent step, and the peculiar spectral features are probably generated in a similar way.[31-33]

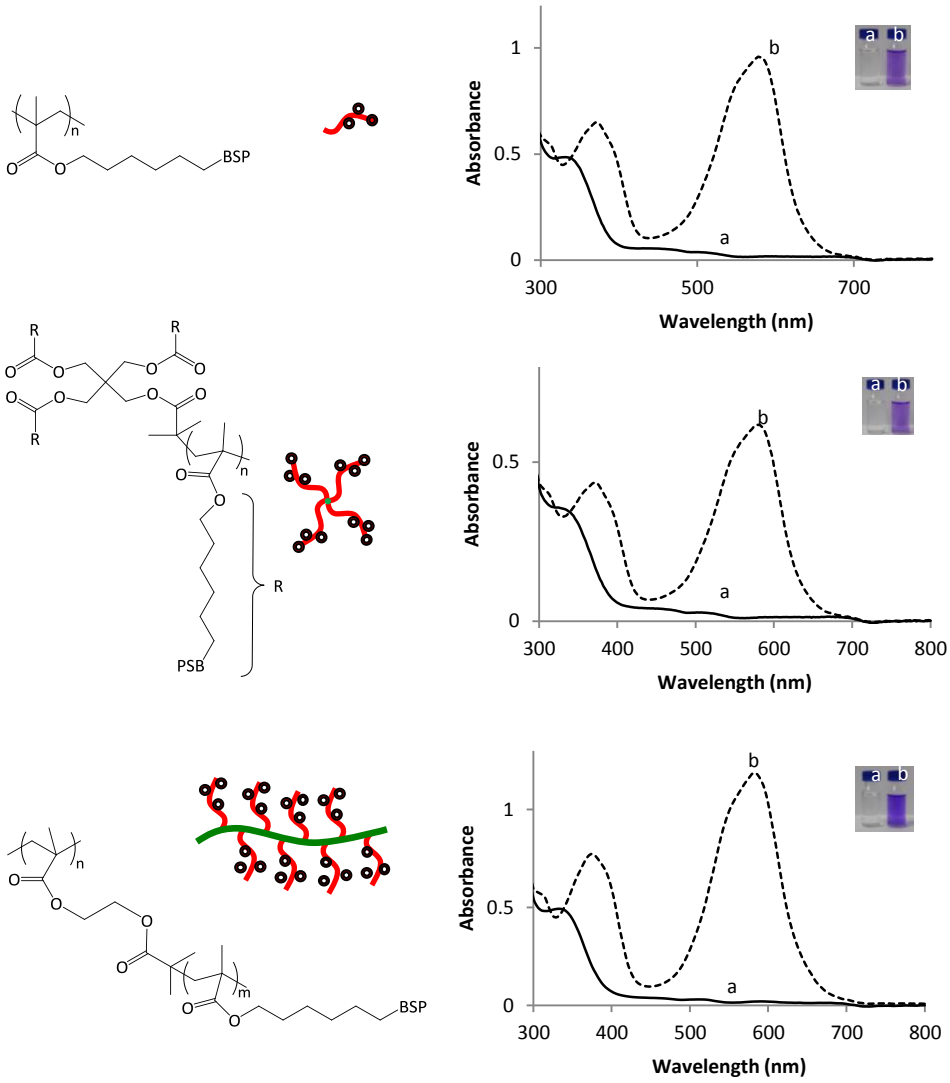

Figure 5.21 Structures, representations and UV-Vis spectra of linear (top), star (middle) and molecular brush (bottom) PBSPHMA before (a) and after (b) 1 minute of UV (365 nm) irradiation.

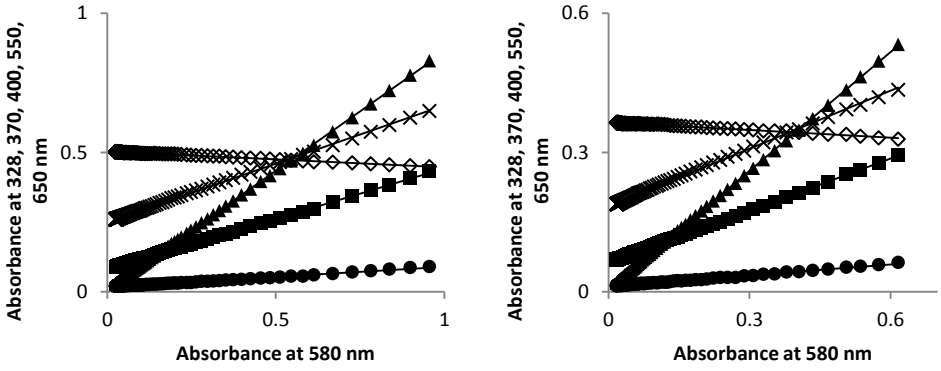

Figure 5.22 E-diagrams for the transition from BMC to BSP form of linear, star-like and molecular brush PBSPHMA in THF, obtained using the corresponding collected spectra. The absorbance values at 328 nm (◊), 370 nm (x), 400 nm (■), 550 nm (▲) and 650 nm (●) are plotted against the absorbance value at 580 nm.

The ring-closure of the BMC to the BSP form is induced upon removal of the UV light source or by irradiation with visible light. Preliminary kinetic studies were performed at room temperature to investigate if the polymeric architecture influences the ring-closure kinetics of the BMC. Therefore the BMC isomer formation was induced in the polymers by exposure to UV light for 1 minute and the decrease in absorbance at λ_{max} was recorded upon removal of UV light. Samples were kept in the dark during the measurements to avoid the influence of ambient light.[34] The reduction of the absorbance at the λ_{max} for the transition from BMC to BSP for the linear PBSPHMA at room temperature is shown in **Figure 5.23**. The ring-closure kinetics of all BSP functional polymers follow first-order kinetics, as expected.[35] The first-order rate constants *k* for the transition of BMC to BSP were determined by plotting ln(At/A0) versus time. A linear correlation between BMC (λ_{max}) and its rate constant was found for each polymer, the *k* values are gathered in **Table 5**. The ring closure kinetics of the transition of BMC to BSP are comparable for the linear and the star-like polymers with a *k* value of 1.10×10^{-2} s^{-1} and 1.01×10^{-2} s^{-1} while in the case of the molecular brush architecture the ring-closure is two times slower. This could be due to higher molecular weight of the molecular brush PBSPHMA, which is M_n 22,100 g/mol (for practical reasons we could not obtain a lower value) while for linear and star-like PBSPHMA the M_n is about half of that, 9,200 g/mol and 10,200 g/mol, respectively (this refers to M_n values before BSP conjugation). In this work it has already been demonstrated that BSP ring-closure kinetics depends on the polymer molecular weight for temperatures higher than room temperature while at room temperature there are no significant variation of the ring-closure kinetics depending on the polymer molecular weight.[15] Another reason could be the effect of the different architecture, probably the BMC units in a molecular brush are closer to each other, compared to the linear and star-like analogue, mutually interacting and generating a favorable environment that stabilizes the BMC isomer, slowing its ring-closure kinetic.

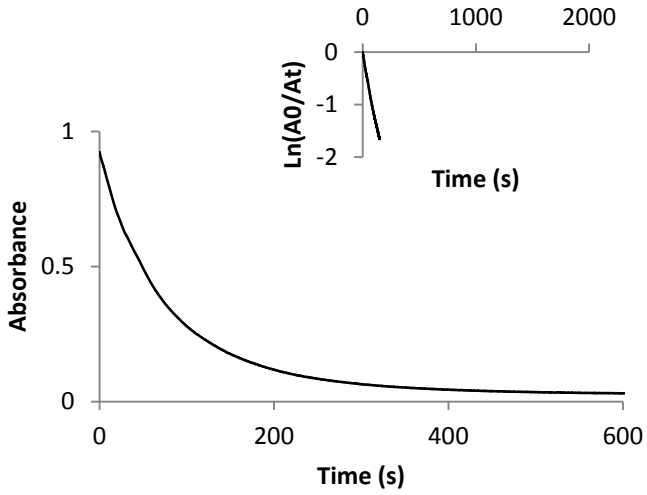

Figure 5.23 Absorbance decrease at λ_{max} (580 nm) in THF as a function of time after removing the UV light source, for the transition of BMC to BSP for the linear polymer at room temperature. A linear correlation between BMC (λ_{max}) and its rate constant is revealed for this polymer.

Table 5 Values of the relaxation rate constant *k* for the transition of BMC to BSP for all the polymers measured in THF at room temperature (λ_{max} 580 nm). The rate constants are compared in terms of ratio to ring-closure kinetics of the single molecule BSP-alkyne.

	Linear PBSPHMA	**Star-like PBSPHMA**	**Brush PBSPHMA**
K_{580} (s^{-1})	$1.10x10^{-2}$	$1.01x10^{-2}$	$5.1x10^{-3}$
Ratio to BSP-alkyne	4.1	4.45	8.2

The switching efficiency of PBSPHMA was studied by measuring the absorbance response behavior of the BMC form after irradiating the sample with UV light (365 nm) for 1 minute several times. The BMC form was allowed to completely reverse back to the BSP form after every measurement and during the experiment the sample was kept in the dark to avoid the interference of ambient light. As shown in **Figure 5.24**, PSBPHMA are able to undergo a number of cycles between high and low absorbance values by repetitive sequence of irradiation with UV light and dark. After the 5^{th} cycle the loss of signal is quite significant for the linear and the star-like polymer and the absorbance value at λ_{max} is about the 50% of the initial value. The molecular brush architecture showed a better photostability as the absorbance value at λ_{max} recorded after the 5^{th} cycle is about 80% of the initial value. As

mentioned previously, the photostability of BSP is lower in solution than in the solid state, therefore these results could be due to the physical state of the sample and investigating the behavior of these polymers in the solid state will help to validate this point.

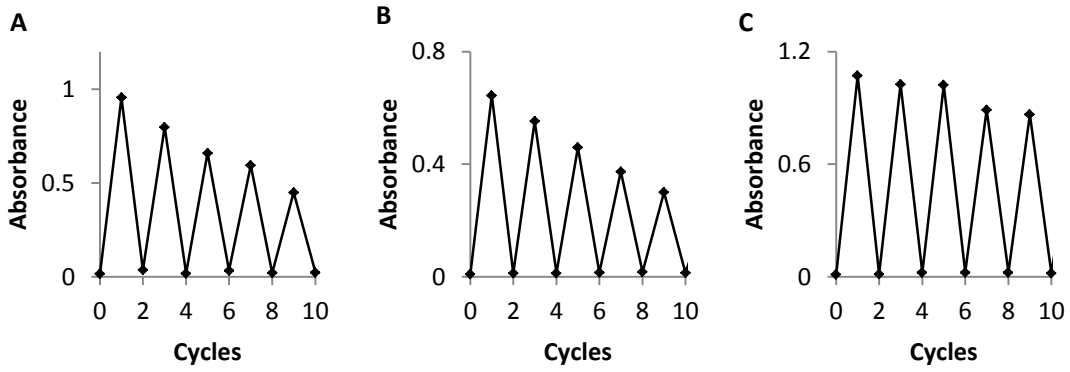

Figure 5.24 Absorbance measured at 580 nm for cyclical switching between BSP and BMC in (A) linear, (B) star-like and (C) PBSPHMA, alternating UV light exposure for 1 minute and thermal relaxation.

5.2.4 Fluorescence spectroscopy of linear, star-like and molecular brush PBSPHMA

The emission of PBSPHMA and the corresponding BMC form in THF ($1x10^{-5}$M for linear and molecular brush polymer and $1x10^{-6}$M for the star-like polymer) was investigated. Stock solutions of linear, star-like and molecular brush polymer were prepared *in situ* by dilution of the corresponding $1x10^{-4}$ M solution in THF, previously prepared and stored in the dark. Spectroscopic studies were firstly performed on linear PBSPHMA. The emission intensity of linear PBSPHMA after excitation at 580 nm was very low (**Figure 5.25**, spectrum a) but increased notably after exposing the sample to UV light (365 nm) for one minute to generate the BMC form in the polymer (**Figure 5.25**, spectrum b). Therefore, the polymer emits only when its photochromic units are in the BMC form, in this case the emission spectrum exhibits one band ($\lambda_{max,em}$ = 660). The excitation spectrum monitored at 650 nm was recorded afterwards and two excitation bands were observed at 360 nm and 560 nm (**Figure 5.25,** spectrum c). The sample was kept in the dark for 10 minutes and a sequence of emission and excitation spectra were recorded, using the same conditions previously set. As shown in **Figure 5.25**, the intensity of the

excitation (spectrum e) and emission (spectrum d) bands decreased and in the emission spectrum and the value of $\lambda_{max,em}$ shifted from 660 nm to 625 nm. No response was observed after maintaining the sample in the dark for 15 minutes.

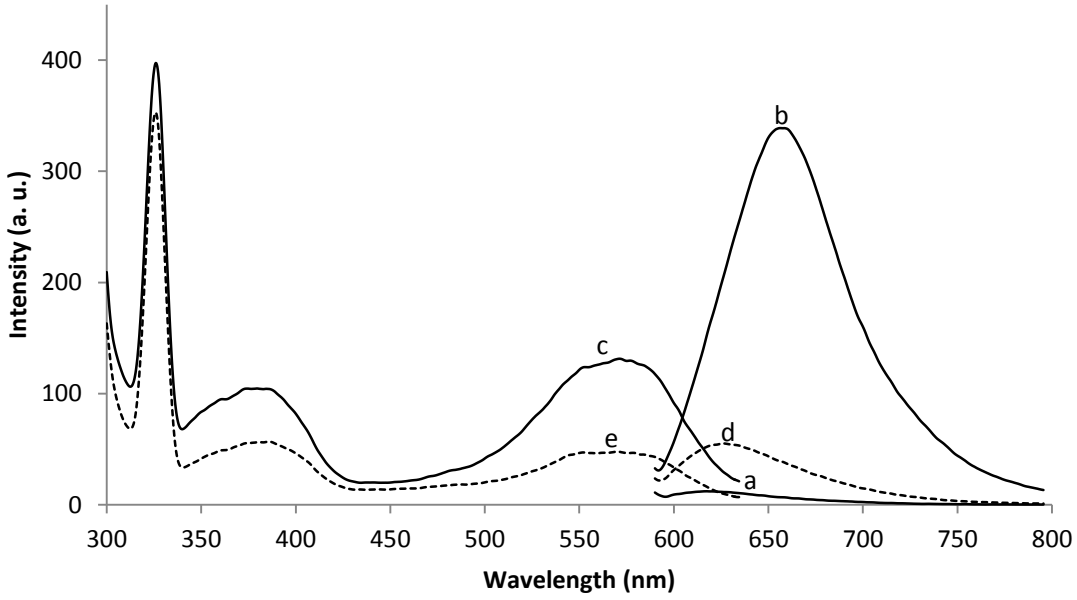

Figure 5.25 Fluorescence spectra of linear PBSPHMA. Emission spectra before (a), after (b) irradiation with UV light (365 nm) for 1 minute and the following excitation spectrum (c) (solid lines); Emission (d) and excitation (e) spectra of the same sample kept in the dark for 10 minutes (dashed lines). All the emission spectra were acquired under 580 nm light excitation and all the excitation spectra were obtained by monitoring 650 nm emission.

Similar spectroscopic studies performed on star-like and molecular brush PBSPHMA lead to analogous results. As shown in figure **Figure 5.26** the emission band of both polymers (λ_{exc} = 580 nm) before irradiation with UV light is very low in intensity (spectra a), while the emission spectra collected after exposure of the samples to UV light for 1 minute (λ_{exc} = 580 nm) displayed a high intensity band ($\lambda_{max,em}$ = 660) (spectra b). Two excitation bands at 370 nm and 560 nm were observed in the polymers excitation spectra monitored at 650 nm (**Figure 5.26**, spectra c). The same samples were kept in the dark for 10 minutes and emission and excitation spectra were recorded using the previously set parameters. The emission bands observed were lower in intensity with the $\lambda_{max,em}$ shifted from 660 nm to 620 nm while the excitation bands showed the same wavelengths with lower intensity (**Figure 5.26**, spectrum d and e, respectively). After keeping the polymer solutions for 15 minutes in the dark no response was observed.

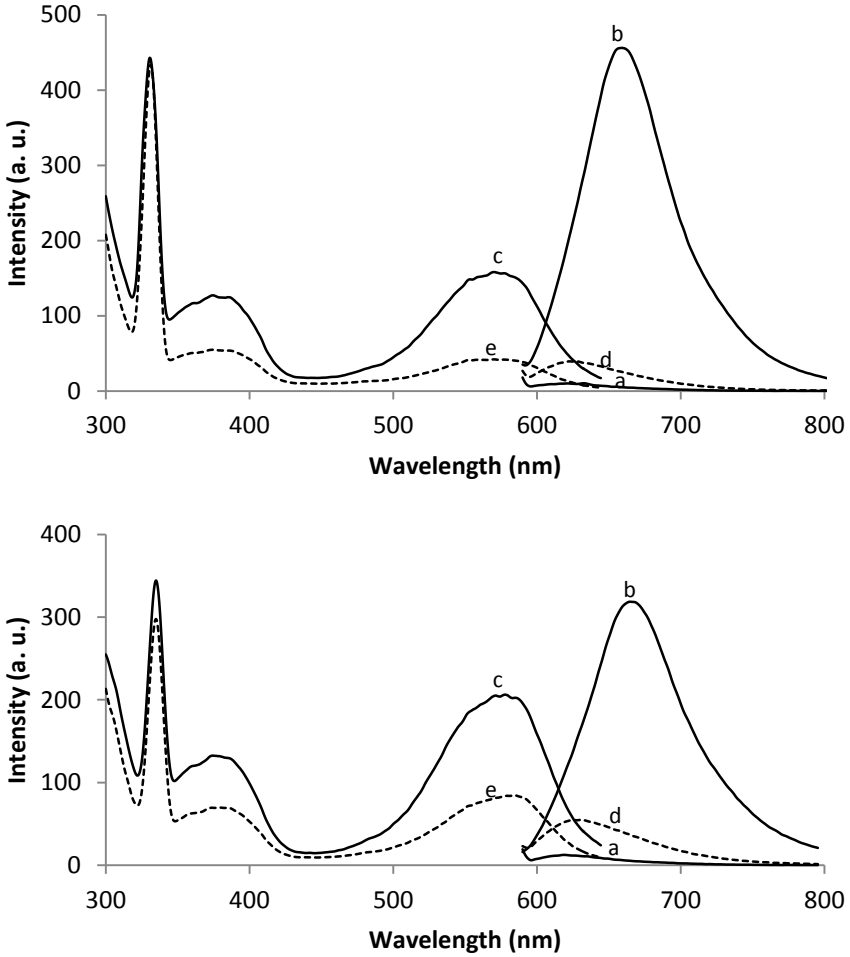

Figure 5.26 Fluorescence spectra of star-like (top) and molecular brush (bottom) PBSPHMA. Emission spectra before (a), after (b) irradiation with UV light (365 nm) for 1 minute and the following excitation spectrum (c) (solid lines); Emission (d) and excitation (e) spectra of the same sample kept in the dark for 10 minutes (dashed lines). All the emission spectra were acquired under 580 nm light excitation and all the excitation spectra were obtained by monitoring 650 nm emission.

5.3 Conclusion and future plans

The incompatibility of the BSP feature and ATRP technique has been studied both directly through ATRP of BSP monomer and indirectly through ATRP of MMA in the presence of a nonreactive BSP derivative. The investigation of ATRP in the presence of spiropyran suggests reaction inhibition if the concentration of spiropyran is larger than the concentration of growing chains (i.e. initiator). This prevents the synthesis of polymers or polymer architectures with a large chain length or density of spiropyran side chains, for example spiropyran functional (meth)acrylates. As an alternative, copper catalyzed cycloaddition (click chemistry) has been shown to be a versatile route to spiropyran functionalized polymers. Combining ATRP and click chemistry enables new well-defined poly(6-benzospiropyran hexylmethacrylate)s bearing a BSP moiety on the side chain of each unit of the polymer with linear, star-like and molecular brush architectures and narrow molecular weight distributions to be synthesized. Preliminary spectroscopic studies were performed on the poly(6-benzospiropyran hexylmethacrylate)s and all the polymers exhibit conventional BSP-BMC photochromism with similar spectral features both in the UV-Vis and the fluorescence spectra. The linear and star-like polymers showed similar behavior with comparable ring-closure kinetics and photostability, while the kinetics of the molecular brush architecture was two times slower and its photostability significantly greater.

Future plans involve an in-depth investigation into the photochromic properties of the polymeric systems produced, and studying their possible applicability as smart materials.

5.4 Experimental part

Materials

1′-(2-hydroxyethyl)-3′,3′-dimethyl-6-nitrospiro[2H-1-benzopyran-2,2′-indoline] was synthesized using a modified literature procedure. 9 Methyl methacrylate (99% purity, Sigma–Aldrich) was purified by vacuum distillation. 2-(trimethylsilyloxy) ethyl methacrylate was purified by filtration through neutral alumina. All the other reagents were purchased from Sigma–Aldrich and used without further purification.

Methods

Molecular weights of polymer were characterized by gel permeation chromatography performed on an Agilent 1200 series equipped with two PL Gel 5 lm Mixed-C 300 x 7.5 mm^2 columns at 40 °C. Tetrahydrofuran (THF) was used as an eluent at a flow rate of 1 mL min^{-1}. Molecular weights were calculated based on PMMA standards. Proton Nuclear Magnetic Resonance spectra were recorded at room temperature with a Bruker Avance 400 (400 MHz) and a Bruker Avance Ultrashield 600 (600 MHz). Deuterated Chloroform ($CDCl_3$) was used as solvent, and signals were referred to the signal of the residual protonated solvent signal. Chemical shifts are reported in ppm and coupling constants in Hertz. Carbon NMR spectra were recorded on Bruker Avance Ultrashield 600 (600 MHz) with total proton decoupling. ATR-FTIR spectra were collected on a Perkin Elmer Spectrum 100 in the spectral region of 650-4000 cm^{-1} and were obtained from 4 scans with a resolution of 2 cm^{-1}. A background measurement was taken before the sample was loaded onto the ATR unit for measurements. Absorption spectra were recorded using a Cary 50 UV–vis spectrophotometer. Emission measurements were carried out with a Perkin Elmer LS 55 Fluorimeter. Quartz cuvettes of 1 cm path length were used. The solutions were irradiated by means of a standard 20W 365 nm UV lamp.

Synthesis of 1'-(2-acryloxyethyl)-3',3'-dimethyl-6-nitrospiro[2H-1-benzopyran-2,2'-indoline] (BSPA)[9]

A solution of 1′-(2-hydroxyethyl)-3′,3′-dimethyl-6-nitrospiro[2H-1-benzopyran-2,2′-indoline] (3.168 g , 9 mmol) and triethylamine (3.6 mL, 25.7 mmol) in dry THF (25 mL) was stirred at 0 °C under N_2 atmosphere for 1 hour. Acryloyl chloride (1 mL,

12.6 mmol) was added dropwise to the mixture. The resulting solution was stirred at 25°C overnight. After evaporation of the solvent, the residue was dissolved in ethyl acetate and saturated aqueous sodium hydrogen carbonate was added. The aqueous phase was extracted with ethyl acetate. The combined organic phase was washed with brine, dried over anhydrous magnesium sulfate and filtered. The solvent was removed under reduced pressure to leave the product as a reddish-brown solid. The crude product was purified by silica gel column chromatography (7/3 *n*-hexane/ethyl acetate as eluent) to give the acrylated spirobenzopyran monomer (2.6 g, 6.4 mmol, 71%) as a yellow solid. ^{1}H NMR (400 MHz, $CDCl_3$, δ, ppm) 1.16 (3H, s, 3'-CH_3), 1.28 (3H, s, 3'-CH_3), 3.40-3.59 (2H, m, NCH_2), 4.30-4.33 (2H, m, OCH_2), 5.82 (1H, dd, *J* = 10.4 Hz, *J* = 1.5 Hz, C*H*$_2$=CH), 5.87 (1H, d, *J* = 10.4 Hz, 2-CC*H*=CH), 6.06 (1H, dd, *J* = 17.4 Hz, *J* =10.4 Hz, CH_2=C*H*), 6.38 (1H, dd, *J* = 17.4 Hz, *J* = 1.5 Hz, C*H*$_2$=CH), 6.70 (1H, d, *J* = 7.5 Hz, ArH), 6.75 (1H, d, *J* = 8.5, ArH), 6.88-6.92 (2H, m, ArH, 2-CCH=C*H*), 7.10 (1H, d, *J* = 7.5, ArH), 7.19-7.23 (1H, m, ArH), 8.00-8.26 (2H, m, ArH); ^{13}CNMR (400 MHz, $CDCl_3$, δ, ppm) δ 19.86, 25.87, 42.43, 52.84, 62.47, 106.49, 106.73, 115.59, 118.42, 119.96, 121.76, 121.86, 122.80, 126.00, 127.88, 128.07, 128.35, 131.29, 135.71, 141.07, 146.63, 159.40, 165.95.

Synthesis of Pentaerythritol Tetrakis(2-bromoisobutyrate) (4Br^{i}Bu)[10]

To a solution of pentaerythritol (0.27 g, 2 mmol) in 16 mL of THF placed in a two-neck round bottom flask, Et_3N (1.24 mL, 8.9 mmol) was added. The mixture was cooled to 0 °C in an ice bath and 2-bromopropionyl bromide (1.10 mL, 8.9 mmol) was added dropwise under N_2. The reaction was stirred overnight and allowed to warm to room temperature. After removing the solvent under reduced pressure, the mixture was extracted with diethyl ether (Et_2O) and washed with $NaHCO_3$(aq). The organic phase was dried over anhydrous $MgSO_4$ and filtered and the solvent removed by rotary evaporation. The crude product, a light brown solid, was recrystallized from Et_2O to give the pure four-arm initiator (0.58 g, 0.8 mmol, 40%) as a white solid. ^{1}H NMR (400 MHz, $CDCl_3$, δ, ppm) 1.94 (24 H, s, CH_3), 4.34 (8H, s, CH_2).

Synthesis of Poly(2-bromoisobutyryloxyethyl methacrylate) (PBiBEMA)[11]

1st step - Synthesis of Poly(trimethylsilyloxyethyl methacrylate) (PHEMATMS)

ATRP was applied for the synthesis of the polymers. All polymerization reactions were carried out in a moisture and oxygen-free glass tube. EBiB (36.8 μL, 0.25 mmol), CuCl (19.8 mg, 0.2 mmol), $CuCl_2$ (6.7 mg, 0.2 mmol), HMTETA (70 μL, 0.25 mmol) were mixed at a 1:0.8:0.2:1 molar ratio in anisole (50% weight). HEMATMS (1.0 g, 5 mmol) was added to the solution at a molar ratio of 10, 20 or 40 with respect to EBiB. The polymerization were carried out at 60 °C for 45, 60 or 120 minutes, respectively, depending on the desired polymer molecular weight. The polymerizations were stopped by cooling the flask to room temperature and exposing the reaction mixture to air. THF was added to the mixtures and the resulting polymer solutions were filtered through a short coloumn of neutral alumina. After removing solvent under reduced pressure, the products were dried under vacuum, collected and used without further purification. The identical reaction was repeated in larger scale, using EBiB (92.5μL, 0.625 mmol), CuCl (49.5mg, 0.5 mmol), $CuCl_2$ (17 mg, 0.125 mmol), HMTETA (170 μL, 0.625 mmol) and HEMATMS (5.0714 g, 25 mmol). The polymerization was carried out for 110 minutes and identical purification procedure was used.

2nd step - Synthesis of Poly(2-bromoisobutyryloxyethyl methacrylate) (PBiBEMA)

A solution of PHEATMS (1.0 g, assuming 5 mmol of TMS groups) in THF (4 mL) was placed in a two-neck round bottom flask, and KF (0.350 g, 6 mmol) and 2,6-di-tert-butylphenol (10.5 mg, 0.05 mmol) were added under N_2. A 0.01 M solution of TBAF in THF (0.5 mL, 0.005 mmol) was added to the flask, followed by the dropwise addition of 2-bromoisobutyl bromide (1.4 g, 6 mmol). The resulting solution was stirred at room temperature overnight. The excess of acid bromide was quenched by adding 0.16 mL of water and 0.16 mL of Et_3N. The mixture was centrifugated to saparate the solid products. The liquid phase was collected, concentrated and purified by dialysis against THF for 48 hours (1000 g/mol average pore size). After removing the solvent under reduced pressure, the product was dried under vacuum to give 0.17 g of polymer in the case of 45 minutes reaction time (PBiBEMA1; M_n = 3,600 g/mol, PDI = 1.1), 0.23 g of polymer in the case of 60 minutes reaction time

(PBiBEMA2; M_n = 4,900 g/mol, PDI = 1.1) and 0.4 g of polymer in the case of 120 minutes reaction time (PBiBEMA4; M_n = 7,300 g/mol, PDI = 1.1). Identical synthetic and purification procedures were followed for the larger scale reaction. Reagent: PHEATMS (5.0g, assuming 25 mmol of TMS groups) in THF (20 mL), KF (1.8 g, 30 mmol), 2,6-di-tert-butylphenol (52.6 mg, 0.25 mmol), a solution of TBAF in THF (2.5 mL, 0.025 mmol), 2-bromoisobutyl bromide (3.75 mL, 30 mmol). 1.9 g of polymer were obtained (PBiBEMA3; M_n = 5,800 g/mol, PDI = 1.2).

Test of Polymerization of Methylmethacrylate (MMA) through ATRP in the presence of BSP-OH-1

All the ATRP tests were performed in a moisture and oxygen-free glass tube. EBiB (18.4 μL, 0.125 mmol), CuCl (9.9 mg, 0.1 mmol), $CuCl_2$ (3.4 mg, 0.025 mmol), HMTETA (35 μL, 0.125 mmol) were mixed at a 1:0.8:0.2:1 molar ratio in anisole (50% weight). MMA (0.52 g, 2.5 mmol) was added to the solution at a molar ratio 20 with respect to EBiB. The test was carried out at 60 °C for 35 minutes. The reaction was stopped by cooling the flask to room temperature and exposing the mixture to air. THF was added to the mixtures and the resulting polymer solution was filtered through a short coloumn of neutral alumina. After removing solvent under reduced pressure, the products were dried under vacuum and collected. This procedure estabilish the reference test (test 1, **Table 2**). All the other tests were performed following the standar procedure with the appropriate modification. In the case of test 2 (**Table 2**) BSP-OH-1 (35.2 mg, 0.1 mmol) was added. In the case of test 3 (**Table 2**) BSP-OH-1 (176 mg, 0.5 mmol) was added. In the case of test 4 (**Table 2**) BSP-OH-1 (352 mg, 1 mmol) was added. In the case of test 5 (**Table 2**) BSP-OH-1 (35.2 mg, 0.1 mmol) was added but the reaction carried out without MMA. In the case of test 6 (**Table 2**) BSP-OH-1 (35.2 mg, 0.1 mmol) was added but the reaction carried out without EBiB.

Synthesis of Poly(2-azidoisobutyryloxyethyl methacrylate) (PAiBEMA)

Sodium azide (0.1 g, 2.3 mmol) was added to a solution of PBiBEMA3 (0.1 g, 0.4 mmol) in dimethylformamide (DMF) (1 mL). The mixture was stirred overnight at room temperature and extracted several times with dichloromethane (DCM). The organic phase was dried over anhydrous $MgSO_4$ and filtered. After removing the

solvent under reduced pressure the product was dried under vacuum to give 0.52 g of polymer (PAiBEMA1, entry 1, **Table 3**; M_n = 6,100 g/mol, PDI = 1.2). The identical synthetic and purification procedure was used for the synthesis of PAiBEMA2 and PAiBEMA3, varying the molar ratio. A molar ratio PAiBEMA3:NaN_3 = 1:0.46 was used in the case of PAiBEMA2 (entry 2, **Table 3**, M_n = 6,000 g/mol, PDI = 1.2). A molar ratio PAiBEMA3:NaN_3 = 1:0.18 was used in the case of PAiBEMA3 (entry 3, **Table 3**, M_n = 6,000 g/mol, PDI = 1.3). In all the cases the presence of the azide groups were observed by FT-IR (cm^{-1}) 2111.

Synthesis of 1'-(propargyl)-3',3'-dimethyl-6-nitrospiro[2H-1-benzopyran-2,2'-indoline] (BSP-alkyne)[22]

1st step - Synthesis of 1-propargyl-2,3,3-trimethylindoleninium tosylate

2,3,3-Trimethylindolenine (1.2 mL, 7 mmol) and 1-tosyl-2-propyne (1.5 mL, 8.7 mmol) were mixed and heated at 78 °C for 3 hours. The reaction mixture was allowed to cool to room temperature. The resulting dark violet crude material was used without further purification.

2nd step - Synthesis of 1-propargyl-2,3,3-trimethylindolenine

20 mL of a 0.5 M solution of KOH (11 mmol) in water were added to 1-propargyl-2,3,3-trimethylindoleninium tosylate (2.6 g, assuming 7 mmol). The resulting mixture was stirred for 45 minutes at room temperature and then extracted with Et_2O. The organic phase was dried over $MgSO_4$ and filtered. The solvent was removed by rotary evaporation, leading to the desired product as a dark orange oil. The product was immediately used in the following step without further purification.

3rd step – Synthesis of 1'-(propargyl)-3',3'-dimethyl-6-nitrospiro[2H-1-benzopyran-2,2'-indoline] (BSP-alkyne)

To a solution of 1-propargyl-2,3,3-trimethylindolenine (2.6 g, assuming 7 mmol) in EtOH (11 mL) 2-hydroxy-5-nitro benzaldehyde (1.64 g, 9.8 mmol) was added. The reaction mixture was heated under reflux for 4 hours. The reaction mixture was allowed to cool to room temperature of its own accord, the solvent was removed

under reduced pressure to give the crude product as a dark purple oil. After purification through silica gel column chromatography (7/3 *n*-hexane/ethyl acetate as eluent) the propargyl spirobenzopyran (0.97 g, 2.8 mmol, 40%) was obtained as a bright yellow solid.^{1}H NMR (600 MHz, $CDCl_3$, δ, ppm): 1.20 (3H, s, 3'-CH_3), 1.30 (3H, s, 3'-CH_3), 2.08-2.10 (1H, m, HC≡C), 3.88 (1H, dd, *J* =18.2 Hz, *J* =2.4 Hz, NCH_2), 4.03 (1H, dd, *J* =18.2 Hz, *J* = 2.7 Hz, NCH_2), 5.09 (1H, d, *J* = 10.2 Hz, 2-CC*H*=CH), 6.75 (1H, d, *J* = 9.9, ArH), 6.82 (1H, d, *J* = 7.8 Hz, ArH), 6.91-6.99 (2H, m, ArH, 2-CCH=C*H*), 7.10-7.14 (1H, m, ArH), 7.21-7.26 (1H, m, ArH), 8.00-8.04 (2H, m, ArH); ^{13}C NMR (600 MHz, $CDCl_3$, δ, ppm): 160.2, 146.1, 141.5, 136.8, 129.4, 128.2, 126.5, 123.0, 122.0, 121.4, 121, 119, 116.5, 108.8, 106.4, 80.2, 80.0, 53.2, 33.0, 26.6, 20.5.

Click reaction of BSP-alkyne onto PAiBEMA

PAiBEMA1 (0.52 g, 0.21 mmol) was dissolved in 4 mL of tetrahydrofuran and BSP-alkyne (0.080 g, 0.23 mmol), 13 µL of an aqueous freshly prepared 4M solution of sodium ascorbate (0.05 mmol) were added. CuBr (15.1 mg, 0.1 mmol) and PMDETA (21.9 µL, 0.1 mmol) were used as catalyst. The reaction mixture was stirred at 40 ^{o}C for 60 h under nitrogen and then purified through dialysis against THF (cut-off 1000 g/mol). The identical synthetic and purification procedure was used to click BSP-alkyne onto PAiBEMA2 and PAiBEMA3. In all the cases the peak at 2111 cm^{-1} due to the azide groups decreased in intensity, as shown by FT-IR, only in the case of PAiBEMA3 the total absence of the peak at 2111 cm^{-1} was recorded.

Synthesis of 6-Azidohexyl Methacrylate (AHMA)[21,30]

1st step - Synthesis of 6-azido-1-hexanol

6-chloro-1-hexanol (3 mL, 22.5 mmol) was added to a solution of NaN_3 (2.3 g, 36.2 mmol) in DMF (4 mL) and water (4 mL). The misxture was heated to 75 °C for 22 h. The reaction mixture was cooled to room temperature, dissolved in 150 mL of water and extracted with Et_2O (6 x 100 mL). The combined organic phase was washed twice with 100 mL of aqueous solution of NaCl, dried over anhydrous $MgSO_4$ and then filtered. After removing the solvent was removed under reduced pressure, the product was dried under vacuum to obtain pure 6-azido-1-hexanol as a yellowish oil. ^{1}H NMR (400 MHz, $CDCl_3$, δ, ppm): 1.33 -1.66 (8H, m, CH_2-CH_2-CH_2-

CH_2), 3.27 (2H, t, *J* = 6.8 Hz N_3-CH_2), 3.64 (2H, t, *J* = 6.8 Hz O-CH_2); FT-IR (cm^{-1}): 2094 (υN_3).

2nd step - Synthesis of 6-Azidohexyl Methacrylate (AHMA)

6-azido-1-hexanol (3.2 g, assuming 22.5 mmol), was reacted with methacryloyl chloride (2.6 mL, 27.0 mmol) in dry DCM (70 mL) at 0 °C in the presence of triethylamine (4.4 mL, 31.5 mmol) for 24 h under inert atmosphere. After removing the solvent under reduced pressure, ethyl acetate and saturated aqueous solution of $NaHCO_3$ were added to the mixture. The aqueous phase was extracted with ethyl acetate (4 x 50 mL) and the combined organic layers were dried over anhydrous $MgSO_4$ and filtered. The solvent was removed under reduced pressure to leave the product as a yellow oil. After purification through silica gel column chromatography (9/1 *n*-hexane/ethyl acetate as eluent) the 6-azidohexyl methacrylate (AHMA) (1.71 g, 8.1 mmol, 72%) was obtained as transparent oil. ^1H NMR (400 MHz, $CDCl_3$, δ, ppm): 1.32-1.75 (8H, m, CH_2-CH_2-CH_2-CH_2), 1.94 (1H, s, CH_3), 3.27 (2H, t, *J* = 6.8 Hz N_3-CH_2), 4.14 (2H, t, *J* = 6.8 Hz O-CH_2), 5.55 (1 H, m, C=CH_2), 6.09 (1 H, m, C=CH_2); FT-IR (cm^{-1}): 2094 (υN_3) and 1714 (υC=O).

Synthesis of Poly(6-azidohexyl methacrylate) (PAHMA)

ATRP was applied for the synthesis of the polymers. All polymerization reactions were carried out in a moisture and oxygen-free glass tube. The initiator used depended on the desired polymer architecture: EBiB (2.6 μL, 0.018 mmol) to obtain the linear polymer, 4BriBu (13.2 mg, 0.018 mmol) to synthetize the star-like polymer and PBiBEMA1 (5 mg, 0.018 mmol) to obtain the molecular brush architecture. The selected initiator (0.018 mmol), CuCl (1.8 mg, 0.018 mmol) and PMDETA (3.8 μL, 0.018 mmol) were mixed at a 1:1:1 molar ratio in isopropyl alcohol (IPA) (50% weight). AHMA (380 mg, 1.8 mmol) was added to the solution at a molar ratio of 100 with respect to EBiB. The polymerization were carried out at 30 °C for 195, 50 or 40 minutes, respectively, depending on the desired polymer architecture. The polymerizations were stopped by cooling the flask to room temperature and exposing the reaction mixture to air. THF was added to the mixtures and the resulting polymer solutions were filtered through a short coloumn of neutral

alumina. The linear and star-like polymers were purified through precipitation into methanol, while the molecular brush polymer was purified through dialisys against THF (cut-off 3,500 g/mol). All the products were dried under vacuum to give 170 mg of linear PAHMA (9,200 g/mol, PDI: 1.2), 105 mg of star-like PAHMA (10,200 g/mol, PDI: 1.2) and 18 mg of molecular brush PAHMA (22,100 g/mol, PDI: 1.2). ^{1}H NMR (600 MHz, $CDCl_3$, δ, ppm): 0.80-1.03 (m, 3H, CH_3 along the polymer backbone), 1.32-1.83 (m, 10H, $CH_2CH_2CH_2CH_2$ and CH_2 along the polymer backbone), 3.34 (m, 2H, CH_2N_3), 3.96 (m, 2H, CH_2O). In all the polymers the presence of the azide groups and the carbonyl groups were observed by FT-IR (cm^{-1}) 2095 and 1728, respectively.

Synthesis of Poly(BSP hexyl methacrylate) (PBSPHMA)

Linear PBSPHMA (85 mg, 0.4 mmol) was dissolved in 6 mL of THF and BSP-alkyne (153 mg, 0.44 mmol), 25 μL of an aqueous freshly prepared 4M solution of sodium ascorbate (0.1 mmol) were added. CuBr (28.7 mg, 0.2 mmol) and PMDETA (42 μL, 0.2 mmol) were used as catalyst. The reaction mixture was stirred at 40 ^{o}C for 60 h under nitrogen. The reaction mixture was cooled to room temperature, filtered through a short coloumn of neutral alumina, precipitated into methanol and further purified through dialysis against THF (cut-off 1000 g/mol). ^{1}H NMR (600 MHz, $CDCl_3$, δ, ppm): 0.55-2.4 (m, 19 H, $CH_2CH_2CH_2CH_2$, CH_2 and CH_3 along the polymer backbone and CH_3 of the benzospiropyran unit), 3.58-4.79 (m, 6H, CH_2O, CH_2N_3, CH_2N), 5.9 (br s, 1H, C-C*H*=CH), 6.46-7.20 (m, 6H,C-CH=C*H* and ArH), 7.45 (br s, 1H, triazole), 7.93 (br s, 2H, ArH). The identical synthetic and purification procedure was used to click BSP-alkyne onto the star-like and molecular brush PBSPHMA. In all the cases the absence of of the azide groups were confirmed by FT-IR.

UV-Vis spectroscopic studies on BSP functional polymer obtained after click Click reaction of BSP-alkyne onto PAiBEMA (40% BSP)

Approximately, $1x10^{-4}$ M stock solution of polymer in DCM was prepared [Note: the polymer concentration for the measurements was calculated based on the polymer M_n from SEC (PMMA standards) and considering the amount of BSP units bonded to the polymer] and stored in the dark at room temperature. The absorbance spectra

of 3 ml of solution were recorded before and after exposure to UV light (365 nm) for 1 minute. For Co^{2+} complexation experiments, 1×10^{-4} M solutions of the polymer were kept in dark before addition of equal molar equivalents of the metal salt.

UV-Vis spectroscopic studies on photochromism of linear, star-like and molecular brush PBSPHMA

Approximately, $0.5x10^{-4}$ M stock solutions of linear and molecular brush PBSPHMA and $0.5x10^{-5}$ M of star-like PBSPHMA in THF were prepared [Note: all polymer concentrations for the measurements were calculated based on the polymer M_n from SEC (PMMA standards) of the corresponding PAHMA precursor polymer] and stored in the dark at room temperature. Then 3 ml of each solution were exposed to UV light irradiation for 1 minute and the absorbance spectra were recorded. The absorbance decrease at λ_{max} (580 nm) was monitored, after removal of the irradiating source, for each polymer every 0.05 second for 800 seconds, in order to evaluate the ring closing kinetic over time. The first-order rate constants were estimated by following the decrease of the absorbance at λ_{max} in time and subsequently examined using the equation $\ln([A_t]/[A_0]) = -kt$ with A_t and A_0 denote the absorbance at λ_{max} at time *t* and at the beginning of the thermal relaxation process, respectively.[36]

E-diagrams were generated by extrapolating the absorbance values at determined wavelengths from each collected spectrum and plotting these values against the absorbance values of a defined wavelength.[31]

For studying switching efficiency the value of absorbance was measured after irradiating the sample with UV light (365 nm) for 1 minute several times. After every measurement the BMC form was allowed to completely reverse back to the BSP form and the sample was kept in the dark during the experiment to avoid the interference of ambient light.

Fluorescence spectroscopic studies on linear, star-like and molecular brush PBSPHMA

Approximately, $1x10^{-5}$ M stock solutions of linear and molecular brush PBSPHMA and $1x10^{-6}$ M of star-like PBSPHMA in THF were prepared [Note: all polymer

concentrations for the measurements were calculated based on the polymer M_n from SEC (PMMA standards) of the corresponding PAHMA precursor polymer] and stored in the dark at room temperature. Fluorescence emission spectra of PBSPHMA were recorded before, after photoisomerisation by exposure to UV light for 1 minute and after maintaining the same sample in the dark for 10 minutes with excitation wavelength was set at 580 nm. Excitation spectra were collected after photoisomerisation upon exposure to UV light for 1 minute and after maintaining the same sample in the dark for 10 minutes. Excitation spectra were monitored at 650 nm.

5.5 References

1. Chen J., Zeng F., Wu S., Zhao J., Chen Q., Tong Z. *Chem. Commun.* **2008**, 5580.
2. Lee H., Wu W., Oh J.K., Mueller L., Sherwood G., Peteanu L., Kowalewski T., Matyjaszewski K. *Angew. Chem. Int. Ed.* **2007**, *46*, 2453.
3. Jin Q., Liu G., Ji J. *J. Polym. Sci. A: Polym. Chem.* **2010**, *48*, 2855.
4. Achilleos D.S., Vamvakaki M. *Macromolecules* **2010**, *43*, 7073.
5. Achilleos D.S., Hatton T.A., Vamvakaki M. *J. Am. Chem. Soc.* **2012**, *134*, 5726.
6. Fries K.H., Driskell J.D., Samanta S., Locklin J. *Anal. Chem.* **2010**, *82*, 3306.
7. Ercole F., Malic N., Harrisson S., Davis T.P., Evans R.A. *Macromolecules* **2010**, *43*, 249.
8. Leea H.I., Pietrasik J., Sheikoc S.S., Matyjaszewski K. *Prog. Polym. Sci.* **2010**;35, 24.
9. Raymo F.M., Giordani S. *J. Am. Chem. Soc.* **2001**, *123*, 4651.
10. Matyjaszewski K., Miller P.J., Pyun J., Kickelbick G., Diamanti S. *Macromolecules* **1999**, *32*, 6526.
11. Nese A., Mosnàcek J., Juhari A., Yoon J.A., Koynov K., Kowalewski T., Matyjaszewski K. *Macromolecules* **2010**, *43*, 1227.
12. Park I., Sheiko S.S., Nese A., Matyjaszewski K. *Macromolecules* **2009**, *42*, 1805.
13. Guglielmetti R.J., Crano J.C. *Organic Photochromic and Thermochromic Compounds*. New York: Plenum Publishers; **1999**.
14. Malatesta V., Hobley J., Salemi-Delvaux C. *Mol. Cryst. Liq. Cryst* **2000**, *344*, 69.
15. Ventura C., Byrne R., Audouin F., Heise A. *J. Polym. Sci. A: Polym. Chem.* **2011**, *49*, 3455.
16. Adelmann R., Mela P., Gallyamov M.O., Keul H., Möller M. *J. Polym. Sci. A: Polym. Chem.* **2009**, *47*, 1274.
17. Golas P.L., Matyjaszewski K. *QSAR Comb. Sci.* **2007**, *26*, 1116.
18. Binder W.H., Sachsenhofer R. *Macromol. Rapid Commun.* **2007**, *28*, 15.
19. Binder W.H., Sachsenhofer R. *Macromol. Rapid Commun.* **2008**, *29*, 952.
20. Tsarevsky N.V., Sumerlin B.S., Matyjaszewski K. *Macromolecules* **2005**, *38*, 3558.
21. Sumerlin B.S., Tsarevsky N.V., Louche G., Lee R.Y., Matyjaszewski K. *Macromolecules* **2005**, *38*, 7540.

22. Bertoldo M., Nazzia S., Zampanob G., Ciardelli F. *Carbohydr. Polym.* **2011**, *85*, 401.

23. Byrne R., Stitzel S.E., Diamond D. *J. Mater. Chem.* **2006**, *16*, 1332.

24. Byrne R., Ventura C., Lopez F.B., Walther A., Heise A., Diamond D. *Biosens. Bioelectron.* **2010**, *26*, 1392.

25. Chibisov A.K., Gorner H. *Chem. Phys.* **1998**, *237*, 425.

26. Gondi S.R., Vogt A.P., Sumerlin B.S. *Macromolecules* **2007**, *40*, 474.

27. Zhang J., Zhou Y., Zhu Z., Ge Z., Liu S. *Macromolecules* **2008**, *41*, 1444.

28. Bräse S., Gil C., Knepper K., Zimmermann V. *Angew. Chem. Int. Ed.* **2005**, *44*, 5188.

29. Kolb HC., Finn MG., Sharpless KB. *Angew. Chem. Int. Ed.* **2001**, *40*, 2004.

30. Cengiz N., Kabadayioglu H., Sanyal R. *J. Polym. Sci. A: Polym. Chem.* **2010**, *48*, 4737.

31. Dürr H., Bouas L.H. *Photochromism: molecules and systems*. Boston: Elsevier; **2003**.

32. Li Y., Zhou J., Wang Y., Zhang F., Song X. *J. Photochem. Photobiol. A* **1998**, *113*, 65.

33. Mauser H., Gaugliz G. *Photokinetics: theoretical fondamentals and applications*. New York: Elsevier; **1998**.

34. Stitzel S., Byrne R., Diamond D. *J. Mater. Sci.* **2006**, *41*, 5841.

35. Gorner H. *Phys. Chem. Chem. Phys.* **2001**, *3*, 416.

36. Flannery J.B. *J. Am. Chem. Soc.* **1968**, *90*, 5660.

Chapter 6

Conclusions and Outlook

6.1 Conclusions

Benzospiropyrans are a particularly interesting class of compounds for use in the development of smart polymers. The unique molecular switch undergoes structural isomerization in response to several external stimuli including light, metal ions, protons and mechanical stress. Incorporating benzospiropyran in a polymer matrix gives the same distinctive properties to the polymer. The use of ATRP permits the preparation of polymers with predetermined molecular weights, narrow molecular weight distributions and the exact positioning of functional units in the polymer. This project aimed at exploiting ATRP for the synthesis of well-defined polymers with photochromic units in defined positions either along the polymer chain or as the polymer end-group and study their photochromic behaviour.

Initially, ATRP was employed to synthetize two sets of PMMA, bearing a single benzospiropyran terminal unit, with different M_n. Different benzospiropyran derivative per set were used to initiate the polymerization: BSP-Br-1 with an electron-withdrawing nitro-group on the benzene ring of the pyran fragment and BSP-Br-2 with an electron donor hydroxyl group in the same position. The photochromic properties of all the benzospiropyran end-functionalized polymers were investigated. The complexation properties of the BSP-Br-2 functionalized polymeric systems were shown and the photonic control of uptake and release of $Cu2^{+}$ ions was demonstrated. The BSP-Br-1 functionalized polymers exhibited conventional photochromism characterized by the UV-induced transition from benzospiropyran to benzomerocyanine in acetonitrile. The light-responsiveness of the polymers was investigated in solution and it was found that the polymer molecular weight influences the photophysical behavior of the benzospiropyran end-group. Moreover, the ability of polymer end-groups to prompt organization was shown by metal ion-binding experiments in which bivalently linked complexes were formed. Comparing the photochromic behavior of the two sets of polymers, it was found that polymers functionalized with BSP-Br-1 responds better to the procured stimulus, as expected. Therefore, it was decided to use the nitro–bearing benzospiropyran derivative for further synthesis of BSP functionalized polymers.

Next, a nitro-benzospiropyran derivative with a propyne functional group was synthesized and its photochromic, solvatochromic and acidochromic properties

investigated by UV-Vis, ^{1}H NMR and fluorescence spectroscopy. The spectral features suggested the presence of more than one BMC-alkyne isomer in solution at room temperature. Exploiting the alkyne functionality of this benzospiropyran compound, commercially available PEG and PPO derivatives were successfully converted into BSP-functionalized polymers through CuAAC. Preliminary spectroscopic studies on these polymers were carried out and their photochromism was shown. All the polymers showed the same spectral features, comparable ring-closure kinetics at room temperature and similar photostability. Therefore, the nature of the polymer backbone linked to the benzospiropyran units, and the molecular weight of the polymer have a small influence on their photochromic behavior at room temperature.

Afterwards, the incompatibility of benzospiropyran as a monomer component in ATRP was investigated. The results revealed that if the concentration of spiropyran is larger than the concentration of growing chains (i.e. initiator), the polymerization was inhibited. This prevented the synthesis of polymers or polymer architectures with a large chain length or density of spiropyran side chains, for example spiropyran functional (meth)acrylates. As an alternative, click chemistry was shown to be a versatile route to spiropyran-functionalized polymers. Combining ATRP and the CuAAC reactions we successfully synthetized well-defined poly(6-benzospiropyran hexylmethacrylate)s that bear a benzospiropyran moiety on the side chain of each unit of the polymer with linear, star-like and molecular brush architectures. Preliminary spectroscopic studies were performed on the poly(6-benzospiropyran hexylmethacrylate)s at room temperature and all the polymers exhibit conventional BSP-BMC photochromism. All the polymers showed the similar spectral features both in the UV-Vis and the fluorescence spectra. The linear and star-like polymers showed similar behavior with comparable ring-closure kinetics and photostability, while the kinetics of the molecular brush architecture was two times slower and its photostability significantly greater.

6.2 Outlook

Photochromic polymers have great potential as light responsive smart materials. The polymers and concepts developed here open opportunities to contribute and advance this exciting field of material science. However, this must involve further in-depth investigation into the photochromic properties of the polymeric systems produced and studying their possible applicability as smart materials. Furthermore, exploiting the ATRP/CuAAC strategy developed for the synthesis of well-defined copolymers that bear both benzospiropyran moiety and different types of functionality on the side chain, in order to create new materials with specific features in addition to the typical benzospiropyran properties could be a future concept. Another important aspect will be the integration of photochromic polymers into actual devices, which in addition to chemical and physical expertise might require the expertise of engineers.